Goethe-Universität Frankfurt

Goethe Center for Scientific Computing

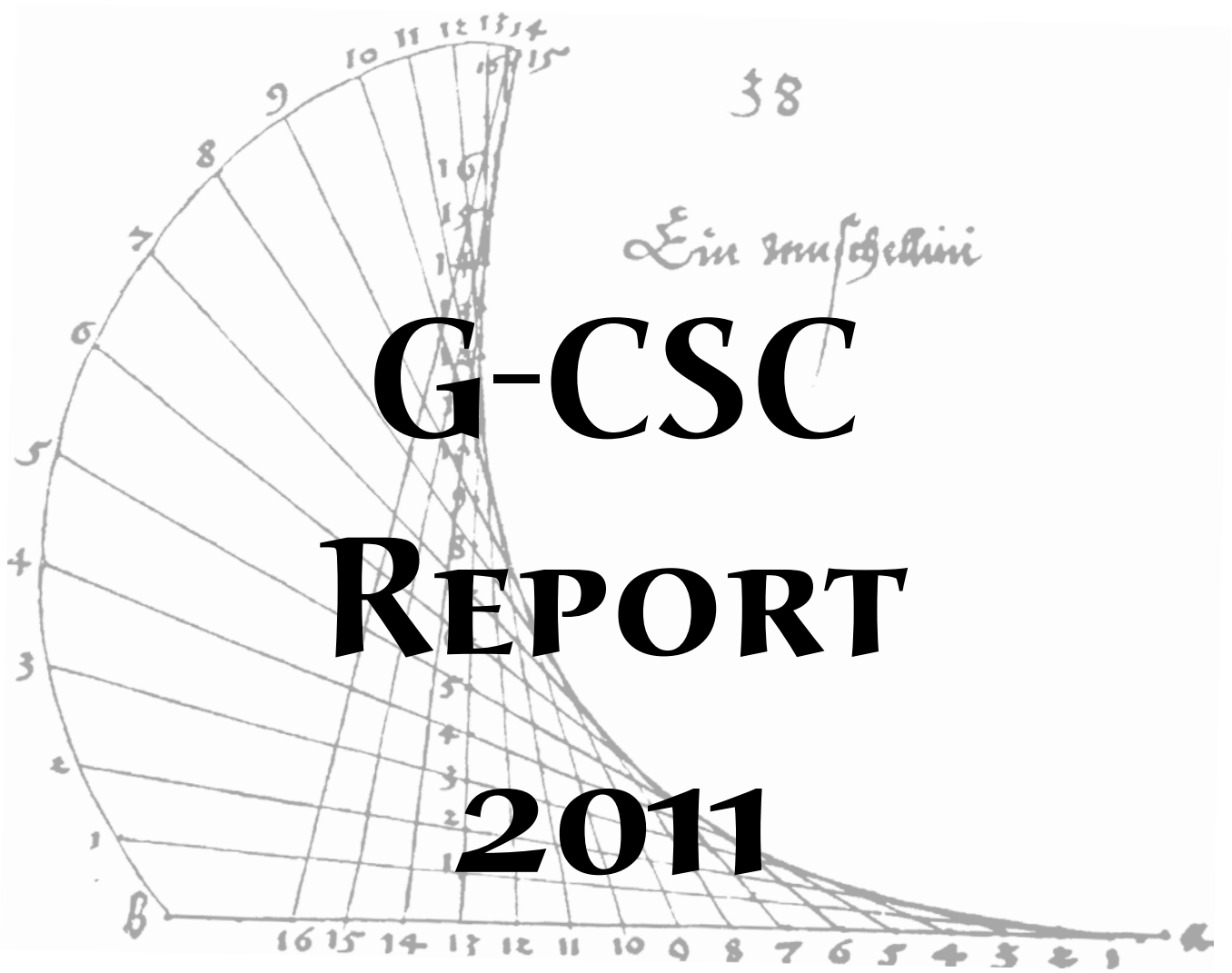

G-CSC Report 2011

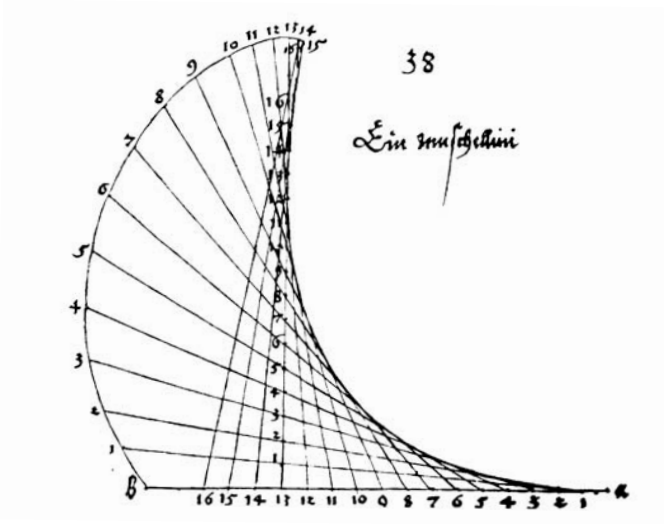

Goethe-Zentrum für Wissenschaftliches Rechnen
Goethe-Universität Frankfurt
Prof. Dr. Gabriel Wittum
URL: http://www.gcsc.uni-frankfurt.de/
E-mail: wittum@g-csc.de
Phone: +49-69-798 25258
Fax: +49-69-798 25268

Table of Contents

Overview

Introduction

The present report gives a short summary of the research of the Goethe Center for Scientific Computing (G-CSC) of the Goethe University Frankfurt. G-CSC aims at developing and applying methods and tools for modelling and numerical simulation of problems from empirical science and technology. In particular, fast solvers for partial differential equations (i.e. pde) such as robust, parallel, and adaptive multigrid methods and numerical methods for stochastic differential equations are developed. These methods are highly adanvced and allow to solve complex problems..

The G-CSC is organised in departments and interdisciplinary research groups. Departments are localised directly at the G-CSC, while the task of interdisciplinary research groups is to bridge disciplines and to bring scientists form different departments together. Currently, G-CSC consists of the department *Simulation and Modelling* and the interdisciplinary research group *Computational Finance.*

The Department Simulation and Modelling (SiM)

In January 2009, 22 researchers moved from Heidelberg to Frankfurt to start this new center. In Heidelberg, the group formed the department "Simulation in Technology" and did research and development of methods for solving typical problems from computational biology, fluid dynamics, structural mechanics and groundwater hydrology. The main focus was on the development of the simulation environment *ug*, which is the first parallel and adaptive multigrid solver for general models based on partial differential equations (pde).

In Frankfurt, the group now forms the department Simulation and Modeling of the G-CSC. Besides continuing the work from Heidelberg, we have now added new topics from finance, neuroscience and sustainable energy. Currently, G-CSC is running a total of thirty projects dealing with the simulation of a very wide variety of application problems, simulation methods and tools.

From 2005-2010, the research focused on applications from the following areas:

A1 Computational Pharmaceutical Science: Diffusion of xenobiotics through human skin.
As early as 1993, we researched diffusion through human skin and predicted diffusion pathways from our simulations. To match experimentally measured data, we had to postulate new diffusion pathways which were not in accordance with traditional assumptions. When we presented the model in 1993 on the annual conference of the "Controlled Release Society" in Washington D.C., the paper was awarded a prize as the best paper of the conference. The results were published; however, pharmacists still kept to their old assumptions on diffusion pathways. In 2003, however, a group from MIT was able to confirm our results experimentally. This shows that simulation is playing an increasingly important role in biosciences as well. Meanwhile we are working on more detailed models. More details can be found in Project A1.

A2 Computational Neuroscience: Detailed modelling and simulation of signal processing in neurons.
Computational neuroscience, i.e. modelling and simulation for getting a deeper understanding of neurons and brain functions is one of the most challenging areas nowadays. Funded by the Bernstein Group DMSPiN (http://www.dmspin.org), we set up a novel approach for detailed modelling and simulation. This approach starts with automatic reconstruction of neuron morphologies by a special image processing. The corresponding tool NeuRA has been awarded the 1st price of the doIT Software Award in 2005. In the last year it has been accelerated to run on GPU clusters. This makes the reconstruction of high-resolution microscopic images possible in real time (A2.1). Another novel approach for automatic classification of neuron cells has been presented (NeuClass, A2.5). Using reconstructed geometries, several processes have been modeled. In A2.2, we describe a project on model-

ling calcium signaling to the cell nucleus. The project was carried out in cooperation with the Bading lab at IZN Heidelberg in the DMSPiN framework. In the project, we obtained results on the relation between calcium signaling and nucleus shape. In A2.3, we model the electric signal transduction in a neuron. To that end, a novel process model is derived from the Maxwell equations resulting in a system of partial differential equations describing the potential as a function in three dimensional space. In A2.4, we investigate the modelling of the replication dynamics of the Hepatitis C Virus in 3D space. Project A2.6 deals with the modelling of the hydrodynamics of synaptic vesicles.

A3 Mathematical Finance: Treating high-dimensional problems.
We have developed a novel approach to computing the fair price of options on baskets. This intriguing problem from financial mathematics is modelled by the Black-Scholes equations. The space dimension equals the number of assets in the basket. Usually, this is done using Monte-Carlo methods, which takes a long time and produces uncertain results. To obtain a faster solution method, we first developed a sparse grid approximation for the Black-Scholes pde and implemented a multi-grid-based solver. We were able to extend this approach to higher-order approximations, allowing the computation of the very important sensitivities ("greeks"). To that end, we combined it with a dimensional reduction, which was surprisingly effective and gives explicit error bounds. With this tool, we are able to compute options on DAX (30-dimensional) in some minutes, whereas state-of-the-art Monte-Carlo methods need about two days without producing any error bounds. For details, see Project A3.1. Project A3.2 uses the same approach to model credit risks. In project A3.3 we develop advanced nuemrical methods for portfolio optimisation.

A4 Process Engineering: Solvers for multidimensional population balances and disperse systems.
Population dynamics in disperse, i.e. spatially resolved, systems is a great challenge for computational science. In industrial practice, all population dynamics processes such as e.g. polymerisation or crystallisation or the growth of bacteria in a stirred reactor happen in a flow. However, coupling the resulting integro-differential equation with the fluid flow is a computational problem which has not yet been solved. We have developed novel fast methods for processing the integro-differential equation and were able to do computations on 2D and 3D property spaces in UG. Then we combined these solvers with our flow solvers and ended up with the first coupled computation of population balance equations with 2D and 3D flow problems. For details see Project A4.

A5 Environmental Science: Groundwater flow and transport, remediation, waste disposal, renewable energy.
We have developed a simulation model for the biological remediation of a chlorine spill in an aquifer. The model was based on a real situation and developed in close co-operation with industry. On the basis of our simulation model, we were able to design a remediation strategy for a concrete application case (see UG brochure, p. 7).

We developed the simulation tool d^3f for computing density-driven porous-media flows in very general domains (A5.1). The tool uses the full model including non-linear dispersion. In this sense, as well w.r.t. the complexity of the problems, it is the most general software available for this kind of problem. With r^3t, we developed a tool for computing the transport, diffusion, sorption and decay of radioactive pollutants in groundwater. This novel software tool allows the simulation of the transport and retention of radioactive contaminants (up to 160 species) in large complex three-dimensional domains (see A5.2). In these projects, we cooperated with S. Attinger and W. Kinzelbach, Zürich, P. Knabner, Erlangen, D. Kröner, Freiburg, and M. Rumpf, Bonn. In a new project, we develp special models for thermohaline flows in fractured porous media (A5.3).

In addition, we develop simulation models for biogas production. In a first effort, we created the software tool VVS. VVS allows to compute the compression process in a crop silo. Currently, we are modeling the fermentation of crops to produce biogas.

We further developed simulation tools and carried out simulations for two-phase flow in porous media and developed and applied methods for the parameter estimation of these problems. To model flow and transport through fractured porous media, we developed a formulation using a lower-dimensional approximation for the

fractures. This was carried out by Volker Reichenberger and Peter Bastian, who is now in the Parallel Computing Group of IWR, Universität Heidelberg, in cooperation with R. Helmig, Stuttgart.

A6 Computational Fluid Dynamics: Incompressible and compressible Navier-Stokes equations, turbulence, Large-Eddy simulation, mixing, aeroacoustics, low Mach-number flow, two-phase flow (gas/liquid), non-Newtonian flows

To compute turbulent flows, we developed a Large-Eddy simulation (LES) model combined with an adaptive multigrid solver. This *uG*-based LES-multigrid simulation model incorporates several subscale models and is so flexible that we were able to compute flows through a static mixer in industrial geometries (see A6.1). A second field of research is aeroacoustics and low Mach-number flow. Here, we developed two kinds of algorithm, one based on the so-called Multiple Pressure-Variables (MPV) ansatz by Klein and Munz, which is based on splitting the pressure, the second one a direct multi-grid approach to this multi-scale problem, coupling acoustics with the Navier-Stokes equations (see A6.2).

We further developed methods and tools to compute multi-phase flows, such as rising air bubbles in water. Here, we use two different basic approaches, the Volume of Fluid method (VOF) and the level-set method.

The former was applied to compute two-phase flow (gas/liquid), and liquid-liquid extraction. We also developed a simulation model for non-Newtonian Bingham flow used for modelling the extrusion of ceramic pastes e.g. for making bricks. This was combined with a tool to optimise design. Based on this tool, the geometry of a measuring nozzle was optimised (see M5). We further coupled our Navier-Stokes solvers with several other problems, e.g. electromagnetics to simulate the cooling of high-performance electric devices, and with population dynamics to describe the development of structured populations in a flow (A4).

A7 Computational Electromagnetics: Eddy-current problems, coupling of electromagnetics with fluid flow
We developed a simulation model for the low-frequency (AC) case of the Maxwell equations. A new estimate for the modelling error was introduced. The model was successfully applied to complicated problems from industry like transformers and high-performance switches (A7.1).

A8 Structural Mechanics: Reduction of numerical sensitivities in crash simulations.
Besides the standard linear elastic problems, we developed methods and tools for solving elasto-plastic problems with non-linear material laws (Neuss 2003; Reisinger and Wittum 2004; Reisinger 2004). We were able to compute reference solutions used to benchmark engineering codes. The research on this topic has been carried out by Christian Wieners. He now holds the chair for Scientific Computing at Karlsruhe University and continues research on this topic there. We also coupled the structural mechanics code with our optimisation tool to carry out topology optimisation (Johannsen et al. 2005).

A10 Numerical Geometry and Visualisation: Reconstruction of Heidelberg Castle before destruction.
The idea of this project is to carry out a virtual reconstruction of Heidelberg Castle before it was destroyed. In co-operation with the History of Arts Institute, we develop a computer model of the castle as it was in 1680. The geometry is prepared for rendering by ray tracing using POVRAY. This geometry will be the basis for a internet computing project on distributed, internet-based visualisation by ray tracing. The project has no support, but is based merely on the work of student helpers.

A11 Computational Musical Acoustics.
Detailed modelling musical instruments requires a lot of new steps to be taken. According to Erich Schumann's theory of formants, we first need to compute the resonances of the instrument. In Project A11, we developed a method and a tool to compute the eigenvalues and eigenvectors of the top plate of a guitar. The results compare well with measured eigenmodes. This is a first step in direction of a complete 3d model of resonances of an instrument.

Moreover, we developed and/or investigated the following methods:

M1 Fast solvers for large systems of equations: Parallel adaptive multigrid methods, algebraic multigrid, frequency filtering, adaptive filtering, filtering algebraic multigrid, homogenisation multigrid, coarse-graining multigrid, interface reduction, domain decomposition.

The development of fast solvers for large systems of equations is the core project from which all the other projects arose. Starting with robust multi-grid methods for systems of pde, we now develop a lot of different methods. A major focus is algebraic multigrid (AMG) methods and their connection to homogenisation. Here, we developed filtering algebraic multigrid (FAMG), a novel approach to constructing multigrid methods directly from the matrix, without knowledge of the pde. Several other new methods from this field have been developed, like automatic coarsening (AC), Schur-complement multigrid (SCMG) and coarse-graining multigrid (CNMG). This is strongly linked with the development of filtering methods. Starting in 1990 with frequency-filtering decompositions, we continued the development of filters as linear solvers. The FAMG ansatz and its parallel version are suited to solving general systems of equations. In the framework of transforming iterations, which we developed years ago, these methods are available for systems of pde.

M2 Multiscale modelling and numerics: Linking homogenisation with numerical multiscale methods, like multigrid solvers, fast computation of effective models and their parameters. Based on the "coarse-graining" approach of S. Attinger, Jena, we developed a new coarse-graining multigrid method, with a nice performance for heterogeneous problems.

M3 Discretisation: Finite volume methods of arbitrary order, modified method of characteristics (MMoC), discontinuous Galerkin methods, Whitney elements, sparse grids, higher order sparse grid methods.

Several discretisation methods have been developed. In particular, methods for the discretisation of advection terms have been investigated, like a novel modified method of characteristics. For stiff problems in time, caused by linear reaction terms (radioactive decay), we developed a special technique for incorporating exact solutions via a Laplace transformation and operator splitting (A5.3). We were also able to establish new sharp error estimates for sparse grids in arbitrary dimensions. This analysis made it possible to generate an extrapolation scheme yielding higher-order approximations with sparse grids (cf. A3). In M2 we describe a new technique to develop finite volume methods of arbitrary order.

M4 Level set methods for free surfaces.

M5 Inverse Modelling and Optimisation: Optimisation multigrid, SQP multigrid, reduced SQP methods.
As early as 1996, we introduced a new multigrid optimisation scheme for optimisation with pdes. Applying a multigrid method directly to the Kuhn-Tucker system corresponding to the optimisation problem, we were able to derive a SQP-type multigrid method (SQP-MG). In the case of a large parameter space, coarse gridding in parameter space is introduced, too. This new approach generates a family of algorithms and allows teh solution of inverse problems in about 3-5 forward solves. We applied it to various kinds of typical optimisation problems, such as inverse modelling and parameter estimation, geometry and topology optimisation and optimal experiment design. The research was conducted by Volker Schulz, who now has the chair for Scientific Computing at the University of Trier. He is continuing this research there.

M6 Numerical methods for high-dimensional problems: We introduced special dimensional reduction algorithms and sparse grid in order to be able to go beyond $d=3$, the typical limit of standard grid methods. The methods were used in financial mathematics (A3) and in population dynamics (A4).

M7 Integro-differential equations: Panel clustering for population balances (see also A4).

M8 Grid generation: Generating combined hexahedral/tetrahedral grids for domains with thin layers (cf. T7).

M9 Image processing: Non-linear anisotropic filtering, segmentation, reconstruction (cf. A2).

M10 Numeric Geometry and Visualisation: Parallel internet based ray tracing. (cf. A10)

Another important issue is the development of software tools:

T1 Simulation system UG: With the simulation system UG we have created a general platform for the numerical solution of partial differential equations in two and three space dimensions on serial and on parallel computers. UG supports distributed unstructured grids, adaptive grid refinement, derefinement/coarsening, dynamic load balancing, mapping, load migration, robust parallel multigrid methods, various discretisations, parallel I/O, and parallel visualisation of 3D grids and fields. The handling of complex three-dimensional geometries is made possible by geometry and grid generation using special interfaces and integrated CAD preprocessors. This software package has been extensively developed in the last four years and has received two awards in this period: in 1999 at SIAM Parallel Processing, San Antonio, Texas, and the HLRS Golden spike award 2001. Based on this platform, simulation tools for various problems from bioscience, environmental science and CFD are being developed. UG is widely distributed around the world; more than 350 groups use it under license.

T2 d^3f: The simulation tool d^3f allows the computation of density-driven groundwater flow in the presence of strong density variations, e.g. around salt domes. This unique software allows a solution of the full equations in realistic geometries for the first time.

T3 r^3t: In cooperation with the GRS Braunschweig, scientists from the universities of Freiburg and Bonn, and the ETH Zürich, a special software package r^3t based on UG was developed. This novel software tool allows the simulation of the transport and retention of radioactive contaminants (up to 160 radionuclides) in large complex three-dimensional model areas.

T4 VRL is a flexible library for automatic and interactive object visualisation on the Java platform. It provides a visual programming interface including meta programming support and tools for real-time 3D graphic visualisation.

T5 SG: As a counterpart to UG, we developed the library SG (structured grids). It makes use of all structures known in logically rectangular grids. Currently, we use it in image processing and computational finance projects. In the future, we will couple it with UG.

T6 ARTE, TKD_Modeller: We developed two grid generators for the treatment of highly anisotropic structures. ARTE generates tetrahedral meshes including prisms in thin layers, TKD_Modeller generates hexahedral meshes for mainly plane parallel domains.

T7 NeuRA: In co-operation with B. Sakmann (MPI), we developed the “Neuron Reconstruction Algorithm” (NeuRA). It allows the automatic reconstruction of neuron geometries from confocal microscopic data using a specially adjusted blend of non-linear anisotropic filtering, segmentation and reconstruction.

T8 NeuGen: A tool for the generation of large interconnected networks of neurons with detailed structure.

T9 NeuTria: A tool for generating three dimensional surfaces for NeuGen objects.

The research is performed in various projects funded by the state of Baden-Württemberg, the Bundesministerium für Bildung und Forschung (BMBF), the “Deutsche Forschungsgemeinschaft” DFG, such as 1 Cluster of Excellence (Cellnetworks), 2 SFBs and priority research programs, the EC and in co-operation with industry. Most projects bridge several of the topics mentioned above. From 2003 to 2009, we acquired more than 5 Mio. EUR grant money.

As early as 1999, we built up our own Fast Ethernet-based, 80-node Beowulf cluster, each with single Pentium II 400 MHz processors and 512 Mbytes memory. Procedures for installing, maintaining and running the cluster have been developed, based on our specific needs and on a low cost basis. This was the prototype which made the nowadays common development of compute clusters from off-the-shelf components possible. Computations with up to 10^8 unknowns have shown significant efficiencies of around 90% on 2000 CPUs.

Theses

Bachelor Theses

1. Handel, Stefan (2005). SurfaceMerge - Ein Postprozessor für die Geometrie- und Gitterdateien zum Simulationssystem UG.
2. Lenz, Herbert (2008). Weiterentwicklung des Verdichtungsvisualisierungssystems VVS für den Einsatz in der Praxis.
3. Wolf, Sergej (2007). Implementierung eines effizienten Parameter-Vererbungsalgorithmus zur Konfiguration des Softwarepakets NeuGen.

Master Theses

1. Föhner, Michaela (2008). Geometry Visualization & Modification Toolkit (GVMT), ein Werkzeug zur Ein-/Ausgabe und Modifikation von UG-Geometrien und UG-Gittern mit der 3D-Grafiksoftware Blender.
2. Giden, Burcu (2009). Process Evaluation Framework.
3. Handel, Stefan (2007). Simulation des Einlagerungsprozesses in Horizontalsilos.
4. Lücke, Monika (2010). Simulation von Auftriebsströmungen in der polaren Grenzschicht.
5. Mlynczak, Peter (2011). Parallelization concepts for the solution of high-dimensional PDEs with applications in finance.
6. Scherer, Martin (2012). Modellierung des Schwellens von Korneozyten im Stratum Corneum.

Diploma Theses

1. Avcu, Yasar (2009). Parallelisierung von Gitteralgorithmen.
2. Gründl, Christian (2006). Berechnung des ökonomischen Kapitals eines Kreditportfolios mit Hilfe partieller Differentialgleichungen.
3. Heinze, Simon (2009). Numerische Berechnung einer hochdimensionalen parabolischen Gleichung aus der Finanzmathematik.
4. Heumann, Holger (2006). Eine Metrik zur Klassifizierung von Neuronen.
5. Hoffer, Michael (2009). Methoden zur visuellen Programmierung.
6. Jungblut, Daniel (2007). Trägheitsbasiertes Filtern mikroskopischer Messdaten unter Verwendung moderner Grafikhardware.
7. Kleiser, Matthias (2006). Reduktion Finite Volumen diskretisierter Navier-Stokes Gleichungssysteme auf winkelperiodischen Rechengebieten.
8. Kolozis, Elena Gianna (2009). 2D-Modellierung eines synaptischen Spaltes.
9. Lemke, Babett (2008). Merkmale dreidimensionaler Objektwahrnehmung - Eine mathematische Beschreibung.
10. Lux, Hanni (2006). Numerical Simulations of Spherically Symmetric Einstein-Yang-Mills-Systems on a de Sitter Manifold.
11. Muha, Ivo (2008). Coarse Graining auf beliebigen Gitterhierarchien.
12. Nägel, Arne (2005). Filternde Algebraische Mehrgitterverfahren.
13. Otto, Corinna (2009). Modellierung der Befüllungsdynamik präsynaptischer Vesikel in einer GABAergen Synapse.
14. Popovic, Dan (2007). Upscaling für die zeitharmonischen Maxwellschen Gleichungen für magnetische Materialen.
15. Queisser, Gillian (2006). Rekonstruktion und Vermessung der Geometrie von Neuronen-Zellkernen.
16. Reiter, Sebastian (2008). Glatte Randapproximation in hierarchischen Gittern.
17. Rupp, Martin (2009). Berechnung der Resonanzschwingungen einer Gitarrendecke.
18. Schoch, Stefan (2008). Numerical Modeling Studies of Condensed-Phase High Energy Explosives.
19. Schröder, Philipp (2008). Dimensionsreduktion eines hochdimensionalen Diffusionsproblems - Physikalische Prozesse im Finanzbereich.

20. Stichel, Sabine (2008). Numerisches Coarse Graining in UG.
21. Urbahn, Ulrich (2008). Entwicklung eines Ratingverfahrens für Versicherungen.
22. Vogel, Andreas (2008). Ein Finite-Volumen-Verfahren höherer Ordnung mit Anwendung in der Biophysik.
23. Voßen, Christine (2006). Passive Signalleitung in Nervenzellen.
24. Wahner, Ralf (2005). Complex Layered Domain Modeller - Ein 3D Gitter- und Geometriegenerator für das Numeriksimulationssystem UG.
25. Wehner, Christian (2007). Numerische Verfahren für Transportgleichungen unter Verwendung von Level-Set-Verfahren.
26. Wanner, Alexander (2007). Ein effizientes Verfahren zur Berechnung der Potentiale in kortikalen neuronalen Kolumnen.
27. Xylouris, Konstantinos (2008). Signalverarbeitung in Neuronen.

PhD Theses

1. Feuchter, Dirk (2008). Geometrie- und Gittererzeugung für anisotrope Schichtengebiete.
2. Hauser, Andreas (2009). Large Eddy Simulation auf uniform und adaptiv verfeinerten Gittern.
3. Jungblut, Daniel (2010). Rekonstruktion von Oberflächenmorphologien und Merkmalskeletten aus dreidimensionalen Daten unter Verwendung hochparalleler Rechnerarchitekturen.
4. Kicherer, Walter (2007). Objektorientierte Programmierung in der Schule.
5 Lampe, Michael (2006). Parallele Visualisierung – Ein Vergleich.
6. Nägel, Arne (2009). Schnelle Löser für große Gleichungssysteme mit Anwendungen in der Biophysik und den Lebenswissenschaften.
7. Queisser, Gillian (2008). The Influence of the Morphology of Nuclei from Hippocampal Neurons on Signal Processing in Nuclei.
8. Schröder, Philipp (2011). Dimensionsweise Zerlegungen hochdimensionaler Probleme mit Anwendungen im Finanzbereich.

Awards

- 1st price of the doIT-Software-Award, 2005
- Poster award at OEESC 2007

Academic Offers to G-CSC(SiM)/SiT Members

- Wittum, Gabriel, FU Berlin, 2005 (W3)
- Johannsen, Klaus, German University Kairo, 2006 (Full Professorship)
- Johannsen, Klaus, Universitetet i Bergen, 2006
- Wittum, Gabriel, U Paderborn 2006 (W3)
- Wittum, Gabriel, U Laramie 2007 (Distinguished Professorship)
- Wittum, Gabriel, U Frankfurt 2007
- Queisser, Gillian, U Frankfurt 2009
- Reichenberger, Volker, European Business School, Reutlingen, 2010

Selected Co-operations

Many projects have been conducted in co-operation with other colleagues from many different disciplines. The level of collaboration varies, depending on the subject and aim of the project. We received a lot of advice, support, and direct co-operation from colleagues from many different disciplines. Otherwise, this interdisciplinary research would not have been possible. We are grateful to all of these colleagues. A selection of the major partners is given below.

National

S. Attinger (UFZ, Leipzig), H. Bading (Uni Heidelberg), A. Draguhn, (Uni Heidelberg), E.-D. Gilles (MPI Magdeburg), W. Hackbusch (MPI Leipzig), M. Hampe (TU Darmstadt), R. Helmig (Uni Stuttgart), R.H.W. Hoppe (Uni Augsburg, University of Houston), W. Juling, (U Karlsruhe), B. Khoromskij (MPI Leipzig), R. Kornhuber (FU Berlin), D. Kröner (Uni Freiburg), H. Monyer (Uni Heidelberg), C.-D. Munz (Uni Stuttgart), A. Reuter (EML Heidelberg), M. Resch (Uni Stuttgart), W. Rodi (Uni Karlsruhe), H. Ruder (Uni Tübingen), M. Rumpf (Uni Bonn), V. Schulz (Uni Trier), C. Schuster (Uni Heidelberg), D. Thevenin (Uni Magdeburg), Ch. Wieners (Uni Karlsruhe)

International

R. Jeltsch (ETH Zürich), W. Kinzelbach (ETH Zürich), S. Sauter (Uni Zürich), U. Langer (Uni Linz), S. Candel (EC Paris), S. Zaleski (Univ. Paris VI), I. Guinzbourg (Cemagref), P. Wesseling (TU Delft), C. Oosterlee (CWI Amsterdam), A. Buzdin (Uni Kaliningrad), R.E. Bank (UCSD), R. E. Ewing (Texas A&M University), R. Falgout (Lawrence Livermore National Laboratory), T. Hou (CalTech), R. Lazarov (Texas A&M University), A. Schatz (Cornell), H. Simon (NERSC, Berkeley), A. Tompson (Lawrence Livermore National Laboratory), R. Traub (IBM), M. Wheeler (University of Texas at Austin), J. Xu (Penn State)

Industry Co-operations

ABB (Ladenburg), BASF AG (Ludwigshafen), Commerzbank AG (Frankfurt am Main), Deutsche Bank (AG) (Frankfurt a. Main), Dresdner Bank AG (Frankfurt a. Main), Fa. Braun GmbH (Friedrichshafen), Fa. Burgmann (Wolfratshausen), Gesellschaft für Reaktorsicherheit mbH (Braunschweig), Fa. Leica-Microsystems Heidelberg GmbH (Mannheim), Steinbeis-Stiftung für Wirtschaftsförderung (Stuttgart), Roche Diagnostics (Mannheim), AEA (Holzkirchen), IBL (Heidelberg), CETIAT (Orsay), IRL (Christchurch, NZ), Schott (Mainz), Porsche (Stuttgart).

Conferences, Workshops and Seminars

Simulation and Modelling organises several conferences, seminars and workshops each year to promote research and exchange on various topics in Computational Science. In recent years, the following events have been organised.

- Modelling Storage in Deep Layers, 11-13 October 2011
- Modelling Barrier Membranes, Frankfurt, 22-24 February 2011
- Competence in High Performance Computing, Schwetzingen, 22-24 June 2010
- SIAM Conference on Computational Issues in the Geosciences, Leipzig, June 2009
- Detailed Modeling and Simulation of Signaling in Neurons, Frankfurt, May 2009
- International Symposium on Scientific Computing, Leipzig, December 2008
- European Multgrid Conference, Bad Herrenalb, October 2008
- Schnelle Löser für partielle Differentialgleichungen, Oberwolfach, June 2008
- Numerics of Finance, Frankfurt, 5-6 November 2007
- Data Driven Modelling and Simulation in Neurosciences, Hohenwart, 14-17 May 2007

G-CSC Members

Research Group Computational Finance:
Prof. Dr. T. Gerstner, Prof. Dr. P. Kloeden (Head), Prof. Dr.. H. Kraft, Dr. S. Mathew, PD Dr. C. Wagner, Prof. Dr. G. Wittum

Department Simulation and Modelling (together with FB12, Informatik)
Staff: A. Baden, Dr. M. Heisig, B. Lemke, E.-M. Vachek, Prof. Dr. G. Wittum (head).

Postdocs: Dr. P. Frolkovic, Dr. A. Grillo, Dr. M. Heisig, Dr. M. Knodel, Dr. M. Lampe, Dr. D. Logashenko, Dr. A. Nägel.

PhD students: I. Heppner, S. Höllbacher, M. Hoffer, B. Lemke, I. Muha, C. Poliwoda, R. Prohl, S. Reiter, M. Rupp, J. Schneider, P. Schröder, M. Stepniewski, S. Stichel, A. Vogel, C. Wehner, K. Xylouris.

Bachelor/Diploma/Master students: M. Breit, A. Elias, S. Grein, T. Klatt, R. Piperkova, M. Scherer.

Junior Professor: Dr. G. Queisser.

Guest member: PD Dr. C. Wagner.

Former Members: Dr. V. Aizinger, Prof. Dr. P. Bastian, Dr. K. Birken, Ph. Broser, A. Croci, L. G. Dielewicz, Dr. T. Dreyer, Dr. J. Eberhard, S. Eberhard, Dr. T. Fischer, M. Föhner, Dr. A. Fuchs, Dr. J. Geiser, Dr. A. Gordner, C. Gründl, Dr. R. Haag, S. Handel, Dr. S. B. Hazra, A. Heusel, J. Hittler, Dr. W. Hoffmann, Dr. B. Huurdeman, D. Jungblut, Dr. M. Kirkilionis, M. Kleiser, Dr. M. Klingel, Dr. A. Laxander, Y. Liu, H. Lux, Dr. B. Maar, Dr. M. Metzner, Dr. S. Nägele, Dr. S. Paxion, D. Popovic, A. Raichle, Dr. V. Reichenberger, Dr. Chr. Reisinger, S. Reiter, Dr. H. Rentz-Reichert, PD Dr.-Ing. W. Schäfer, Th. Schönit, Prof. Dr. V. Schulz, Dr. N. Simus, D. Singh, U. Stemmermann, Dr. O. Sterz, C. Voßen, R. Wahner, A. Wanner, W. Weiler, Prof. Dr. Chr. Wieners, Chr. Wrobel, L. Zhang, G. Zhou, R. F. Ziegler.

The Interdisciplinary Research Group Computational Finance (CoFi)

Computational finance is a newly developing branch of numerical mathematics and scientific computing, which is concerned with deevlopment, analysis and implementation of computational problems which arise in the banking, finance and insurance industries.

The recent appointment of Prof. Dr. Thomas Gerstner to a professorship in computational finance in the Institute of Mathematics at the Goethe University is a unique event in Germany, indeed the first professorship of its kind in a university in Germany.

The appointment of Prof. Gerstner and the concentration of the banking industry in Frankfurt am Main has motivated the establishment of the “Interdisciplinary Research Group in Computational Finance” in the Goethe Centre of Scientific Computing of the the Goethe University in Frankfurt am Main under the leadership of Prof. Dr. Peter Kloeden. It will bring together researchers from different departments of the university and banks who are active contributors to the field of computational finance.

The group will have close links with the House of Finance on the Goethe University.

A regular Computational Finance Colloquium is planned and will take place in the House of Finance.

Members: Prof. Dr. Thomas Gerstner (Mathematics), Prof. Dr. Peter Kloeden (head, Mathematics), Prof. Dr. Holger Kraft (House of Finance), Dr. Stanley Mathew (Mathematics), PD Dr. Christian Wagner (The Boston Consulting Group, G-CSC), Prof. Dr. Gabriel Wittum (Computer Science, G-CSC)

Projects: CF1: Asset Management in Insurance/CF2: Valuation of Performance Dependent Options/CF3, A3.1: The Numerical Pricing of Options with Many Risk Factors/CF4, A3.2: Credit Risk Estimation/CF5, A3.3: Portfolio Optimisation

A1: Modelling Barrier Membranes

Arne Nägel, Dirk Feuchter, Michael Heisig, Christine Wagner, Gabriel Wittum

The investigation of barrier membranes is important in various fields of engineering and life sciences. For many industrial applications, notably in food packaging, coatings and chemical separations, the study of chemical diffusion and transport of substances is of great significance. Closely linked transport through biological barrier membranes plays a vital role in pharmaceutical research and development. This is true not only for clinical studies where drugs are applied in different epithelia barrier membranes (e.g., intestine, lung, blood-brain barrier, skin) but also for the risk assessment of substances in various exposure scenarios. Until now in-vitro test systems are used to give some information about the in-vivo situation and replace animal experiments. In order to increase capacity, speed, and cost-effectiveness of such studies significantly, in-silico test systems with an adequate predictive power have to be developed. As an archetypical example of a biological barrier membrane we have investigated the diffusion of drugs through skin by numerical simulation.

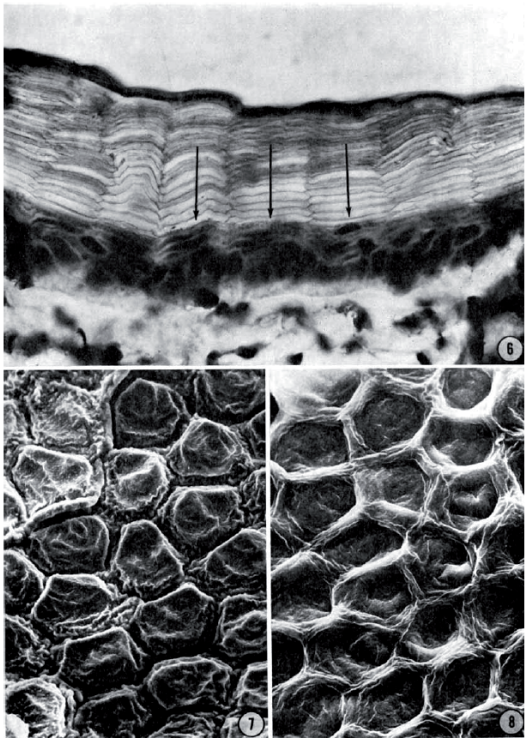

Figure 1. Micrographs of cross-sections of mouse skin (6) and mouse stratum corneum (7,8) (from Menton, 1976)

The barrier function of mammalian skin is primarily located in the outermost epidermal layer, the stratum corneum (SC). This morphological unit consists of dead, flattened, keratinised cells, the corneocytes, which are embedded in a contiguous layer of lipid (Figure 1). Investigations of the stratum corneum are hampered by enormous difficulties regarding equipment and experiments. This is the reason, why the physical properties of this skin layer have hitherto been grasped insufficiently. The numerical simulation of drug diffusion through the stratum corneum contributes to understanding of the permeation process.

In a simulation with high resolution of geometric details, the mathematical challenge first of all comes from the complicated structure. This leads to a large number of degrees of freedom. Secondly the associated bio-physical properties induce discontinuities which makes the use of robust multigrid methods mandatory.

This project began with the development of a two-dimensional model for the diffusion of xenobiotics through the human stratum corneum (Heisig et al. 1996). In this model, we showed that, in addition to the commonly cited lipid multilamellar pathway, intracorneocyte diffusion must exist to match the experimental data. Ten years later this was confirmed experimentally using dual-channel high-speed two-photon fluorescence microscopy (Yu et al. 2003). Since these first steps, the model has been refined in various aspects:

In cooperation with researchers from the Saarland University the development of a virtual skin model has been addressed. In this context the geometry has been extended by an additional compartment for the deeper skin layers (DSL). An illustration is

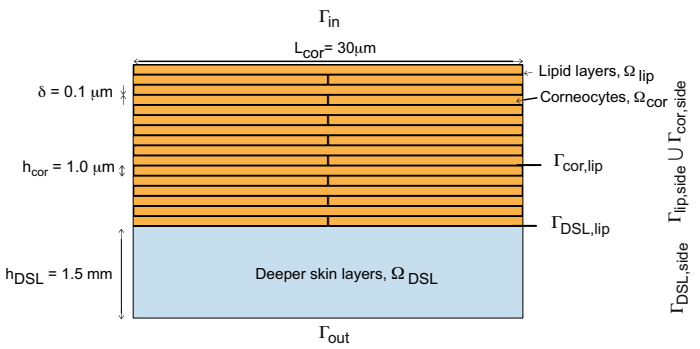

Figure 2. 2D model of the stratum corneum and deeper skin layers (from Naegel et al. 2008)

shown in Figure 2. All phases are modelled with homogeneous diffusivity. Lipid-donor and SC–DSL partition coefficients are determined experimentally, while corneocyte–lipid and DSL–lipid partition coefficients are derived consistently with the model. Together with experimentally determined apparent lipid- and DSL-diffusion coefficients, these data serve as direct input for computational modelling of drug transport through the skin. The apparent corneocyte diffusivity is estimated based on an approximation, which uses the apparent SC- and lipid-diffusion coefficients as well as corneocyte–lipid partition coefficients. The quality of the model is evaluated by a comparison of concentration–SC-depth profiles of the experiment with those of the simulation. For two representative test compounds, flufenamic acid (lipophilic) and caffeine (hydrophilic) good agreements between experiment and simulation are obtained (Hansen et al. 2008; Naegel et al. 2008; Nägel 2009b; Naegel et al. 2011) which is shown for caffeine in Figure 3. Moreover the results provided hints, that additional processes, such as keratine binding, were also important to consider. The role of this particular effect was then studied numerically, before an appropriate experimental design was developed (Hansen et al. 2009).

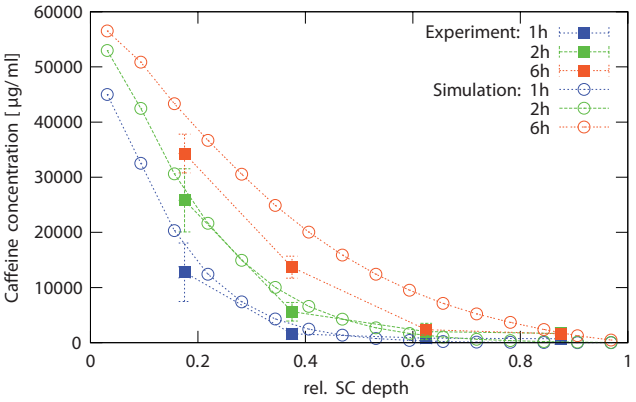

Figure 3. Concentration-depth profile for caffeine (from Naegel et al. 2008)

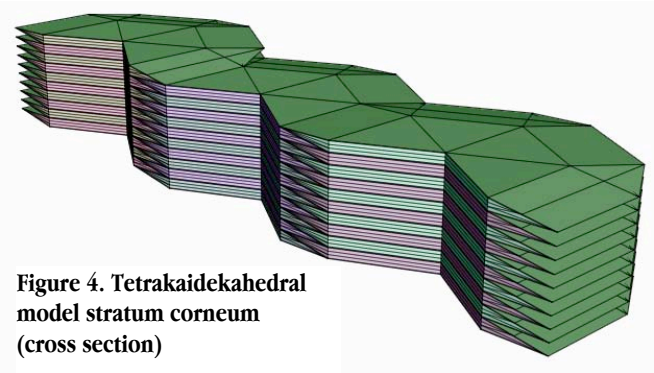

Figure 4. Tetrakaidekahedral model stratum corneum (cross section)

With respect to geometry, several cellular models in both two and three space dimensions are supported now. The most elaborate and most flexible cell model is based on Kelvin's tetrakaidekahedron (TKD). This 14-faced structure features a realistic structure and surface-to-volume ratio and may therefore serve as a general building block for cellular membranes (Feuchter et al. 2006; Feuchter 2008). An example for a stratum corneum membrane consisting of ten cell layers is shown in Figure 4. Simpler models are based, e.g., on cuboids (Wagner 2008). In Figures 5 and 6 time-dependent concentration profiles within tetrakaidekahedral and cuboidal model membranes are shown.

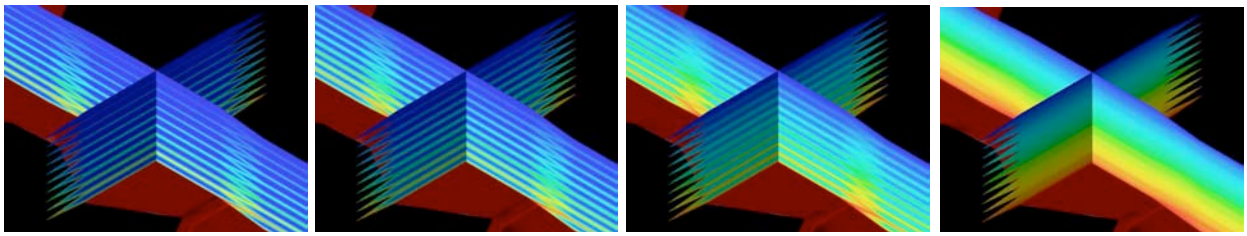

Figure 5. Evolution of concentration in tetrakaidekahedral model stratum corneum (from Nägel et al. 2006).

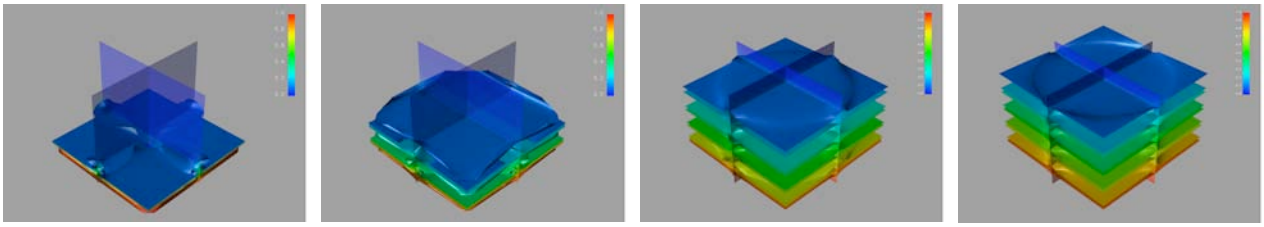

Figure 6. Evolution of concentration in cuboid 3D model (from Wagner 2008)

The barrier property of a membrane is described by two parameters: the permeability and the lag time. Using numerical simulation the influence of the cell geometry on the permeability and lag time of two- and three-dimensional membranes has been studied (Naegel et al. 2009a; Nägel 2009b; Naegel et al. 2011). In Figure 7, the relative permea-

bilities of three different geometries, i.e., ribbon (2D), cuboid (3D) and tetrakaidekahedron (3D) are shown as a function of a normalised corneocyte diffusivity. Similarly, the influence of the horizontal cell overlap is shown in Figure 8. As one can observe for small overlap the TKD model is comparable to the cuboid model, but for increasing overlap it approaches the irrealistic 2D brick-and-mortar model, which has a very good barrier function. Hence it can be seen that in 3D the TKD geometry provides a more efficient barrier than the cuboid geometry. The results confirm that tetrakaidekahedral cells with an almost optimal surface-to-volume ratio provide a barrier membrane, in which a minimal amount of mass is used in a very efficient manner.

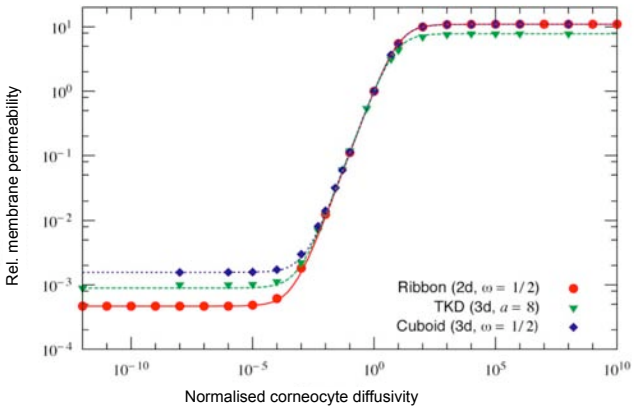

Figure 7. Relative membrane permeability for ribbon, TKD and cuboid model membranes as a function of normalised corneocyte diffusivity (from Naegel et al. 2009a)

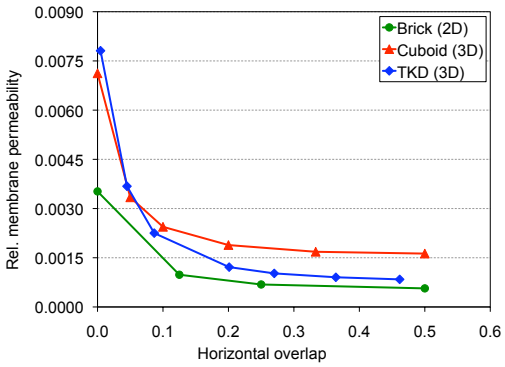

Figure 8. Relative membrane permeability depending on the overlap for different model geometries (from Muha et al. 2011)

The results are also closely linked to homogenisation theory (Muha et al. 2011).

In transdermal therapeutic systems (TTS), substances are often presented to skin in small volumes of solution per area of exposure and various exposure times. In these situations, the amount of skin absorption will be less than would be calculated using a model for infinite dose exposures. Therefore, an extended model is needed to account for the limited capacity of the small vehicle volume and limited exposure time to apply drugs to the skin. This has been accomplished with a non-steady-state model of skin penetration under finite dose conditions (Naegel et al. 2012b; Naegel et al. 2012c; Selzer et al. 2012).

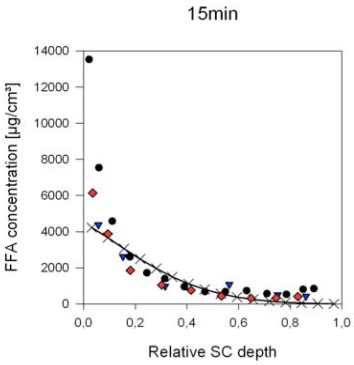

Figure 9. Flufenamic acid (FFA) concentration-SC-depth profile for t = 15 min (from Naegel et al. 2012b)

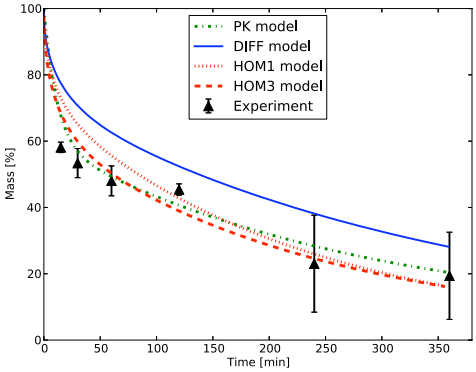

Figure 10. Flufenamic acid mass profiles over time of the vehicle compartment (from Selzer et al. 2012)

Finite dose skin penetration concentration-SC-depth profiles for flufenamic acid and caffeine have been determined. As shown in Figure 9, good agreements between experiment and simulation are obtained (Naegel et al. 2012b). A pharmacokinetic model (PK) and two different diffusion models (DIFF, HOM) have been compared which allow to compute the mass profiles over time in the vehicle, SC, DSL, acceptor and lateral compartment. As it is shown in Figure 10 for the FFA vehicle compartment, the simulations reproduce the experimental results (Selzer et al. 2012).

All methods and tools for this research are implemented as a module within the UG framework. The mechanisms include, e.g., adsorption, metabolic activity and co-permeation of substances (Naegel et al. 2012a). For skin penetration

experiments, both finite and infinite dose formulations are supported. By continuing research and extending the existing models, we expect that, once again, computer simulation is going to play a key role in understanding, which factors determine the behaviour of biological and artificially designed membranes.

References

Feuchter, D., Heisig, M., & Wittum, G. (2006). A geometry model for the simulation of drug diffusion through stratum corneum. Computing and Visualization in Science, 9(2), 117-130.

Feuchter, D. (2008). Geometrie- und Gittererzeugung für anisotrope Schichtengebiete. PhD thesis, University of Heidelberg.

Hansen, S., Henning, A., Naegel, A., Heisig, M., Wittum, G., Neumann, D., Kostka, K., Zbytovska, J., Lehr, C. M., & Schaefer, U. F. (2008). In-silico model of skin penetration based on experimentally determined input parameters. European Journal of Pharmaceutics and Biopharmaceutics, 68(2), 352–367.

Hansen, S., Naegel, A., Heisig, M., Wittum, G., Neumann, D., Kostka, K., Meiers, P., Lehr, C. M., & Schaefer, U. F. (2009). The Role of Corneocytes in Skin Transport Revised - A Combined Computational and Experimental Approach. Pharmaceutical Research, 26, 1379-1397.

Heisig, M., Lieckfeldt, R., Wittum, G., Mazurkevich G., & Lee, G. (1996). Non steady-state descriptions of drug permeation through stratum corneum. I: the biphasic, brick and mortar model. Pharmaceutical Research, 13, 421-426.

Menton, D. N. (1976). A minimum-surface mechanism to account for the organization of cells into columns in the mammalian epidermis. American Journal of Anatomy, 145, 1-22.

Muha, I., Naegel, A., Stichel, S., Grillo, A., Heisig, M., & Wittum, G. (2011). Effective diffusivity in membranes with tetrakaidekahedral cells and implications for the permeability of human stratum corneum. Journal of Membrane Science, 368(1-2), 18-25.

Nägel, A., Feuchter, D., Hansen S., Henning, A., Neumann, D., Lehr, C. M., Schäfer, U. F., Wittum, G., & Heisig, M. (2006). Modelling drug diffusion through stratum corneum using in silico techniques. 10th International Conference on Perspectives in Percutaneous Penetration, April 18-22, La Grande-Motte, France.

Naegel, A., Hansen, S., Neumann, D., Lehr, C., Schaefer, U. F., Wittum, G., & Heisig, M. (2008). In-silico model of skin penetration based on experimentally determined input parameters. Part II: Mathematical modelling of in-vitro diffusion experiments. Identification of critical input parameters. Eur. Journal of Pharmaceutics and Biopharmaceutics, 68, 368-379.

Naegel, A., Heisig, M., & Wittum, G. (2009a). A comparison of two- and three-dimensional models for the simulation of the permeability of human stratum corneum. European Journal of Pharmaceutics and Biopharmaceutics, 72, 332-338.

Nägel, A. (2009b). Schnelle Löser für große Gleichungssysteme mit Anwendungen in der Biophysik und den Lebenswissenschaften. PhD thesis, University of Heidelberg.

Naegel, A., Heisig, M., & Wittum, G. (2011). Computational modeling of the skin barrier. Methods Molecular Biology 763, 1-32.

Naegel, A., Heisig, M., & Wittum, G. (2012a, in press). Detailed modeling of skin penetration - an overview. Adv Drug Deliv Rev.

Naegel A., Hahn T., Lehr C.-M., Schaefer U.F., Heisig M., & Wittum G. (2012b). Finite dose skin penetration: Concentration depth profiles - Comparison between experiment and simulation. Manuscript submitted for publication.

Naegel A., Heisig, M., Wittum, G., K.H. Schaller, H. Drexler, & Korinth, G. (2012c). Prospective evaluation of a sophisticated predictive mathematical model to simulate the percutaneous penetration of caffeine. Manuscript submitted for publ.

Selzer D., T. Hahn T., Naegel A., Heisig M., Neumann D., Kostka K.H., Lehr C.M., Schaefer U.F., & Wittum G. (2012). Finite dose skin mass balance including the lateral part - Comparison between experiment, pharmacokinetic modeling, and diffusion models. Manuscript submitted for publication.

Wagner, C. (2008). Dreidimensionale digitale Rekonstruktion des humanen Stratum corneum der Haut in Kombination mit Simulation substantieller Diffusion durch das Stratum corneum. PhD thesis, Tierärztliche Hochschule Hannover.

Yu, B., Kim, K. H., So, P. T., Blankschtein, D., & Langer, R. (2003). Visualization of oleic acid-induced transdermal diffusion pathways using two-photon fluorescence microscopy. Journal of Investigative Dermatology, 120(3), 448-455.

A2.1, M8, T6: NeuRA: The Neuron Reconstruction Algorithm

Philip Broser, Alexander Heusel, Daniel Jungblut, Gillian Queisser, Sebastian Reiter, Roland Schulte, Christine Voßen, Gabriel Wittum

In recent years, novel microscopy methods have been developed allowing for a never imagined precision in detection of microstructure of the brain. Confocal and multi-photon microscopy have become a principal technique for high-resolution fluorescence imaging in biological tissues because it provides intrinsic optical sectioning and exceptional depth penetration. Thus, 3D fluorescence images of neurons including their entire dendritic morphology can be obtained within their native environment. To use this new knowledge in modeling, novel algorithms for extracting morphology information are necessary.

Automatic reconstruction allows the fast, high-throughput determination of characteristic anatomical features, for instance the dendritic branching pattern of neuronal cells, unlike standard manual reconstruction techniques, which are time-consuming and highly dependent on the experience of the anatomist. In vitro methods also suffer from scaling problems due to shrinkage in fixed tissue. Automatic reconstruction will help to establish large databases of neuronal morphologies for modelling of cellular and network signal processing.

In order to address this issue, we designed a software tool NeuRA, which allows the automatic reconstruction of neuronal morphology (Broser et al. 2004, Queisser et al. 2008). To accomplish the task of automatic reconstruction, NeuRA provides the four main components:

1. Inertia based filter for the native image data
2. Segmentation of the data
3. Reconstruction of the branching pattern
4. Export of the data in common file format.

In practice, the signal-to-noise ratio in such data can be low, especially when dendrites in deeper layers of the cortex are imaged in vivo. Typically, discontinuities in the fluorescence signal from thin dendrites are encountered, as well as a noisy fluorescence background not originating from the labelled neuron, and the combination of these difficulties strongly requires a suitable pre-processing of the data before reconstruction.

To address the problem of noise, we use a novel inertia-based filter for 3D volume data which enhances the signal-to-noise ratio while conserving the original dimensions of the structural elements and closing gaps in the structure (Broser et al 2004, Queisser et al. 2008). The key idea is to use structural information in the original image data - the local moments of inertia - to control the strength and direction of diffusion filtering locally. In the case of a dendrite, which can be locally approximated as a one-dimensional tube, diffusion filtering is effectively applied only parallel to the axis of the tube, but not perpendicular to it. Thus, noise is averaged out along the local axis of the dendrite, but dendritic diameters are not affected.

The second release of NeuRA, *NeuRA 2,* supports multiple GPUs. Since 2-photon and confocal microscopy significantly improved within the last years, three dimensional microscope images of neuron cells with a resolution of 2048x2048x400 are available now. To process these large data, NeuRA 2 uses the massively parallel architecture of state-of-the-art graphic processing units (GPUs) and is able to distribute the data among multiple GPUs at single computers or computer clusters, allowing to process images of a size of up to several GBytes in a few minutes. To accomplish the four substeps above, in NeuRA 2 additional algorithms have been incorporated to give the user more possiblities. In particular, a multi-scale enhancement filter has been implemented.

The object-oriented software design of NeuRA 2 strictly encapsulates data access, data processing and workflow control, allowing the fast processing of large images as well as the easy extension with other image processing operators. NeuRA 2 automatically checks the available GPUs and divides the input image in suitable overlapping sub-images of a size suited for the single GPUs. Linear interpolation in the overlap regions, when reassembling the single subimages, guarantee continuous output images. The NeuRA 2 user interface allows a comfortable reconstruction of the data, including a preview mode to adapt the parameters of the image processing operators on the fly.

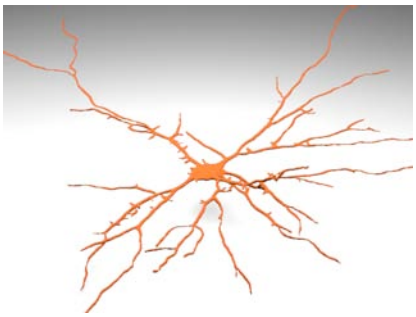

Figure 1. Reconstruction of a neuron cell (data from Jakob v. Engelhardt, Hannah Monyer)

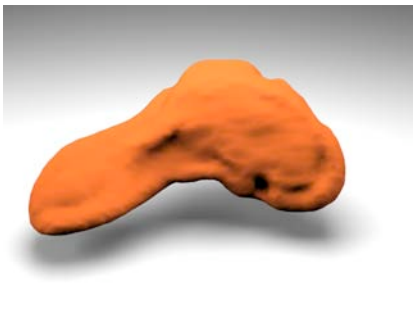

Figure 2. Presynaptic bouton Figure (data from Daniel Bucher, Christoph Schuster)

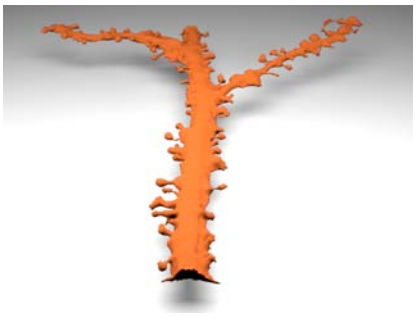

Figure 3. Dendrite segment with spines (data from Andreas Vlachos, Thomas Deller)

Using general noice reduction and segmentation methods rather than model-based techniques, NeuRA 2 is not limited to reconstruct neuron cells (Figure 1). It can also be used to generate surface meshes from archaeological (Figure 5; Jungblut et al. 2009b) or medical computer tomography images (Figure 6), as well as nuclei (Queisser et al. 2008) or other neurobiological microscopy images, like presynaptic boutons (Figure 2) or dendrite segments with spines (Figure 3).

Figure 5. Reconstruction of a ceramic vase

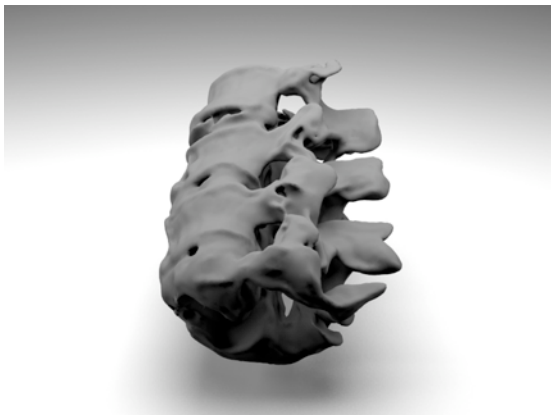

Figure 6. Reconstruction of a cervical spine

References

Broser, P. J., Schulte, R., Roth, A., Helmchen, F., Waters, J., Lang, S., Sakmann, B., & Wittum, G. (2004). Nonlinear anisotropic diffusion filtering of three-dimensional image data from 2-photon microscopy. Journal of Biomedical Optics, 9(6), 1253–1264.

Jungblut, D., Queisser, G., & Wittum, G. (2012). Inertia Based Filtering of High Resolution Images Using a GPU Cluster. Computing and Visualization in Science, 14(4), 181-186.

Jungblut, D., Karl, S., Mara, H., Krömker, S., & Wittum, G. (2009). Automated GPU-based Surface Morphology Reconstruction of Volume Data for Archeology. SCCH 2009.

Queisser, G., Bading, H., Wittmann, M., & Wittum, G. (2008). Filtering, reconstruction, and measurement of the geometry of nuclei from hippocampal neurons based on confocal microscopy data. Journal of Biomedical Optics, 13(1), 014009.

A2.2: Modelling the Nuclear Calcium Code

Gillian Queisser, Gabriel Wittum

Calcium regulates virtually all cellular responses in the mammalian brain. Many biochemical processes in the cell involved in learning, memory formation as well as cell survival and death, are regulated by calcium (Bading 2000, Milner 1998, West 2002). Especially when investigating neurodegenerative deseases like Alzheimer‘s or Parkinson‘s disease the calcium code plays a central role. Signalling from synapses to nucleus through calcium waves and the subsequent relay of information to the nucleus that activates transcriptional events was of special interest in a project together with the Bading lab at the IZN in Heidelberg.

Electron microscopy studies in hippocampal rat tissue carried out at the lab revealed novel features of the nuclear membrane morphology (Wittmann et al., 2009). While current text book depictions show the nucleus to have a spherical form, these electron micrographs showed infolded membrane formations of both nuclear membranes (Figure 1, left).

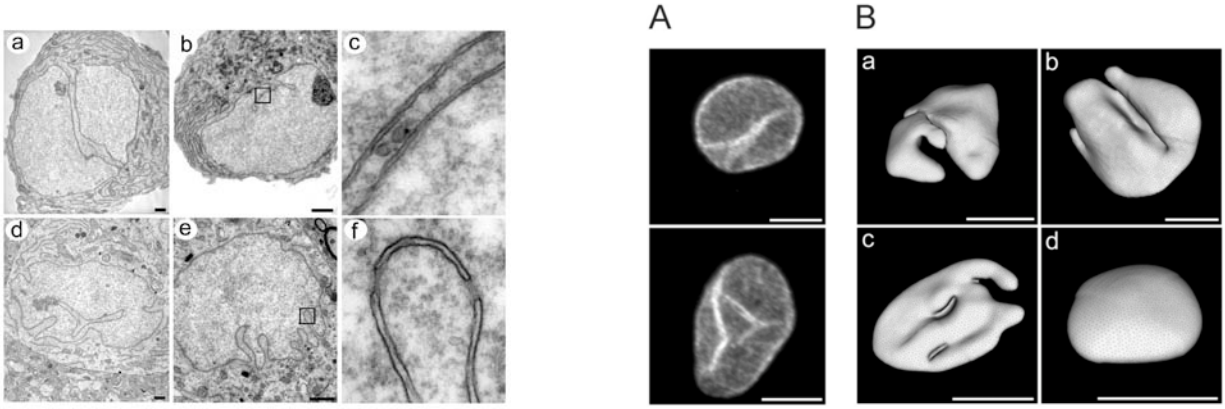

Figure 1. Left: Electron microscopy slices through various hippocampal nuclei (a,b,d,e). The micrographs show infolded envelope formations of both nuclear membranes (c). As seen in f, the infoldings contain nuclear pore complexes as entry points for cytosolic calcium. Right: Confocal slices of two different nuclei (A). This data is used to reconstruct nuclei in 3-d (B). The 3-d reconstructions show the formations of nuclei ranging from highly infolded to nearly spherical.

To assess the realistic morphologies of hippocampal nuclei and to investigate the influence of the diverse structures on nuclear calcium signalling, we used NeuRA (Queisser et al. 2008) to reconstruct the nuclear membrane surface from confocal microscopy recordings (Figure 1, right). As a first result one could ascertain, that the hippocampal area contains a large quantity of highly infolded nuclei, where the nuclear envelope divides nuclei into microdomains. Furthermore, measuring surface and volume of infolded and spherical nuclei showed that all nuclei are nearly equal in their volume but infolded nuclei have an approx. 20% larger surface than spherical ones (Wittmann et al., 2009). This surface increase is proportional to the increase in nuclear pore complexes (NPCs) on the membrane through which cytosol can freely diffuse into the nucleus. This observation, and the visible compartimentalisation of nuclei led us to investigate the morphological effect on nuclear calcium signalling.

Therefore we developed a mathematical model describing calcium diffusion in the nucleus, calcium entry through NPCs including the realistic 3-d morphology. The discrete representation of the PDE-based biophysical model is solved using the simulation platform *ug*. Information stored in calcium signals is mainly coded in amplitude and frequency. We therefore investigated these parameters w. r. t. various nuclear morphologies. Figure 2 shows the differences in calcium amplitude within single nuclei, w. r. t. compartment size. Due to changes in the number of NPCs and differences in diffusion distances, small compartments elicit higher calcium amplitudes than large compartments. This can have a substantial impact on the biochemical events downstream of calcium and therefore affect gene transcription in the cell. Furthermore, infolded nuclei show visible differences in resolving high frequency calcium signals compared to spherical nuclei and large compartments respectively.

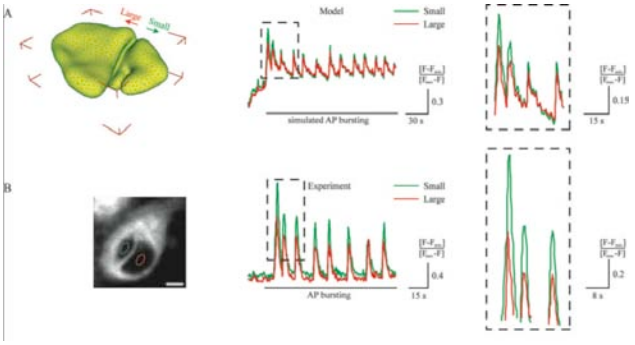

Figure 2. Measuring the calcium signal in two unequal nuclear compartments shows, that smaller compartments elicit higher calcium amplitudes in model simulations (top) and experimental calcium imaging (bottom). This shift in amplitude can have effects on biochemical, transcription related processes.

Figure 3 shows that given a 5 Hz stimulus to the cell, small compartments are more adept at resolving this frequency than large compartments. We therefore ascertain, that hippocampal neurons fall into categories of "frequency resolvers" and "frequency integrators" (see ExtraView Queisser et al. for more detail). The effects of nuclear morphology on amplitude and frequency seen in simulations, were then verified in experimental settings (see Figures 3 & 4). In an attempt to evaluate the effect of these changes in the nuclear calcium on events closely related to transcription, the phosphorylation degree of the protein histone h3, involved in gene transcription and chromosomal reorganisation, was related to the degree of nuclear infolding. As a result, experiments show, that with increasing degree of nuclear infolding the degree of histone h3 phosphorylation increases as well (see Figure 4). We could therefore show a novel feature of nuclear calcium signalling. The structures of hippocampal nuclei are highly dynamic and show nuclear plasticity upon recurrent cellular activity. The capability of a neuron to adapt its organelle's morphology adds an extra layer of complexity to subcellular information processing, and could therefore be necessary in higher brain function.

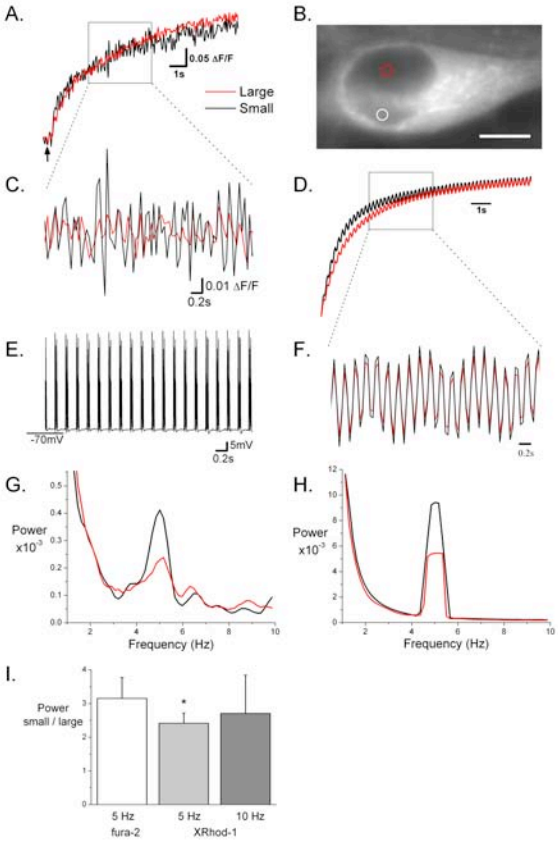

Figure 3. Stimulating an infolded nucleus (A, E, D) with unequal sized compartments (B) shows, that smaller compartments are more adept at resolving the high-frequency signal (C, F). Both power plots in experiment (G, I) and model (H) show a stronger 5 Hz resolution in the small compartment.

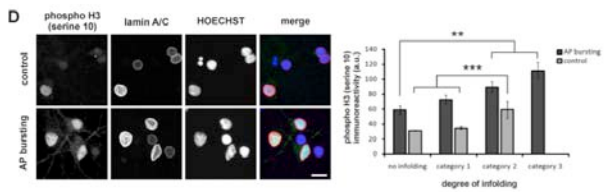

Figure 4. Measurements of histone H3 phosphorylation in respect to degree of nuclear infolding (ranging from weakly to strongly infolded). Phosphorylation degree increases proportionally with the degree of infolding.

Remark: All images are taken from Wittmann et al. 2009

References

Queisser, G., Wiegert S., & Bading H. (2011). Structural dynamics of the nucleus: Basis for Morphology Modulation of Nuclear Calcium Signaling and Gene Transcription. Nucleus, 2(2), 98-104.

Queisser, G., Wittmann, M., Bading, H., & Wittum, G. (2008). Filtering, reconstruction and measurement of the geometry of nuclei from hippocampal neurons based on confocal microscopy data. Journal of Biomedical Optics, 13(1), 014009.

Wittmann, M., Queisser, G., Eder, A., Bengtson, C. P., Hellwig, A., Wiegert, J. S., Wittum, G., & Bading, H. (2009). Synaptic activity induces dramatic changes in the geometry of the cell nucleus: interplay between nuclear structure, histone H3 phosphorylation and nuclear calcium signaling. The Journal of Neuroscience, 29(47), 14687-14700.

A2.3: Electric Signalling in Neurons

Konstantinos Xylouris, Gabriel Wittum

The brain is a unique human organ which concentrates all information humans receive from their surroundings. All perceptions and sensations as well as consciousness are somehow connected with the function of this organ and considering the tremendous inputs it receives, processes and from which it is able to form new thoughts it must be extremely dynamical in its work. To put it simply, the brain provides a representation of our outer world while paralle facilitating the evaluation and formation of the information perceived.

Although science is far away to understand the brain's role in consciousness and behavior, it is clear that the brain is a huge network of small entities called neurons, whose activity somehow determines the way it works. Indeed these pieces are basically units being either on or off.

Roughly speaking, physiologically the neurons' membrane consists of a bi-lipid layer separating the intracellular space from the extracellular one. These spaces are filled with ionic liquids which are exchanged through the membrane according to its properties. This is why, a potential difference is created accross the membrane balancing the effecting electrochemical forces and whose value tells whether the neuron is active or not.

In this project, starting with Maxwell's equations, the aim is to form a set of equations which describe the neurons signal processing as a function of its three-dimensional geometry, its membrane properties and the involved intracellular and extracellular potentials. As a simplification, it is assumed that the variation of the magnetic field is negligible as well as that the intra- and extracellular spaces are purely resistive, i.e. there are no free charges. Then according to Faraday's law, the electric field becomes rotation free, and thus is describable by the negative gradient of an electric potential (Figure 1).

On the other hand, according to Gauß' Law the intracellular and extracellular potential must spread in harmony to Laplace's equation (Figure 1) since there are no free charges. Taking now into consideration, the continuity equation of electric charges, you obtain the adequate Neumann-boundary-conditions for the Laplace problems while making use that there is a flux accross the membrane and that the electric fluxes in the spaces follow the Ohmic Law(Figure 1).

$$
\begin{aligned}
rot\ \vec{E} = -\frac{d\vec{B}}{dt} &= 0 \quad \text{(Faraday's Law)} \\
\Rightarrow \vec{E} &= -\nabla\Phi \\
div\ \vec{E} = \frac{\rho}{\epsilon_0} &= 0 \quad \text{(Gauß' Law)} \\
\Rightarrow -div\nabla\Phi = -\Delta\Phi &= 0 \\
div\ \vec{j} + \epsilon_0\frac{d\rho}{dt} = div\ \vec{j} &= 0 \quad \text{(continuity equation)} \\
div\ \vec{j} = -div(\sigma\nabla\Phi) + div(\delta_{membrane}(x)j_{HH}) &= 0 \ \text{(Ohmic Law)} \\
\Rightarrow -div(\sigma_{in,out}\nabla\Phi_{in,out}) &= 0 \quad \text{in } \Omega_{in,out} \\
-\sigma_{in,out}\nabla\Phi_{in,out}\cdot n_{in\to out} &= j_{HH} \quad \text{on } \Gamma
\end{aligned}
$$

Figure 1. Derivation of the three-dimensional cable equation

In order to solve the arising system of partial differential equation, in which the membrane potential, the intracellular potential and the extracellular potential is involved, we make use of a trick and reduce the system in finding two of these quantities.

The membrane potential is defined as difference between the intracellualar and extracellular potential. For the sake of obtaining a space equation for the membrane potential, the extraclelular potential is extended to the intracellular space obaying the problem in Figure 2. This problem is in a sense a natural extension since then the membrane potential also obeys a Laplace equation and since the extracellular potential becomes continuous over the whole domain.

$$-\sigma_{in}\Delta\Phi_{out}^{IN} = 0 \quad \text{in } \Omega_{in}$$
$$\Phi_{out}^{IN} = \Phi_{out} \quad \text{on } \Gamma$$

Figure 2. Problem defining the extension for the extracelluar potential to the intracellular space

Therefore, the problem for the membrane potential becomes as shown in Figure 3.

$$-\sigma_{in}\Delta V_m = 0 \quad \text{in } \Omega_{in}$$
$$-\sigma_{in}V_m \cdot n_{in\to out} = j_{HH}(V_m) + \sigma_{in}\nabla\Phi_{out}^{IN} \cdot n_{in\to out} \quad \text{on } \Gamma$$

Figure 3. Membrane potential problem

With the aid of these equations, now one can adequately compute the signal's propagation on a three dimensional membrane (Figure 5). Furthermore, you receive the characteristic current dipole behavior of the neuron (Figure 4).

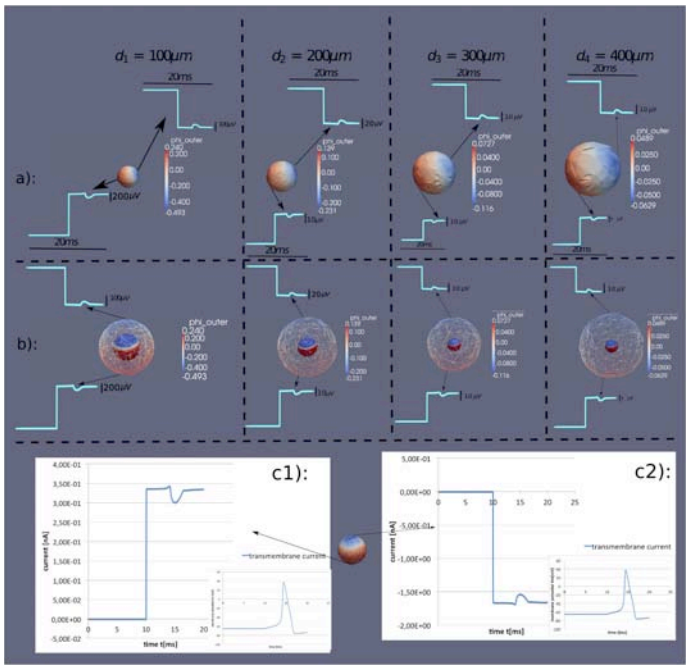

Figure 4. Current dipole behavior

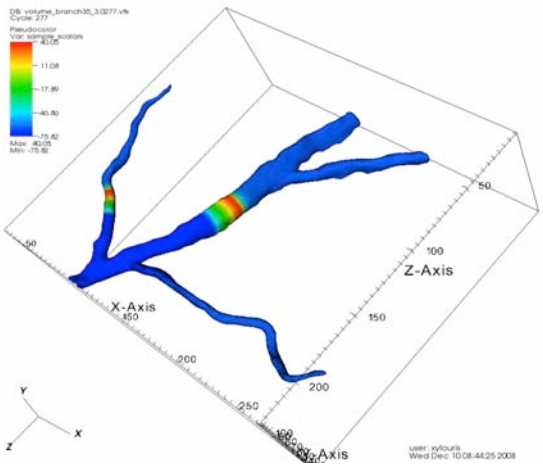

Figure 5. Propagation on a 3D neuron

References

Gold, C., Henze, D. A., Koch, C., & Buzaki, G. (2006). On the Origin of the Extracellular Action Potential Waveform: A Modeling Study. Journal of Neurophysiology, 95, 3113-3128.

Voßen C., Eberhard J., & Wittum G. (2007). Modeling and simulation for three-dimensional signal propagation in passive dendrites. Computing and Visualization in Science, 10(2), 107-121.

Xylouris, K., Queisser G., & Wittum G.(2010). A Three-Dimensional Mathematical Model of Active Signal Processing in Axons. Computing and Visualization in Science, 13(8), 409-418.

Xylouris, K (2012). Generalized cable equation for signal processing in neurons. PHD thesis.

A2.4: Modelling Replication Dynamics of Hepatitis C Virus in 3D Space

Markus Knodel, Alfio Grillo, Paul Targett-Adams, Eva Herrmann, Gabriel Wittum

Hepatitis C virus is the major cause of nowadays liver diseases in western countries. The Heptatitis C virus (HCV) infection is caused by blood-to-blood contacts to infected persons. HCV causes in nearly all cases a chronic liver infection. Within several years, many patients develop liver chirrhosis and even liver cancer. Therefore, many of them need liver transplantation or die, in each case their life quality is reduced strongly. There exist several genotypes of HCV, for some of them medical treatments could be developed (combined Interferon and Ribivarin therapy) which help a significant part of the patients, however for several genotypes there is no treatment available up to now. In particular, there is no vaccinatiojn available and this could hold on for many years still. Recently, there was progress with respect to the development of new antiviral drugs which block viral processing in parts, but nevertheless there is only few progress in understanding the complete replication dynamics and the experimental possibilities are rather restricted due to the lack of small animal model systems, i.e. the virus only replicates in high developed primates and only up to some extend in cell cultures. Even though there exist some mathematical models which allowed for understanding of some basic relations, no one of these take into account the spatial structure of the liver cells in which the virus gets replicated. Therefore, our aim is to apply our instrument of in silico 3D simulation techniques to this field in order to allow for new insights with respect to viral replication fror the sake of modeling in detail the effects of new antiviral agents allowing for more effective strategies with respect to the development of new antiviral agents.

HCV is an enveloped, positive stranded RNA virus and belongs to the family of Flaviviridiae, to which also belong e.g. yellow and Dengue fever. Once it fuses with the membrane of a hepatocyte (liver cell), it gets endocytosed. Inside the cytosol, the RNA gets uncoated and gets translocated to the rough Endoplasmatic Reticulum (rough ER / rER). There, it fuses with ribosomes and this causes the translation of a big number of the viral polyprotein. The polyprotein gets cleaved in parts by cellular proteases and in other parts by viral proteases. There are as well structural and nonstructural proteins. At first, the structrural proteins are cleaved by cellular proteases. The structural proteins will later enclose the new viral RNA (which will be produced in forthcoming steps by replication of the existing one). In particular, the core protein C will have to enclose the RNA and the envelope proteins E1 and E2 will bind to the surface in order to enable the entry to other cells once the new viral particle will have been freed by the actual cell. However before being able to do so, first the nonstructural proteins have to cause the reproduction of the existing RNA. This gets done in the following way: After when the structural proteins are cleaved by cellular proteases from the polyprotein (and a small protein called p7 of which the function is not clear so far'), the rest of the polyprotein cleaves independently of cellular processes. In particular, at first the nonstructural protein NS2 cleaves autocatalytically. Then the combination of the NS3 and NS4a (NS3/4a protease) frees the RNA polymerase NS5b, the multifunctional NS5a (which is especially related to the suppression of the cellular immune response) and the NS4b. Finally also NS3 and NS4a are seperated. The NS4b protein causes on top of the membrane of the ER the growing of regions of the so-called membranous web, which is the accumulation of many small vesicles. Soon there exist several regions on the surface of the ER where this vesicular places are located, the bigger of these regions are more or less spatially fixed whereas the smaller ones are "jumping" around presumably randomly. Once these web regions exist, the RNA polymerase NS5b proteins get translocated into them. For not understood reasons, at some step the so far only existing (old) viral RNA translocates into one of these web regions causing its own reproduction by the NS5b polymerase. At intermediate steps, negative stranded RNA gets produced and combines with the plus-stranded one to double stranded RNA (dsRNA) allowing for producing new plus-stranded RNA. In parts the new RNA will translocate again to ribosomes causing the production of new polyproteins, others will go to other web

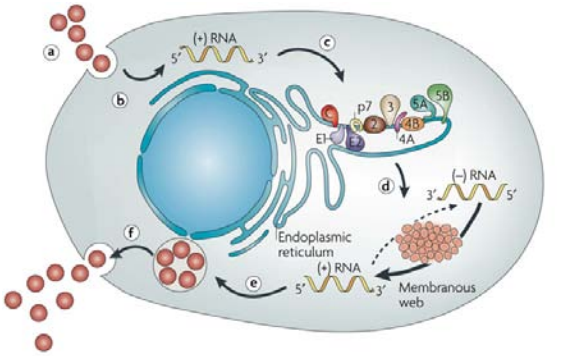

Figure 1. The Hepatitis C life cycle: Uncoating and translation of the RNA, cleavage of the polyprotein, creation of the membranous web, reproduction of the RNA and assembly and exocytosis of new viruses

regions causing production of additional RNAs. Thus the circle of RNA reproduction gets cloesd. At some step, core proteins accumulates at the surfaces of so-called lipid droplets, forming hulls, and into this hull, RNA will get incorporated. The E1 and E2 proteins will fuse with the surface, and in some not understood way new complete viruses will leave the cell on the usual secretory pathway within vesicles passing in particular also the Golgi apperatus. The mature viruses will get exocytosed finally at the surface of the cell. The aim of antiviral agants is to block one or several of the reproduction steps.

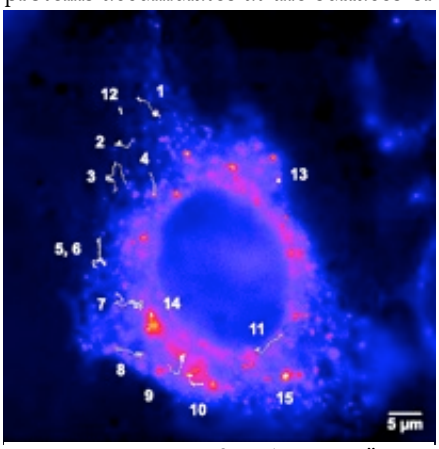

Figure 2. Regions of replication ("membranous web") at the ER

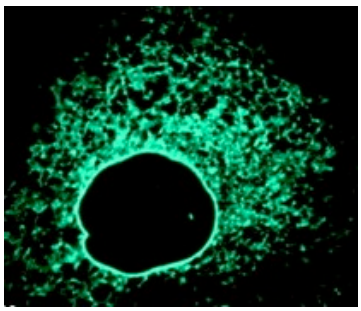

Figure 3. Confocal flouroscence microscopy image of calnexin, an ER marker

We are creating a biophysical model of the replication of the virus within the complete spatio-temporal domain of single hepatocytes. Therefore we are reconstructing the geometry of the ER of hepatocyte confocal flouroscence microscopy image z-stack data (using NeuRA2) corresponding to calnexin marker which localizes on the surface of the ER. On top of this geometry we will do simulations of the dynamics of the viral proteins and RNA (using UG) allowing for precise predictions with respect to the effects of antiviral agents hence allowing for more effective pharmaceutical development.

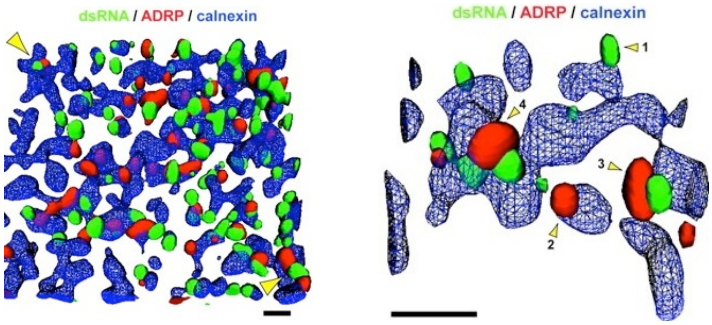

Figure 4a and b. 3D reconstructions of the ER (marked by calnexin), the double stranded viral RNA and the lipid droplets (marked by ADRP). Actually redone using NeuRA

References

Dahari, H., Ribeiro, R. M., Rice, C. M., & Perelson, A. S. (2007). Mathematical Modeling of Subgenomic Hepatitis C Virus Replication in Huh-7 Cells. Journal of Virology, 81(2), 750-760.

Kwong, A. D., Kauffman, R. S., Hurter, P., & Mueller, P. (2011). Discovery and development of telaprevir: an NS3-4A protease inhibitor for treating genotype 1 chronic hepatitis C virus. Nature Biotechnology, 29, 993–1003.

Moradpour, D., Penin, F., & Rice, C. M. (2007). Replication of hepatitis C virus. Nature Reviews Microbiology, 5, 453–463.

Targett-Adams, P., Boulant, S., & McLauchlan, J. (2008). Visualization of Double-Stranded RNA in Cells Supporting Hepatitis C Virus RNA Replication. Journal of Virology, 82(5), 2182-2195.

Targett-Adams, P., Graham, E. J. S., Middleton, J., Palmer, A., Shaw, S. M., Lavender, H., Brain, P., Tran, T. D., Jones, L. H., Wakenhut, F., Stammen, B., Pryde, D., Pickford, C., & Westby, M. (2011). Small Molecules Targeting Hepatitis C Virus-Encoded NS5A Cause Subcellular Redistribution of Their Target: Insights into Compound Modes of Action. Journal of Virology, 85(13), 6353-6368.

Wölk, B., Büchele, B., Moradpour, D., & Rice, C. M. (2008). A Dynamic View of Hepatitis C Virus Replication Complexes. Journal of Virology, 82(21), 10519-10531.

A2.5: NeuClass: Neuron Classification Tools

Holger Heumann, Gabriel Wittum

In the age of technological leaps in the neuroscientific world, a multitude of research areas, computational tools, mathematical models and data-aquiring methods have emerged and are rapidly increasing. Not only is data mass exploding, but also different data types and research approaches account for large diversification of data and tools. At the G-CSC ongoing research of an interdisciplinary nature brought about the need for organised and automatic data & tool structuring. Furthermore, we see a central data & tools management as an optimal means for scientific knowledge exchange, especially in decentralised research projects.

In addition to the automatic reconstruction of neuron morphologies by *NeuRA*, a new tool has been developed for the automatic classification of cells, *NeuClass*. This is a typical entry point of data into the database. Thus we developed a new approach for the classification of neuron cells.

The shape of neuronal cells strongly resembles botanical trees or roots of plants. To analyse and compare these complex three-dimensional structures it is important to develop suitable methods. In (Heumann and Wittum 2009) we review the so called tree-edit-distance known from theoretical computer science and use this distance to define dissimilarity measures for neuronal cells. This measure intrinsically respects the tree-shape. It compares only those parts of two dendritic trees that have similar position in the whole tree. Therefore it can be interpreted as a generalisation of methods using vector valued measures. Moreover, we show that our new measure, together with cluster analysis, is a suitable method for analysing three-dimensional shape of hippocampal and cortical cells.

The corresponding tool NeuClass has been applied to many experimental data available. Figure 2 shows such a classfication obtained by NeuClass.

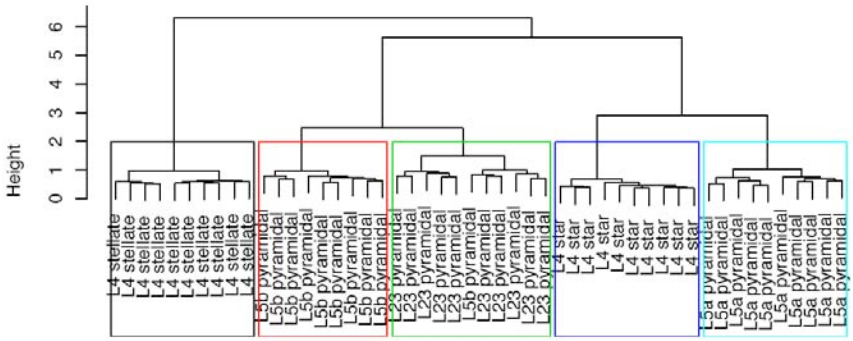

Figure 2. The tree-edit distance discriminates well between the different cell types

The algorithm performed nicely. In spite of the fact that complexity of the tree-edit distance algorithm used is not optimal, all the computations from (Heumann and Wittum 2009) were performed in at most a few minutes. On larger datasets it may be useful to parallelise the algorithm which is straightforward. Besides complexity issues, it should further be investigated using more cell datasets, what parameters should be used for characterisation of cells.

References

Heumann, H. & Wittum, G. (2009). The tree-edit distance. A measure for quantifying neuronal morphology. Neuroinformatics, 7(3), 179-90.

Zhang, K. (1996). A constrained edit distance between unordered labeled trees. Algorithmica, 15, 205–222.

Zhang, K., Statman, R., & Shasha, D. (1992). On the editing distance between unordered labeled trees. Information Processing Letters, 42, 133–139.

A2.6: Modelling the Hydrodynamics of Synaptic Vesicles

Susanne Höllbacher, Gabriel Wittum

In the brain, most neuronal cells are connected by chemical synapses, transmitting information from one cell to another. The activity at synapses is much more than a 0-1-coding within information processing. So called synaptic vesicles - small fluid droplets (40nm diameter) enclosed by a bilipid membrane and filled with the neurotransmitter - play a prominent role within the whole transmission process. In the neuronal cells of most central nervous systems, about 200-500 such droplets reside in one single synaptic ending. In order to sustain and adapt the ability to send signals, i.e. discharge neurotransmitter at one single connection, the vesicles have to refill and cycle within the synapse adequately. Up to now, the underlying mechanisms of the cycling are largely unknown. Our simulations shall give an insight into the dynamics the whole population of hundrets of vesicles. The approach for a model of the interaction of this nanoscale particles (the vesicles) is the simulation of their motion within the hosting fluid, the cytosol. Consequently, the Navier-Stokes equations build the governing equations of the modes system.

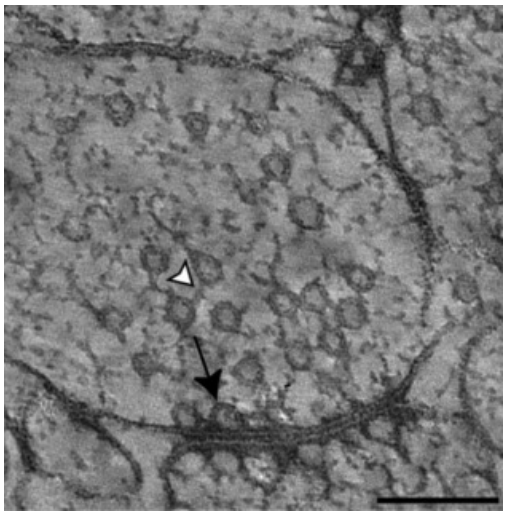

Figure 1. Sections from the tomographic reconstruction of a synapse. Docked synaptic vesicles (black arrow) and filaments between the synaptic vesicles (white arrowhead). Scale bar 200 nm. (L. Siksou et al. 2007)

According to the regime within a biological cell like the synapse, the fluid dynamics can strongly be simplyfied:

First, the cytosol itself does not undertake large fluctuations within a single, tiny synapse of approxymately 500nm in diameter. With a viscosity of the cytosol being 10-fold bigger than the viscosity of water, a characteristical lenth scale of 40 nm (= diameter of the vesicle) and an average velocity of a diffusing vesicle of about 0.1 μm/s, Reichert (2006), the Reynolds number $Re = UL/v$ (U is the characteristic velocity, L is the characteristic length and v is the fluid viscosity) is very small. Consequently, the inertial forces within the fluid can be neglected and this low-Reynolds regime can be described by the linear incompressible Stokes equations.

Second, the momentum relaxation time for colloids (particles of size $< 0.1\ \mu$m) suspended in water ranges from 1-100 ns. Therefor, this so called "overdamped" fluid dynamics can be modeled by the stationary Stokes equations, Reichert (2006).

Finally, the fluid equations are solved coupled with the equations of the motion of the particles. This so called "direct numerical simulation" (DNS) of particle motion in fluids has allready been investigated, addressing problems like sedimentation of particles in gravity driven flows. Our approach is inspired by the ideas of Glowinsky et al. (2001), who has been done the most important work within this field. He handles the coupling of fluid and particle motion by treating the entire fluid-particle domain as a single fluid and imposing a rigid motion constraint at regions occupied by a particle. The numerical implementation follows the approach of Wagner et al. (2001). Using an extension of the ansatz function space within the finite volume method, the rigidity constraint is implicitly captured by the discretization. This method was implemented using an existing finite volume discretisation for the Navier-Stokes equations, the collocated discretisation from Nägele and Wittum (2007). Since rigid motion can simply be expressed by it translational and rotational component, as a consequence of the extension three further degrees of freedom for each particle arise in the algebraic system of equations. They can either be prescribed or treated as free variables being result of the fluctuations of the whole system.

As a first proof of concept, artificial scenarios were investigated. Figure 2 shows the velocity field of a channel flow with one single particle in the middle of the channel. The usual boundary conditions for this problem describe a parabolic inflow entering the channel from the left and passing out of the channel at the right, and no slip boundary conditions on the bottom and top of the channel.

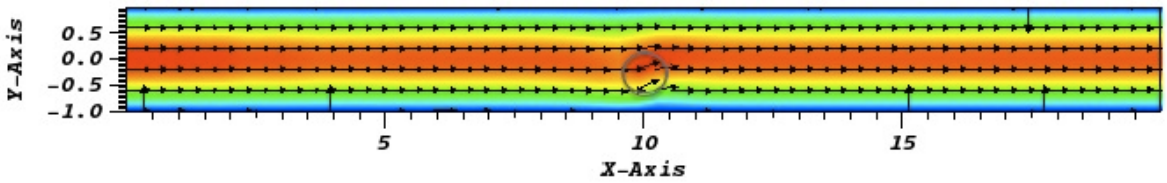

Figure 2. Velocity field of the channel problem with one inserted particle in the middle of the channel

Varying now the horizontal location of the particle within of the channel, the velocity of the inserted particle - passively driven by the sourrounding flow field - changes. This dependence is ploted in Figure 3. As to be expected, the particle being located in the lower or upper half of the channel approaches the center (blue triangles, contour). With decreasing distance from the center its velocity in x-direction increases (blue triangles, filled). The rotational velocity changes orientation passing the zero-line of the y-axis (red squares).

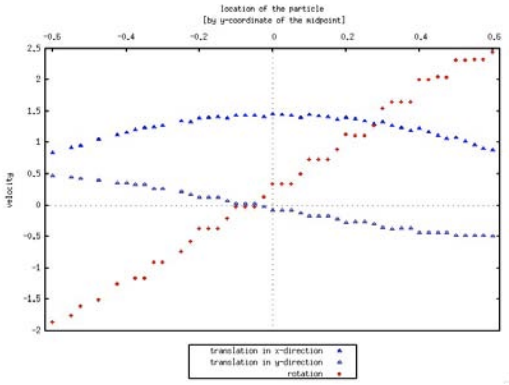

Figure 3. Plot of the free velocities of an inserted particle

In order to apply these technique to the simultaion of synaptic vesicles, certain features has to be added, like the geometrical information of the location of certain vesicles, the morphological properties of the synapse and the biological forces dominating this regime. This will be part of the ongoing work.

References

Glowinski, R., Pan, T.W., Hesla, T.I., Joseph, D.D., & Périaux, J. (2001). A Fictitious Domain Approach to the Direct Numerical Simulation of Incompressible Viscous Flow past Moving Rigid Bodies: Application to Particulate Flow. Journal of Computational Physics, 169(2), 363-426.

Nägele, S., & Wittum, G. (2007). On the influence of different stabilisation methods for the incompressible Navier-Stokes equations. Journal of Computational Physics, 224(1), 100-116.

Reichert, M. (2006). Hydrodynamic Interactions in Colloidal and Biological Systems. Dissertation, URL: http://ub.uni-konstanz.de/kops/volltexte/2006/1930/.

Wagner, G. J., Moes, N., Liu, W. K., & Belytschko, T. (2001). The extended finite element method for rigid particles in Stokes Flow. International Journal for Numerical Methods in Engineering, 51, 293–313.

A3.1, CF3: The Numerical Pricing of Options with Many Risk Factors

Philipp Schröder, Christoph Reisinger, Gabriel Wittum

A very large and increasing number of products traded on financial markets has the form of derivative securities. It is common that these products depend on several uncertain quantities that have to be modelled as stochastic parameters. Two particular examples in this wide range of products are FX options on the exchange rate between two currencies, where the dynamics of the interest rates on the two markets is also crucial, or basket options, which depend on the average of a possibly very large selection of stocks. It is common to express the risky assets and stochastic parameters in terms of Brownian motions, giving rise to parabolic PDEs for the option price. The need for efficient techniques to price these contracts faster and more reliably than by means of state-of-the-art Monte Carlo methods is enormous.

The focus of our research is multivariate systems such as those mentioned above with a special emphasis on high-dimensional problems. First, taking into account the correlation of the processes, a reduced model with a low superposition dimension is derived. This allows a very accurate extrapolation of the solution from lower-dimensional problems. The resulting parabolic equations are discretised on sparse grids with a drastically reduced number of points compared to the conventional spaces. The combination technique allows a further decoupling into discrete subspaces. These linear systems are solved by a suitable multilevel solver in linear complexity . The robust solution is essential for the speed-up of the parallel implementation of the method.

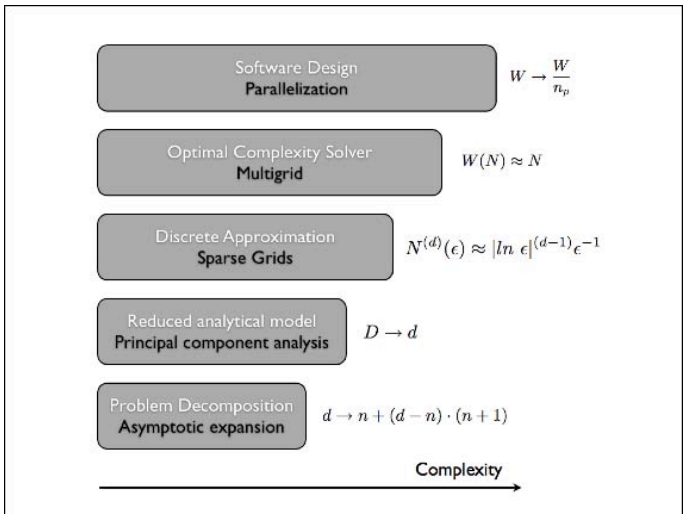

Figure 1. Complexity reduction for option pricing problem

Dimensional reduction

High-dimensional processes often show a typical correlation pattern corresponding to a characteristic form of the spectrum: a dominating component represents the movement of the market, the other eigenvalues decay exponentially. Asymptotic analysis can be used to study the perturbations of simple one-factor models. For the classical Black-Scholes model, an analytic expansion of the solution in terms of these small parameters has been derived. As an alternative, the solution is extrapolated from two-dimensional auxiliary problems that mimic the directional derivatives with respect to the spectrum. The latter idea can be carried over to more general situations. Recently, a theoretical background to explan the good practical results of the asymptotic expansion has been devoloped (Schröder 2012).

Sparse grids and multigrid methods

Sparse grids are known to break the “curse of dimensionality”, i.e. the exponentially increasing number of grid points in high dimensions. The combination technique exploits an astonishing extrapolation property of a particular family of hierarchical subspaces: Assuming some form of the error expansion for the discretisation scheme, the com-

bination of solutions on decoupled Cartesian grids shows the same asymptotic error as the sparse finite element solution and deteriorates only by logarithmic factors in comparison with the full high-dimensional Cartesian grid. In the course of this project, the above statement could be proven and closed form error estimates for the sparse-grid solution in arbitrary dimensions have been derived.

The parallel implementation gave very accurate results for real-world scenarios in up to six dimensions. A solver of linear complexity is crucial for the load balancing. A multilevel technique with "plane" smoothing, applied recursively in lower-dimensional hyper-planes, proved robust for the present anisotropic and degenerate parabolic operators coming from bounded stochastic processes. Extensions to American options involve adapted transfer operators at the free boundary and show comparable convergence.

Results

The plot shows the price u of a European option on a basket of two uncorrelated stocks S_1 and S_2 with different volatilities. The triangle indicates the pay-off, which serves as terminal condition. The sparse grid has been transformed such that the kink in the pay-off is captured exactly and graded in the direction orthogonal to the kink. This preserves the discretisation order despite the lack of smoothness and provides a suitable refinement in that region.

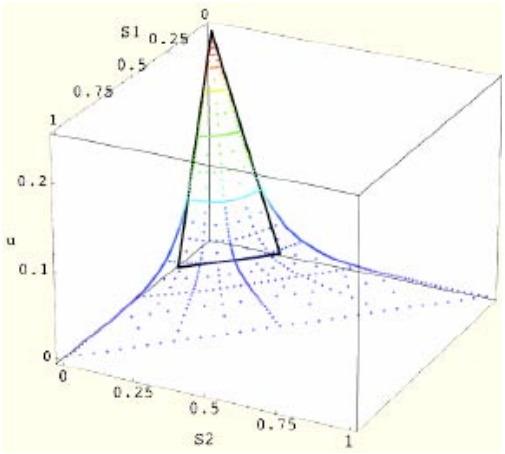

Figure 2. Result and payoff function (black) of two-asset basket option

For visualisation's sake, we show only two-dimensional results in the figure above. Nevertheless, comparison with solutions obtained by a large number of Monte Carlo runs shows that our approach yields remarkably accurate prices within a few minutes with errors below 0.1 % even for very large baskets like the DAX (30 dimensions).

References

Reisinger, C. (2004). Numerische Methoden für hochdimensionale parabolische Gleichungen am Beispiel von Optionspreisaufgaben (Numerical Methods for High-Dimensional Parabolic Equations on the Example of Option Pricing Problems). PhD thesis, University of Heidelberg.

Reisinger, C., & Wittum, G. (2004). Multigrid Methods for Anisotropic Equations and Variational Inequalities. Computing and Visualisation in Science, 7(3-4), 189-197.

Reisinger, C., & Wittum, G. (2007). Efficient Hierarchical Approximation of High-Dimensional Option Pricing Problems. SIAM Journal on Scientific Computing, 29(1), 440-458.

Schröder, P., Gerstner, T., & Wittum, G. (2012). Taylor-like ANOVA Expansion for high dimensional Problems in Finance. Manuscript submitted for publication.

A3.2, CF4: Credit Risk Estimation in High Dimensions

Philipp Schröder, Gabriel Wittum

Credit risk influences many important banking processes and functions like credit decisions and pricing, portfolio management, estimation of portfolio losses, building of loan loss reserves, etc. Thus, the correct quantification of credit risk is crucial for a bank. The credit risk basically consists of four components: loan exposure, (payment) default probability of the borrower (PD), potential recovery after default due to collateral, and (default) correlation of the borrowers.

The modelling of customers default correlations is an important research area. Borrower correlations are currently only considered in sophisticated credit portfolio models. Nevertheless, these correlations are as well important. for the calculation of default probabilities of complex exposure structures (for instance loans to a group of linked companies) or for the calculation of the joint default probability of borrower and guarantor. Recently, modern numerical analysis techniques have been successfully applied to option pricing problems (Reisinger 2004). As option pricing and Merton-type credit portfolio models are based on the same rationale, the objective of our recent research was to combine the classical Merton-type portfolio model (Merton 1974) with advanced numerical methodologies like sparse grids and multigrid solvers in order to obtain an efficient borrower correlation model.

Since the resulting partial differential equations are of high dimensionality, different approaches have been taken to increase efficiency of the used algorithms.

Dimensional reduction

As many problems from finance, the estimation of joint default probabilities for large portfolios suffers from the so called „curse of dimension“ due to the high number of underlying risk drivers. Statistical analysis (e.g. Analysis of Variance, Principal Component Analysis) of the underlying processes however often shows, that the original problem can be decomposed into problems of lower dimension. Furthermore only some of the lower dimensional subproblems have significant contribution to the total variance of the problem. The picture below shows an ANOVA analysis of two-dimensional subproblems a 30D highly correlated credit portfolio can be decomposed in. Subproblems that contribute to the total variance of the problem significantly are shown in brown.

Asymptotic expansion can be used to extrapolate the solution of the fully dimensional problem via a linear combination of the individual solutions to the subproblems. For the classical Merton Firm Value model, an expansion of the solution in terms of these subproblems has been derived (Schröder 2009).

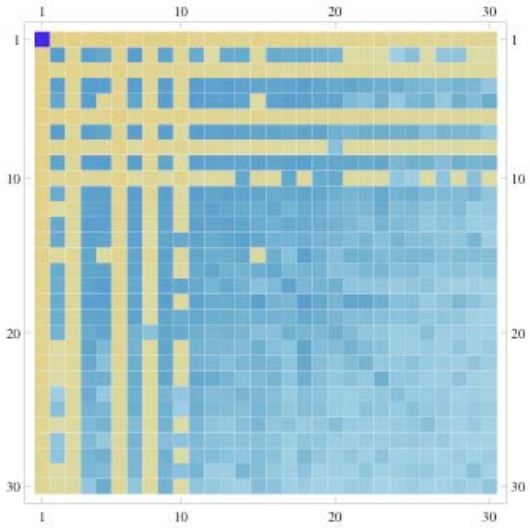

Figure 1. ANOVA Analysis of two-dimensional subproblems

Recently, a higher order expansion has been developed. Additionally, a theoretical background for the good practical results has been developed (Schröder 2011, Schröder 2012)

Parallelization

The parallel implementation of a sparse grid extrapolation technique gave very accurate results together with good scalability results for real-world scenarios up to six dimensions. Current research is aimed on the developement of an additional layer for the parallelization, i.e. a parallelization of the calulation of the subproblems solutions.

Results

Asymptotic expansion and sparse grid combination technique enabled us to efficiently calculate the default risk for a portfolio of 50 higly correlated credits with relative errors below 0.1%.

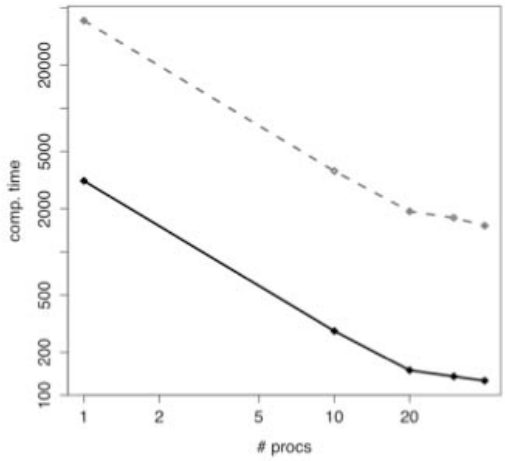

Figure 2. Scaleup for six-dimensional problem

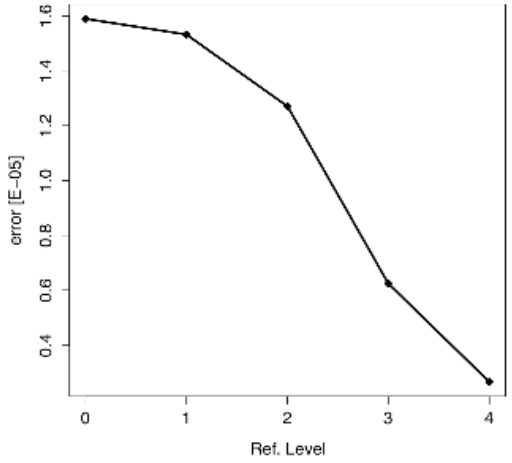

Figure 3. Absolute Error for six-dimensional problem

References

Merton, R. C. (1974). On the pricing of corporate debt: The risk structure of interest rates. The Journal of Finance, 29(2), 449-470.

Mlynczak, P. (2011). Parallelization concepts for the solution of high-dimensional PDEs with applications in finance. Master thesis, Universität Frankfurt.

Reisinger, C. (2004). Numerische Methoden für hochdimensionale parabolische Gleichungen am Beispiel von Optionspreisaufgaben (Numerical Methods for High-Dimensional Parabolic Equations on the Example of Option Pricing Problems). PhD thesis, Universität Heidelberg.

Schröder, P., Avçu, Y., Wagner, C. & Wittum, G. (2009). Calculation of Default Probability (PD) solving Merton Model PDEs on Sparse Grids. Proceedings of the 23rd IPDPS, IEEE International Symposium on Parallel&Distributed Processing, pp.1-6.

Schröder, P. (2011). Dimensionsweise Zerlegungen hochdimensionaler Probleme mit Anwendungen im Finanzbereich, PhD thesis, Universität Frankfurt, submitted.

Schröder, P., Gerstner, T., & Wittum, G. (2012). Taylor-like ANOVA Expansion for high dimensional Problems in Finance, Manuscript submitted for publication

A3.3, CF5: Portfolio Optimisation

Mathias Höfer, Holger Kraft, Gabriel Wittum

An important problem in modern continuous time finance is the so-called Merton's Lifetime Portfolio Problem. Whereas the former portfolio selection approach by Markowitz regards an isolated portfolio without dynamic effects, this time-dependent model becomes more realistic (Merton 1969). Succeeding authors constructed generalised models, which made it difficult or even impossible to find closed-form solutions. Numerical methods can handle these kind of higher dimensional problems.

The task is finding an optimal strategy for the level of consumption and investment in different risky assets to reach maximum expected utility. The regarded model consists of two important parts. First, an economy, which is modelled by the interest rate and diverse market prices e.g. of shares or bonds. The dynamics of these market characteristics are expressed in terms of correlated stochastic processes based on the Brownian Motion. Secondly, the consumer/small investor is modelled by his utility function, which shows his risk aversion and his consumption requirements, furthermore his income is modelled stochastically similar to the market processes. The optimal value function (maximum expected utility) is composed of the discounted utility of running consumption and the discounted final wealth. This problem of stochastic control theory can be transformed to a controlled partial differential equation, the so-called Hamilton-Jacobi-Bellman Equation. Ignoring the maximization problem, this equation is a convection-diffusion equation with source terms, whereby the choice of the investment strategy has linear effects on the drift-terms and quadratic influence on the diffusion. Changes of consumption level itself causes non-linear amendments.

Classical solvers require finite control possibilies in each discretized time step (Lion and Mercier 1980). The principle work flow of the solver is an alternating process of finding the maximizing strategy parameters and computing the partial differential equation. Integrating a gradient descent optimizer enables continous investment and consumption choise. The capabilies of SG2 can be used to construct a fast HJB-solver with the described method.
The concept of sparse grids allows decreasing the number of grid points substantially (Reisinger and Wittum 2007). Constructing a hierarchy of coarser grids gives the opportunity to identify relevant strategy-combinations and consider them on finer levels as initialisation for the optimiser. This adapted nested iteration method offers the opportunity to reduce calculation time. Combining the solution of HJB-equation and the corresponding strategy-vectors with typical sparse-grid-methods leads to demanded solution.

Illustrating a 3-dimensional problem, one can see the optimal strategy of an exemplary consumer in diverse market environments.

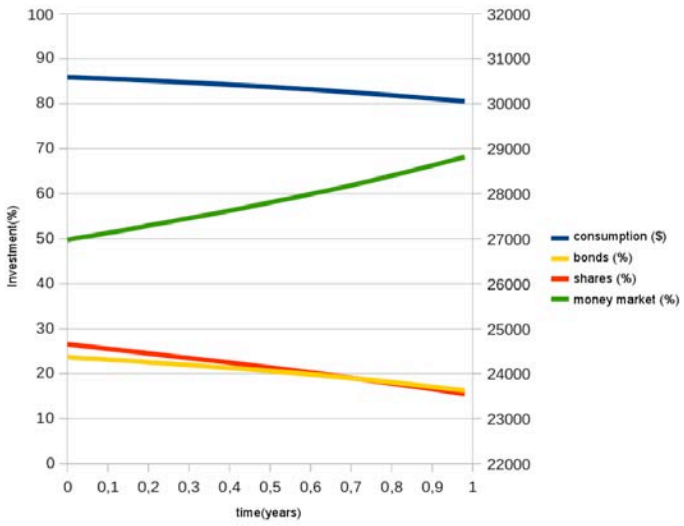

Figure 1. Optimal investment strategy and consumption of a small investor.

Figure 1 illustrates the opimal investment strategy and the consumption of a small investor. During the optimisation horizont his portfolio changes to less risky structure. Investments in bonds and shares are reduced and his capitel in the money markets increased.

Using market parameters with a negative correlation of bonds and shares enables a hedging strategy (Figure 2). More capitel can be invested in risky assets, since a negative price trend of shares related to increasing bond prices.

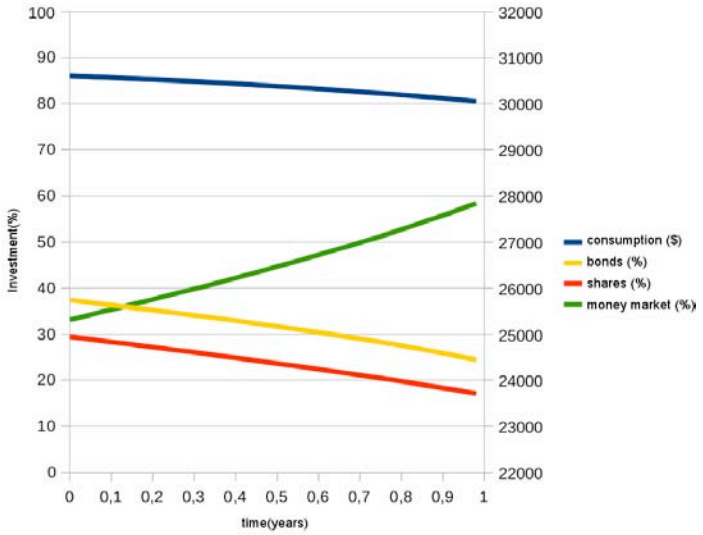

Figure 2. Hedging strategy

References

Bick, M., Kraft, R., & Munk, C. (2009). Investment, Income, Incompleteness. Series Finance and Accounting, No. 202, Working Paper. Retrieved from http://www.finance.uni-frankfurt.de//wp/1823.pdf

Lion, P.-L., & Mercier, B. (1980). Approximation numérique des équations de Hamilton-Jacobi-Bellman. Revue d'Automatique, d'Informatique et de Recherche Opérationnelle - Analyse numérique, 14, 369-393.

Merton, R. (1969). Lifetime portfolio selection under uncertainty: the continuous case. Review of Economical Statistics, 51, 247-257.

Reisinger, C. (2004): Numerische Methoden für hochdimensionale parabolische Gleichungen am Beispiel von Optionspreisaufgaben. Dissertation, Fakultät Mathematik, Universität Heidelberg.

Reisinger, C., & Wittum, G. (2007). Efficient Hierarchical Approximation of High-Dimensional Option Pricing Problems. SIAM Journal for Scientific Computing, 29(1), 440-458.

A4.1: Simulation of Crystal Growth and Attrition in a Stirred Tank

Dmitry Logashenko, Torsten Fischer, Gabriel Wittum

Crystallisation from solution in stirred crystallisers is one of the economically most important industrial separation and purification processes. It is applied as a large scale continuous process for the production of inorganic (e.g. potassium chloride, ammonium sulphate) and organic (e.g. adipic acid) materials. On a small scale it is often applied as a batch operation to produce high purity pharmaceuticals or fine chemicals (e.g. aspartame, L-ascorbine). This process includes two classes of physically different but strongly coupled phenomena. The first one is the crystallisation itself, typically described by means of population models. The second one consists of the spatial flow and the transport induced by the stir.

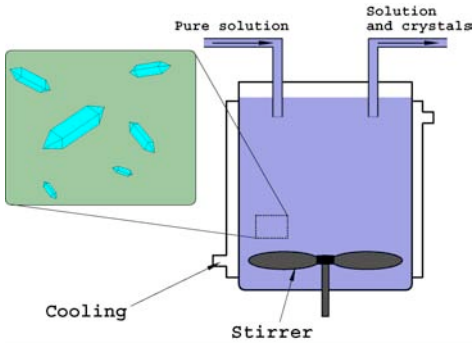

Figure 1. Scheme of the stirred crystalliser

We consider a continuous stirred crystalliser (cf. Figure 1). The pure solution (without crystals) is pumped in at the inflow and the suspension of the crystals leaves the tank at the outflow so that the volume of the fluid in the tank is constant. The crystalliser is cooled from the outside so that the solution in it is oversaturated. The attrition of the crystals happence only on the stirrer whereas the growth takes place everywhere in the tank. The fluid in the crystalliser is suspension whose density and viscosity depend on the concentration of the crystals and the dissolved substance.

The main feature of this model is its hight dimensionality: 2 or 3 spatial dimentions for the flow and the transport are extended with one additional dimention for the population dynamics. (We assume that the crystals have only one inner parameter - the length.) A practically relevant description of complicated behaviour of the crystallisation process requires a fine numerical resolution in this crystall length dimension. Furthermore, the population balance equations include integral terms that need special numerical treatment. This leads to a high computational complexity of the simulations that can be only achieved under the use of parallel architectures and adaptive techniques.

The geometric space is covered with an unstructured grid. On it, the coupled flow and transport equations are discretised to one nonlinear algebraic system (we use the implicit time scheme) that can be then solved by the fixed-point or Newton iteration. The arising linear systems are handled by the geometrical multigrid method with the ILU-smoothers. The unstructured grid is adaptively refined during the time stepping according to an error indicator. At every node of this grid, we introduce a uniform mesh for the discretisation of the population balance equations.

Figure 2 presents the results of the simulation of crystallisation of potassium nitrate in a stirred tank (cf. Logashenko et al. 2006). The inflow is placed at the upper part of the left wall and the outflow at the lower part of the right one (s. the upper left picture in this figure). The stirrer is located in the middle of the crystalliser. The pictures correspond to time 300 s from the beginning of the process, when the tank was filled with the suspension of the middle-sized crystals. The spatial unstructured grid consists of about 12500 nodes, the population mesh has 51 points (at every node of the spatial grid). This simulation shows the fine spatial structuring of the process.

Similar results of the simulation in a 3d crystalliser are illustrated in Figure 3. The pictures have here the same meaning as on Figure 2 and represent an early stage (1.5 s) of the process.

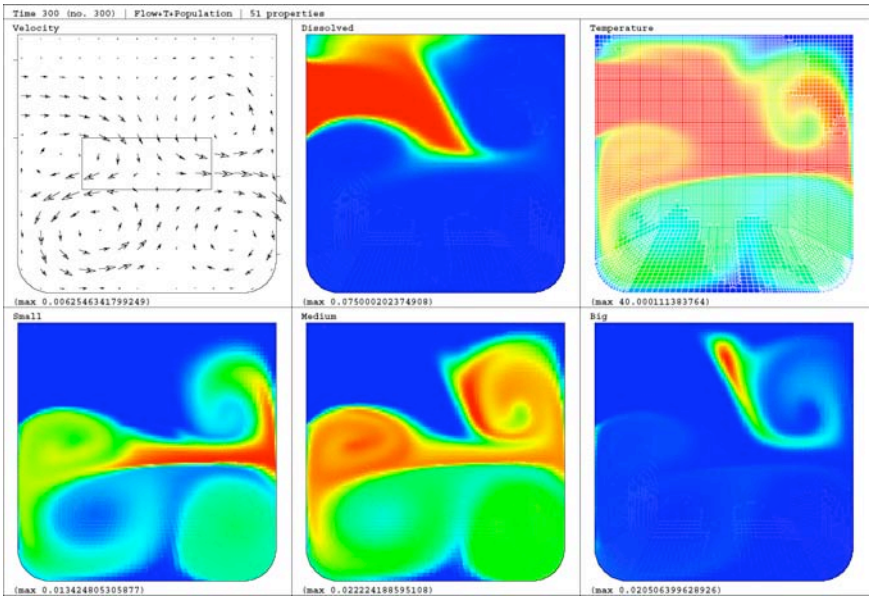

Figure 2. Crystallisation of potassium nitrate in a stirred tank (2d simulation)

Upper pictures (f.l.t.r.): the flow velocity field [m/s], the molar fraction of the substance in the solution and the temperature [^{o}C]. Lower pictures: the integral volume fraction for lengths 0-0.1 mm, 0.1-0.5 mm and 0.5-1 mm.

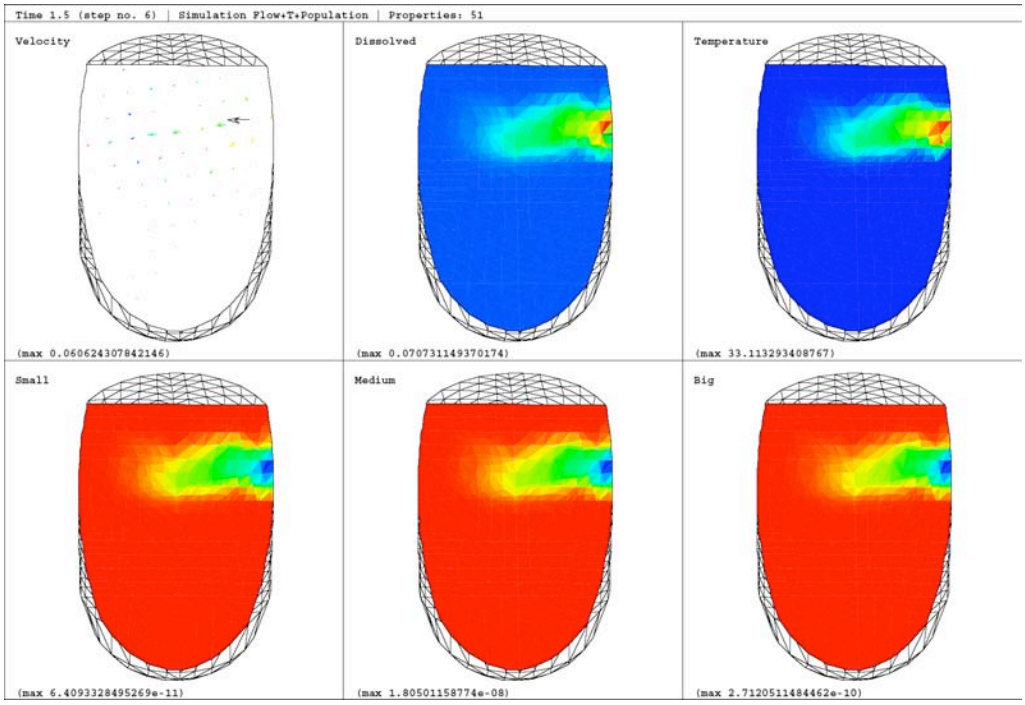

Figure 3. Crystallisation of potassium nitrate in a stirred tank (3d simulation)

The meaning of the plots is the same as for Figure 2.

References

Fischer, T., Kirkilionis, M., Logashenko, D. & Wittum, G. (2006): Fast Numerical Integration for Simulation of Disperse Systems. Mathematical Models and Methods in Applied Sciences, 16(12), 1987-2012.

Logashenko, D., Fischer, T., Motz, S., Gilles, E.-D., & Wittum, G. (2006). Simulation of Crystal Growth and Attrition in a Stirred Tank. Computing and Visualization in Science, 9(3), 175-183.

A5: Environmental Science
A5.1: Density-Driven Flow in Porous Media

Alfio Grillo, Michael Lampe, Gabriel Wittum

A leading topic in hydrogeology and environmental science is the investigation of salinity- and thermohaline-driven fluid flow in porous media of hydrological relevance. The porous medium and the fluid are usually identified with a soil and groundwater, respectively. The name given to these two types of groundwater flow depends on the causes that have either brought the fluid out of mechanic equilibrium or altered its dynamic state. Salinity-driven flow is due to the non-uniform change of the mass density of the fluid consequent to mixing together water and brine (the latter is a mixture of water and various salts). Temperature-driven flow is triggered by exposing the fluid to thermal gradients or mixing together flows at different temperatures. Thermohaline-driven flow is the combined effect of the just mentioned types of flows. In all these cases, in order to observe flow, it is necessary that the alteration of the density of the fluid favours fluid motion. Within the context sketched above, some of the most typically studied problems are sea-water intrusion into coastal aquifers, upconing of hypersaline water from deep aquifers, flow around salt domes or sedimentary rocks, and contamination of aquifers caused by waste. Some of the reasons for undertaking these studies are the managment of freshwater supplies (especially in arid or urbanised zones) and the solution forcast and remediation problems (for example, in the neighbourhood of nuclear waste repositories).

Our research focussed on the mathematical modelling, numerical simulation, and physical interpretation of some peculiar phenomena of thermohaline-driven flow that can be captured through the analysis of dedicated benchmark problems. The theoretical aspects of our investigations are inspired by Hassanizadeh (1986) and Bear (1972). Numerical simulations were carried out by using the sofware packages $\mathcal{UG}$ and d^3f (Fein 1998). A summary of our results, which also covered the study of thermodiffusion in porous media, was provided by Grillo et al. (2011). More detailed, three-dimensional simulations of thermohaline-driven flow as well as brine and heat transport were done in the publications by Grillo et al. (2010) and Lampe et al. (2010), where the buoyancy of a brine parcel was studied. The simulations consist of a generalisation of the benchmark proposed by Oldenburg and Pruess (1999). Some of our results are shown in the following figures. Recently, we extended our results to the case of fractured porous media (Grillo et al. 2012, Stichel et al. 2012).

Some results of the simulations concerning the buoyancy of a brine parcel are reported in the figures. The peculiar phenomenological features of this example can be summarised as follows. In the case of negative buoyancy, brine is transported downward faster than heat because of a retardation factor, which slows down heat convection. The mass fraction of the brine distributes by generating several "fingers" which result from the interplay of down- and up-swelling of fluid motions. Heat, instead, is mainly confined in the region occupied by the original configuration of the parcel. When the brine starts to leave this region, fluid density in the parcel becomes smaller and eventually the parcel begins to experience even positive buoyancy. This leads to the separation of brine and heat from the initial parcel: brine moves downwar and heat slowly upward. At the sides of the parcel, the brine exhibits a "fountain"-like motion. Indeed, brine enters colder regions where it again leads to higher fluid density, and is then convected downward. In the case of positive buoyancy, brine is transported upward faster than heat (also in this case because of the retardation factor). Above the initial parcel, brine is cooled down, which leads to higher density of the fluid, and moved downward along the sides of the parcel. Since heat is again confined mostly to the initial parcel, while brine moves away, the density of the fluid in this zone becomes even smaller, which enhances the initial buoyancy.

However, the separation of heat from the initial parcel is hindered by a density "lid" built up by cold brine (highest density) flowing aroung the parcel (hot, low-brine, relatively low density).

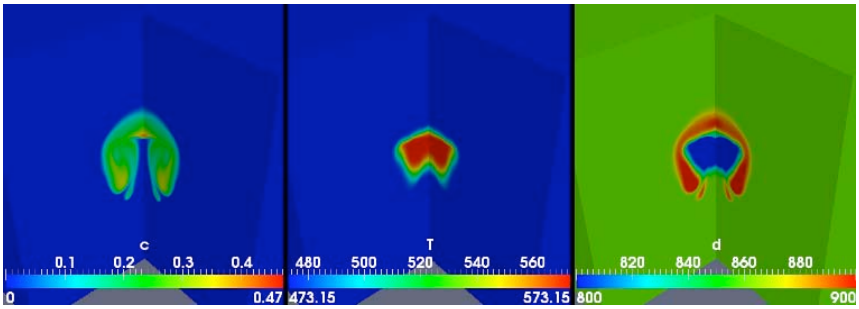

Figure 1. Evolution in the case of positive buoyancy (from left to right: mass fraction, temperature, and density)

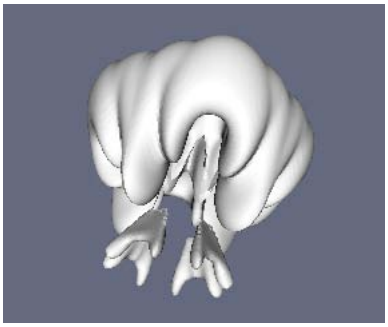

Figure 3. Isosurfaces of mass fraction (0.15) in the case of positive buoyancy

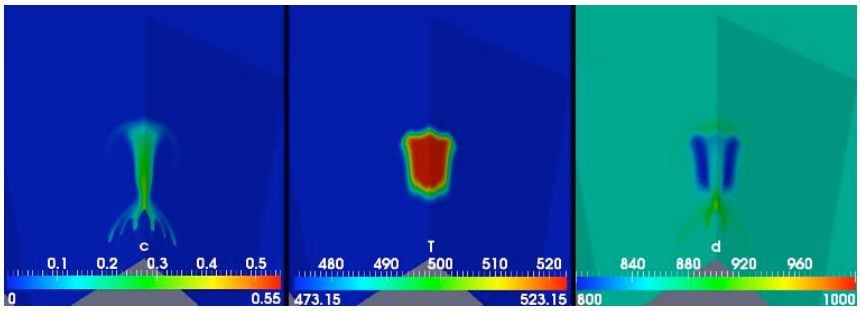

Figure 2. Evolution in the case of negative buoyancy (from left to right: mass fraction, temperature, and density)

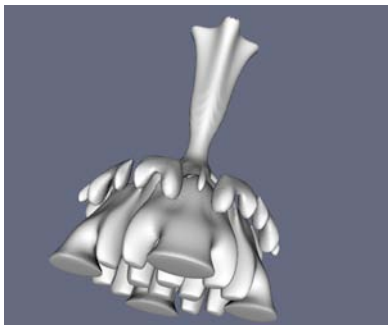

Figure 4. Isosurfaces of mass fraction (0.15) in the case of negative buoyancy

References

Bear, J. (1972). Dynamics of fluids in Porous Media. New York: Dover Publication, INC.

Fein, E. (1998). Ein Programmpaket zur Modellierung von dichtegetriebenen Strömungen. Braunschweig: GRS-139, ISBN 3-923875-97-5.

Grillo, A., Lampe, M., Logashenko, D., Stichel, S., & Wittum, G. (2012). Simulation of salinity- and thermohaline-driven flow in fractured porous media. Journal of Porous Media, 15(5), 439-458.

Grillo, A., Lampe, M., & Wittum, G. (2011). Modelling and Simulation of temperature-density-driven flow and thermodiffusion in porous media. Journal of Porous Media, 14(8), 671-690.

Grillo, A., Lampe, M., & Wittum, G., (2010). Three-dimensional simulation of the thermohaline-driven buoyancy of a brine parcel. Computing and Visualization in Science, 13, 287-297.

Hassanizadeh, S. M. (1986). Derivation of basic equations of mass transport in porous media, Part II. Generalized Darcy's and Fick's Laws. Advances in Water Resources, 9, 207-222.

Lampe, M., Grillo, A., & Wittum, G. (2010). Software Framework UG: Parallel simulation of a three-dimensional benchmark problem for thermohaline-driven flow. In W.E. Nagel et al. (Eds.), High Performance Computing in Science and Engineering '10. Berlin: Springer-Verlag. DOI10.1007/978-3-642-15748-6_40

Oldenburg, C. M., & Pruess, K. (1999). Plume separation by transient thermohaline convection in porous media. Geophysical Research Letters, 26(19), 2997-3000.

Stichel, S., Logashenko, D., Grillo, A., Reiter, S., Lampe, M., & Wittum, G. (2012). Numerical methods for flow in fractured porous media. In J.M.P.Q. Delgado (Ed.), Heat and Mass Transfer in Porous Media, Advanced Structured Materials (vol. 13, pp. 83-113). Berlin: Springer.

A5.2, T4: The Software Tool r^3t and Flux-Based Level-Set Methods

Peter Frolkovic, Jürgen Geiser, Michael Lampe, Christian Wehner, Gabriel Wittum

The software tool r^3t (radionuclide, reaction, retardation and transport, c.f. Frolkovic 2003), based on the UG library, can solve very large systems of coupled partial differential equations describing the transport and retention of radioactive contaminants with up to 160 species numerically. Computational results from other UG applications for groundwater flows in complex 3D geological formations can be used as the input for r^3t . Modelling physical parameters is performed by using user-friendly configuration and script files. Computations on several parallel computer platforms are possible.

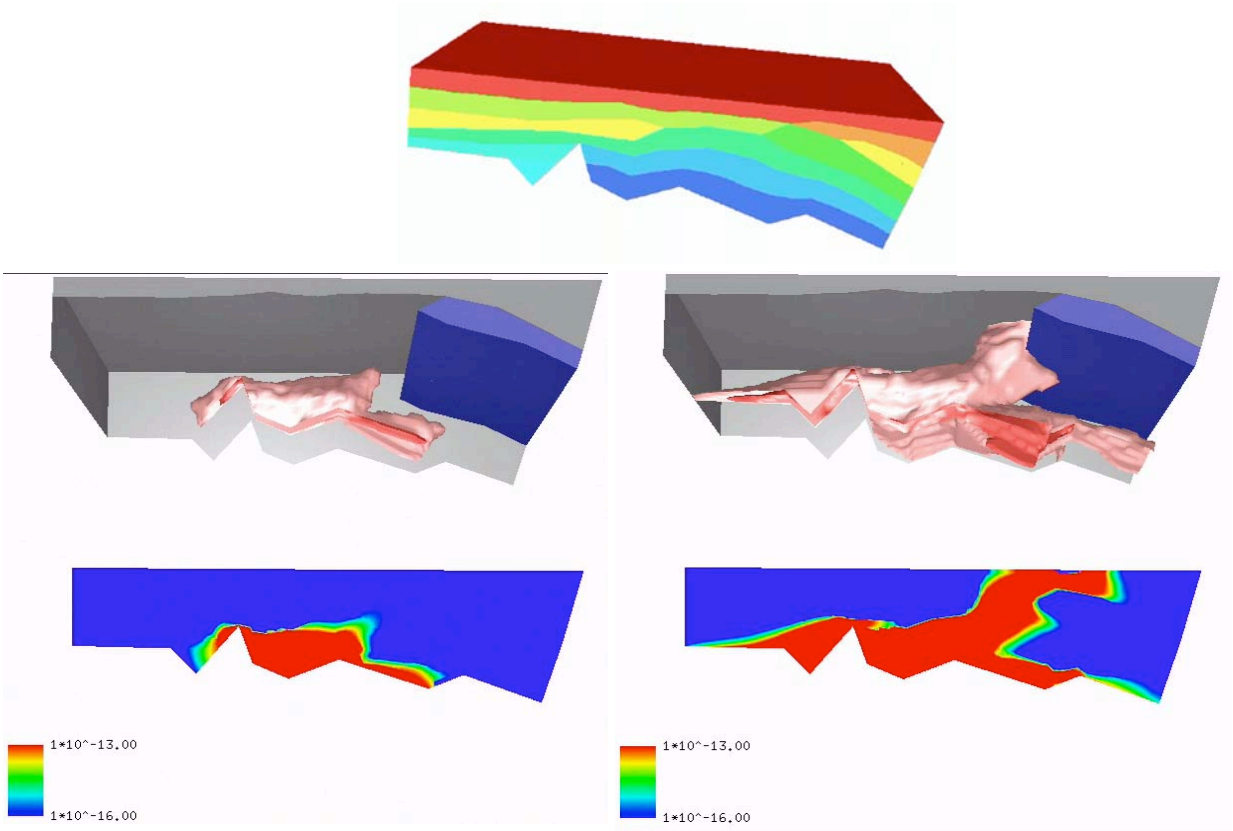

Figure 1. From top to bottom: layered 3D-domain, development of the U_{238} component

r^3t can solve very general mathematical models of the transport and retention of radionuclides, including non-linear kinetic sorption and non-linear precipitation with a solution-dependent solubility limit (Frolkovic and Geiser 2000). Several novel algorithms had to be developed to solve typical applications with r^3t. First, the so-called flux-based method of characteristics was designed and successfully implemented (Frolkovic 2002a). This method enables us to solve convection-dominated transport problems on general 2D/3D unstructured grids using very large time steps (with no CFL restriction). In such a way, extremely large simulation times that are required by typical risk scenarios for radioactive waste disposal (up to 10000 years) can be realised with r^3t .

The discrete minimum and maximum principle is fulfilled by the scheme (i.e. solutions are oscillation-free), and the discrete local and global mass-balance property is preserved. Such combinations of important numerical properties are novel for this type of method on general computational grids. The flux-based method of characteristics was further extended for a system of convection-dominated transport equations that are coupled through the decay of radioactive contaminants. In the case of different retardation factors for each transported radionuclide (as occurs in practice), a very large time-splitting error will occur if standard operator-splitting methods are used with large time steps. We proposed a novel method minimising such errors (Frolkovic 2004).

Furthermore, to obtain very precise numerical solutions for the coupled system of transport equations with different retardation factors, a novel algorithm with no time-splitting error was developed and implemented for *r^{3}t*, (Geiser 2004). It is based on a second-order explicit finite volume discretisation scheme with the usual CFL restriction for the time steps.

For the case of a non-linear retardation factor due to sorption of Freundlich or Langmuir type, a new algorithm was developed to obtain very precise numerical solutions for one-dimensional problems with arbitrarily small diffusion (Frolkovic and Kacur 2006). Again, very large time steps that do not satisfy the CFL restriction can be used with this method.

Finally, the finite volume discretisation and the flux-based method of characteristics were extended for transport equations in non-divergence form. This extension is important not only for transport problems with a non-divergence-free velocity field (Frolkovic and De Schepper 2001; Frolkovic 2002b), but it is very promising for problems with moving interfaces depending on their geometrical properties (Frolkovic and Mikula 2007a, b).

References

Frolkovic, P. (2002a). Flux-based method of characteristics for contaminant transport in flowing groundwater. Computing and Visualization in Science, 5(2), 73-83.

Frolkovic, P. (2004). Flux-based method of characteristics for coupled transport equations in porous media. Computing and Visualization in Science, 6(4), 173-184.

Frolkovic, P. (2002b). Flux-based methods of characteristics for transport problems in groundwater flow induced by sources and sinks. In S.M. Hassanizadeh et al. (Eds.), Computational Methods in Water Resources 2, 979-986. Amsterdam: Elsevier.

Frolkovic, P. (2003). The simulator and the methods used. In E. Fein (Ed.), r^{3}t - A program suite to model transport and retention in porous media, GRS-192, 99-169. Braunschweig: (GRS)mbH.

Frolkovic, P., & Geiser, J. (2000). Numerical simulations of radionuclides transport in double porosity media with sorption. In A. Handlovicova et al. (Ed.), Algoritmy 2000, pp. 28-36. Slovak University of Technology, Bratislava.

Frolkovic, P., & Kacur, J. (2006). Semi-analytical solutions of contaminant transport equation with nonlinear sorption in 1D, Computational Geosciences, 3(10), 279-290.

Frolkovic, P., & Lampe, M., & Wittum, G. (2011). Numerical simulation of contaminant transport in groundwater using software tools r^{3}t. Manuscript submitted for publication.

Frolkovic, P., & Mikula, K. (2007a). High-resolution flux-based level set method. SIAM Journal on Scientific Computing, 29(2), 579-597.

Frolkovic, P., & Mikula, K. (2007b). Flux-based level set method: A finite volume method for evolving interfaces. Applied Numerical Mathematics, 57(4), 436-454.

Frolkovic, P., & De Schepper, H. (2001). Numerical modelling of convection dominated transport coupled with density driven flow in porous media. Advances in Water Resources, 24(1), 63-72.

Frolkovic, P., & Wehner, C. (2009). Flux-based level set method on rectangular grids and computations of first arrival time functions. Computing and Visualization in Science, 12(5), 297-306.

Geiser, J. (2004). Diskretisierungsverfahren für Systeme von Konvektions-Diffusions-Dispersions-Reaktions-Gleichungen und Anwendungen. PhD thesis, University of Heidelberg.

A5.3: Fractured Porous Media

Sabine Stichel, Dmitry Logashenko, Alfio Grillo, Sebastian Reiter, Gabriel Wittum

Simulation of groundwater flow and solute transport in fractured porous media is currently one of the most active research fields and is of great practical importance. Fractures influence flow and transport processes essentially. Espeacially, the often high conductivity in the fractures leads to their representation as preferential fast pathways for contaminant transport. Because of their long and thin geometry, fractures are difficult to handle numerically: on the one hand, computational grids covering the whole domain where hydrology is simulated usually cannot resolve the thickness of fractures. On the other hand, the simulations on finer grids resolving the fractures even in smaller domains encounter specific difficulties with numerical solvers that demonstrate poor performance in this case.

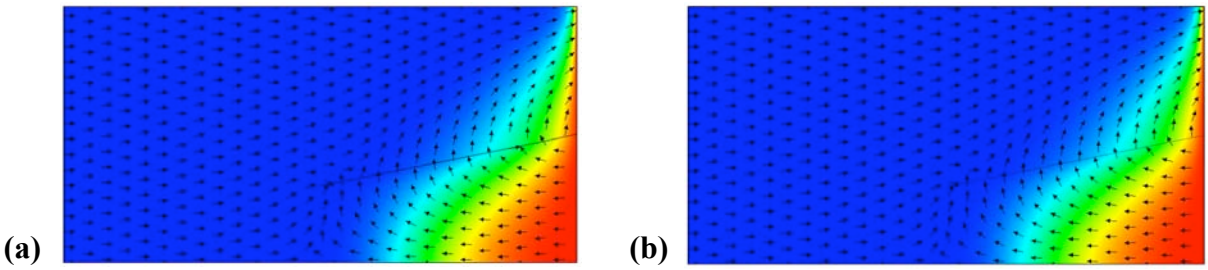

Figure 1. Simulation of the Henry problem with a fracture: (a) d-dimensional, (b) (d-1)-dimensional

Therefore we follow two approaches. In the first one, useful for simulations in large domains with many fractures, we represent the fractures by low-dimensional hypersurfaces. We develop special models based on averaging of unknowns in the fractures in the direction orthogonal to the fracture surfaces (Grillo et al. 2009a,b,2010a) by employing an upscaling method exposed in Bear (1979). Initially, the fracture is regarded as a full-dimensional porous medium filled by a two-constituent fluid, which consists of water and brine. The equations describing the macroscopic behaviour of the medium are given by the balance of mass of the contaminant and the fluid-phase as a whole. It is assumed that the fluid-phase velocity and the diffusive mass flux of the contaminant are given by Darcy's and Fick's laws, respectively. Subsequently, these balance equations are averaged according to a procedure known as "average along the vertical" (see Bear 1977). This leads to a set of equations describing an equivalent low-dimensional porous medium. In order for these equations to be consistent, surface physical quantities (mass density, concentration, velocity and mass flux) have to be introduced, and the vector fields describing Darcy's and Fick's laws have to be projected onto the tangent space of the equivalent lower-dimensional fracture. The gravity force in the fracture is treated in a special way. It should be also pointed out that the normal components of these vector fields account for the interaction of the fracture with the surrounding medium. The explicit determination of the way in which such an interaction takes place, and its numerical treatment require the self-consistent expression of normal mass fluxes.

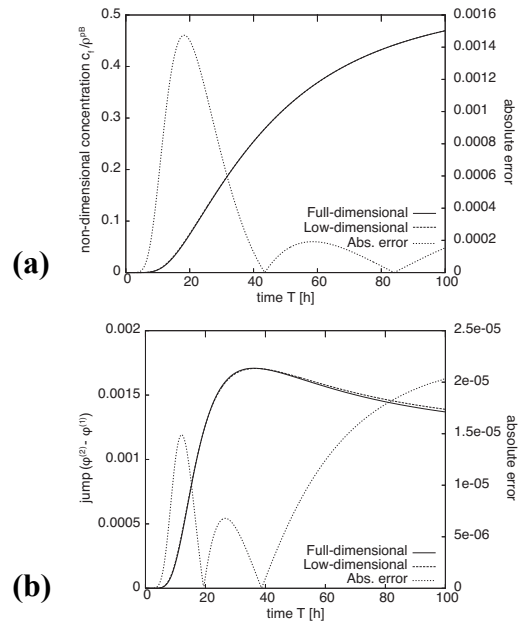

Figure 2. Comparison of the d- and the (d-1)-dimensional simulations: (a) non-dimensional concentrations in the fracture, (b) jumps of the non-dimensional concentrations at the fracture interfaces

Numerically, the low-dimensional hyperfaces are represented by so-called degenerated grid elements. For discretisation, the vertex-centered finite volume method, in particular based on the low-dimensional finite volumes in fractures (Grillo et al. 2010a), is used. Conventional numerical methods, like Newton iteration with geometrical multigrid method for linearised equations, demonstrate very good performance for this type of problems.

Although the approach presented above demonstrates good performance, it does not allow to resolve many specific phenomena taking place in the fractures themselves. In the second approach, we consider the fractures as full-dimensional subdomains and develop special numerical solvers that overcome the difficulties arising in the numerical solution of the discretised model that occur due to strong anisotropy of the grid in the fractures and the essential difference of hydraulic parameters in the fractures and the surrounding medium. To this end a dimension transfer is introduced in the grid hierarchy, resolving the fractures as full-dimensional objects on the finest grid level, but treating them as low-dimensional objects on the coarse grids. This allows to retrieve the good convergence properties of the solver.

Figure 1 presents results of a 2d simulation of density-driven flow and contaminant transport in the so-called Henry problem with a fracture added to the domain. The simulation was performed using both methods presented above. Permeability in the fracture is 10000 times larger than in the surrounding medium, and porosity is 2 times greater. On the right wall, we impose the maximum brine concentration, whereas there is a slow inflow of pure water through the left wall (the two other walls are impermeable.) The flow in the domain is mainly induced by gravity and the vertical pressure gradient at the right wall. Figure 2 shows that for thin fractures the two methods deliver the same results (Grillo et al. 2010a). Though, for increasing fracture width the second approach should be used as there are vortices produced inside the fracture (cf. Figure 3). Some implications of the presence of vorticity and an extension of the model to the case of thermohaline-driven flow have been discussed by Grillo et al. (2012) and Stichel et al. (2012). The influence of vorticity on the stability of the flow is part of current research. For this especially 3D simulations (Reiter et al. 2012) are needed. The appearance of vortices in some fractures also implies that the validity of Darcy's law should be questioned. Therefore, a Forchheimer correction for the velocity is introduced and currently analyzed.

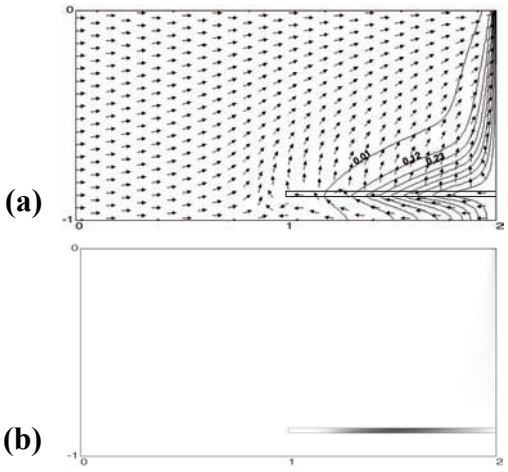

Fig 3. Simulation of the Henry problem with a thick fracture: (a) concentration isolines, (b) vorticity

References

Bear, J. (1977). On the Aquifer's Integrated Balance Equations. Advances in Water Resources, 1, 15-23.

Bear, J. (1979). Hydraulics of Groundwater. Mineola, NY: Dover Publications, Inc.

Grillo, A., Logashenko, D., & Wittum, G. (2009a). Mathematical Modelling of a Fractured Porous Medium. Mini-Workshop "Numerical Upscaling for Flow Problems: Theory and Applications", Oberwolfach Report No. 12/09.

Grillo, A., Logashenko, D., & Wittum, G. (2009b). Study of a Transport Problem in a Two-Dimensional Porous Medium. In the Proccedings of COSSERAT+100, Int. Conference on the Legacy of "Theorie des Corps Deformables" by E. and F. Cosserat in the centenary of its publication. Ecole des Ponts ParisTech, 15-17 July 2009.

Grillo, A., Logashenko, D., Stichel, S., & Wittum, G. (2010a). Simulation of density−driven flow in fractured porous media. Advances in Water Resources, 33(12), 1494-1507.

Grillo, A., Lampe, M., Logashenko, D., Stichel, S., & Wittum, G. (2012). Simulation of salinity−and thermohaline−driven flow in fractured porous media. Journal of Porous Media, 15(5), 439-458.

Stichel, S., Logashenko, D., Grillo, A., Reiter, S., Lampe, M., & Wittum, G. (2012). Numerical methods for flow in fractured porous media. In J. Delgado (Ed.), Heat and Mass Transfer in Porous Media, Advanced Structured Materials, 13, Springer, 83-113.

Reiter, S., Logahenko, D., Stichel, S., Grillo, A., & Wittum, G. (2012). Models and simulations of variable−density flow in fractured porous media. Manuscript submitted for publication.

A5.4: Modelling Biogas Production

Ivo Muha, Johannes Schneider, Alfio Grillo, Gabriel Wittum

Biogas is the result of a cascade of biochemical reactions which produce methane out of the digestion of an organic input material. One possible organic material is crop. The process of biogas production starts with the collection of crops and finishes with the availability of methane. In order to optimise biogas production, the whole process has to be investigated. The first step of the process consists in harvesting the crops and storing them in appropriate silos. The storage problem arises because the crops, being harvested only a few times per year, have to be stored for quite a long time before being employed for gas production. If the crops were not stored in an optimal way, the digestion process would already begin while the substrate is in storage. Consequently, the total amount of methane, which could actually be produced in the biogas reactor, would decrease significantly. For this reason, the optimisation of the storage–process is also quite important.

During harvesting, crops are put into the silo by special delivery vessels. In the remaining time a vehicle tries to compress the stored crops in order to remove as much air as possible to prevent aerobic degradation and rotting of the stored crops. The next layer of harvested crops can be put into the silo, only after finishing the compression of the current top layer. This compression process is typically responsible for delays in harvesting, since trucks carrying harvested crops have to wait until compression is finished before unloading.

To give compression vehicle's drivers better control over the compression process, we developed a software tool. The developed software VVS (VerdichtungsVisualisierungsSoftware) helps the driver of the vehicle to visualise where the compression is not finished yet (see Figure 2). With this information, an optimal compression of the crops can be achieved and therefore a nature preserving usage of resources is supported.

Additionally, some other useful information is provided. For example, a 3D view of the silo itself can be drawn showing the different layers of the stored crops, which develop from the fact that the total amount of crops is not stored in the silo at once (see Figure 1). For using the latter feature, the software tool UG is used (Lang and Wittum 2005; Feuchter 2008). Full details about VVS can be found in (Muha et al. 2009).

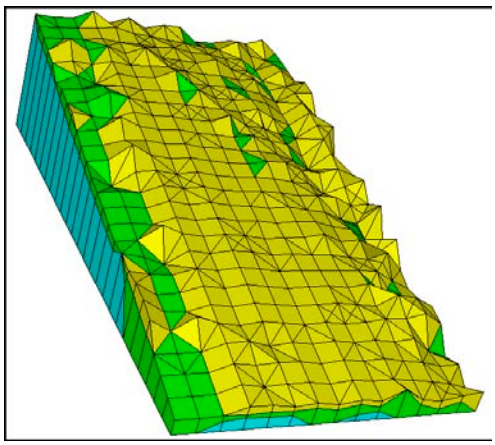

Figure 1. Visualisation of different silage-layers

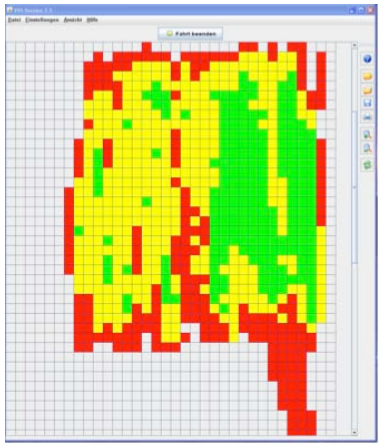

Figure 2. Visualisation process

After the storage–process has already been investigated, the focus of the current work is modelling of the biogas reactor itself. ODE based anaerobic digestion models have been common in the community since years, (Garcia et al. 1999). The Anaerobic Digestion Model no. 1 (ADM1) was published by the IWA TaskGroup (Batstone et al. 2002) and was since then used many times for modeling biogas reactors.

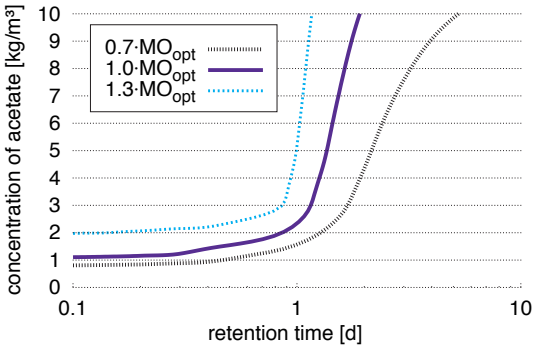

Figure 3. Optimal hydraulic retention time

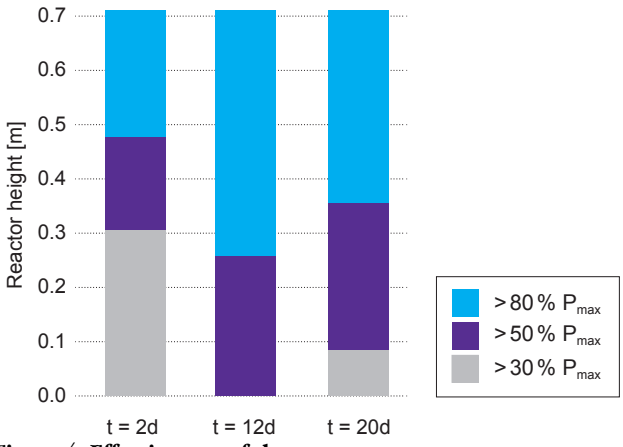

Figure 4. Effectiveness of the reactor

Since ADM1 consists only of ordinary differential equations, we generalised ADM1 to include spatial resolution. In addition, a 3D model for diffusion and flow inside the biogas reactor was developed and coupled with the generalized version of ADM1. The arising partial differential equations are highly nonlinear and are discretized with the finite volume method. The obtained set of linear equations is then solved by using the simulation framework *UG*.

The developed software was then, e.g., used to obtain the optimal hydraulic retention time depending on acetate concentration in the process liquid (see Figure 3). This information is crucial for a stable operation of biogas plants. Furthermore a measure for the effectiveness of the reactor P_{max} was defined and it was shown that current reactors are not working effectively (see Figure 4). A full discussion can be found in (Muha et al. 2012a).

Currently, the software is used to get some fundamental understanding of the anaerobic digestion process in 2–phase biogas reactors (Muha et al. 2012b).

References

Batstone, D. J., Keller, J., Angelidaki, I., Kalyuzhyni, S. V., Pavlovstathis, S. G., Rozzi, A., Sandersw, T. M., Siegrist, H., & Vavilin, V. A. (2002). Anaerobic Digestion Model No. 1. IWA TaskGroup on Mathematical Modelling of Anaerobic Digestion Processes, IWA Scientific Technical Report No. 13. London, UK: IWA Publishing.

Feuchter, D. (2008). Geometrie- und Gittererzeugung für anisotrope Schichtengebiete. Dissertation, Universität Heidelberg.

García-Ochoa, F., Santos, V.E., Naval, L., Guardiola, E., & López, B. (1999). Kinetic model for anaerobic digestion of livestock manure. Enzyme and Microbial Technology, 25, 55-60.

Lang, S., & Wittum, G. (2005). Large scale density driven flow simulations using parallel unstructured grid adaptation and local multigrid methods. Concurrency and Computation, 17(11), 1415-1440.

Muha, I., Grillo, A., Heisig, M., Schönberg, M., Linke, B., & Wittum, G. (2012a). Mathematical modeling of process liquid flow and acetoclastic methanogenesis under mesophilic conditions in a two−phase biogas reactor. Bioresource Technology, 106, 1-9.

Muha, I., Lenz, H., Feuchter, D., Handel, S., & Wittum, G. (2009). VVS eine Software zur Optimierung des Einlagerungsprozesses in Horizontalsilos. Bornimer Agrartechnische Berichte, 68, 35-43.

Muha, I., Zielonka, S., Lemmer, A., Schönberg, M., Linke, B., & Wittum, G. (2012b). Do two stage biogas reactors seperate the processes? Bioresource Technology. In preparation.

A6: Computational Fluid Dynamics
A6.1, M3: Turbulence Simulations and Application to a Static Mixer

Andreas Hauser, Vadym Aizinger, Andreas Vogel, Gabriel Wittum

In order to produce an accurate numerical solution for a turbulent flow problem of practical interest one has to make difficult choices involving some tradeoffs between computational efficiency and physical relevance. The 'brute force' approach of direct numerical simulation (DNS) needs no modelling assumptions, it incurs, however, huge computational overhead and is too expensive for most practical applications. In the Reynolds averaged Navier-Stokes equations (RANS) all turbulent motion modes are modeled by employing rather limiting assumptions; schemes of this type have been shown to perform poorly for large classes of important flow problems. The large eddy simulation (LES) represents a compromise between both approaches in which the large flow structures are computed explicitly and only the small ones need to be modeled. In spite of this reduction in the size of the numerical problem, the LES is still computationally intensive for complex flow problems, and the quality of the LES model deteriorates fast as the grids become too coarse. Since in a general flow situation flow regimes may vary widely in both time and space, significant computational savings can be achieved if the simulation software has the ability to flexibly adjust local mesh resolution to produce a numerical solution of required accuracy at minimum computational cost. This calls for an adaptive mesh refinement algorithm. However, most known adaptive grid refinement techniques are based on the assumption that the mathematical model does not change when the grid is refined. This assumption does not hold in the case of the LES model: The cutoff wave number of the turbulence model depends on the grid resolution, thus, changing grids means changing models.

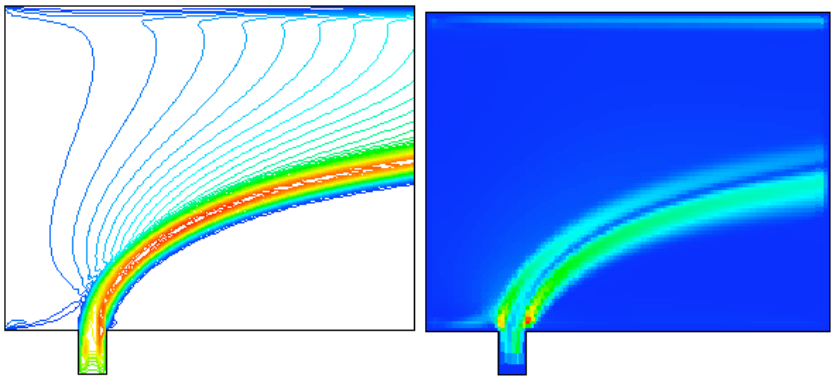

Figure 1. Kinetic energy (top) and eddy viscosity (bottom) for JICF-problem in quasi-steady state

To take advantage of adaptive methods in the LES context, we developed and tested a number of LES specific ***a posteriori*** error indicators. In particular, we looked at error indicators of four different types: Residual based indicators (estimating the size of the residual of the discrete Navier-Stokes equations), hierarchical basis based indicators (comparing our numerical solution to a solution in a higher dimensional discrete space), gradient jump based indicators (estimating jumps of gradients of the numerical solution over the element boundaries), and maximum indicators (heuristic indicators measuring values of a given quantity, in this case the turbulent eddy viscosity).

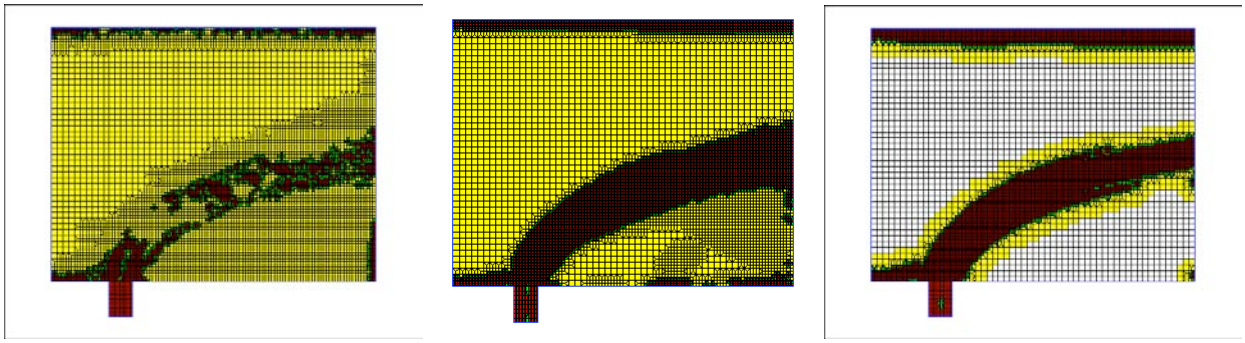

Figure 2. Jet in cross flow grid adaptively refined by residual, hierarchical, and maximum indicators (from left to right)

The grid adaptivity algorithms were applied to the well known jet-in-crossflow (JICF) problem in the configuration shown in Figure 1. In this setting, a fast jet of fluid exiting an orifice interacts with the ambient fluid moving in cross-wise direction. Figure 2 illustrates adaptively refined grids produced with the help of the residual, hierarchical basis, and maximum indicators. An evaluation of the modelling and discretisation components of error lead to a conclusion that the residual based indicator performs best of all tested error indicators.

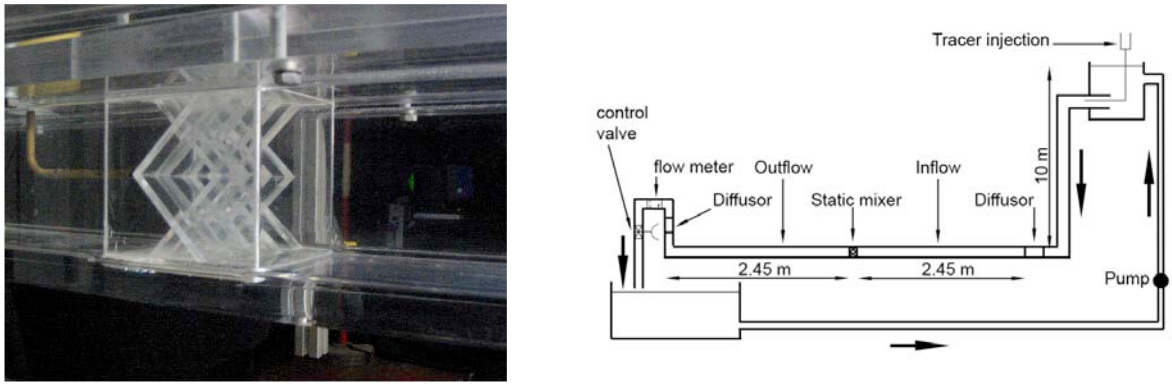

Figure 3. Side view of the static mixer (left), experimental setup (right)

An important application of advanced numerical techniques developed for incompressible flow is a static mixer problem where two or more fluids are mixed solely by the combined effect of advection and turbulence induced by the mixer geometry. This problem requires an additional equation to represent transport and mixing of a passive tracer. Simulation results were compared to the experiments performed by the group of Prof. Thévenin at the University of Magdeburg. Figure 3 illustrates the mixer geometry and the experimental setup.

One of the most important goals of this simulation was to reproduce experimental values of mixing quality indicators such as temporal or spatial mixing efficiency. It turned out that even on those grids that were too coarse to resolve fine flow and mixing structures the values of mixing indicators downstream from the highly turbulent zone right after the mixer were reasonably close in both, experimental and numerical cases. A comparison of the spatial efficiency (SMD) indices of the experimental measurements vs. laminar and turbulent numerical simulations is given in Figure 4. To improve the representation of mixing in the highly turbulent zone right after the mixer an adaptive mesh refinement scheme customised for mixing simulations appears to be a very promising avenue of further research.

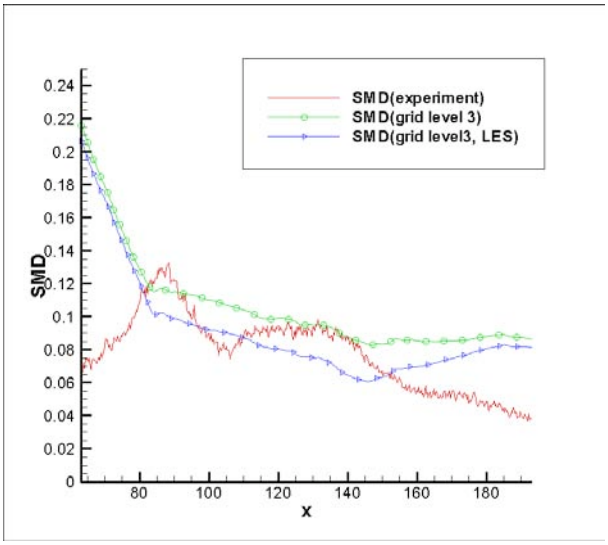

Figure 4. Comparison of spatial mixing efficiency index in the xy-plane cut after the mixer

References

Aizinger, V., Hauser, A., Wittum, G. (2010). Simulation of Flow and Transport in a Static Mixer Using Adaptive and Higher Order Numerical Methods. In H. Bockhorn et al. (Eds.), Heat and Mass Transfer, Micro and Macro Mixing: analysis, simulation and numerical calculation (pp. 245-262). Berlin: Springer

Gordner, A., Nägele, S., & Wittum, G. (2006). Multigrid methods for large-eddy simulation. In W. Jäger et al. (Eds.), Reactive Flows, Diffusion and Transport. Berlin: Springer.

Hauser, A., Wittum, G. (2006). Parallel Large Eddy Simulation with UG. High Performance Computing in Science and Engineering '06. Berlin: Springer.

Hauser, A., Wittum, G. (2008). Analysis of Uniform and Adaptive LES in Natural Convection Flow. In J. Meyers et al. (Eds.), Quality and Reliability of Large-Eddy Simulations (pp. 105-116). Dordrecht: Springer.

A6.2: Discontinuous Galerkin Method for Incompressible Navier-Stokes Equations

Vadym Aizinger, Gabriel Wittum

A high order adaptive numerical scheme for the incompressible Navier-Stokes equations is the ultimate goal of our work with the Discontinuous Galerkin (DG) method. A discretisation based on this method was developed and fully integrated in the UG package, including the time stepping algorithms as well as non-linear and linear solvers. A series of benchmarking tests comparing the performance and cost of the DG implementation to the node-centred second order Finite Volume solver (our standard package for the incompressible Navier-Stokes equations) produced encouraging results showing expected efficiency gains connected with the high order scheme. In particular, we simulated flow in a 2D driven cavity with Re= 10000. Figure 1 provides a comparison of vertical and horizontal midline velocity profiles for different grid levels and discretisations. These plots confirm that for large flow features high order numerical solutions can be more accurate on far coarser meshes than the standard Finite Volume method: E.g., compare the fourth order DG solution at grid level 2 (64 elements, 960 degrees of freedom) to the Finite Volume solution at grid level 5 (4096 elements, 2113 degrees of freedom). The advantages of high order methods appear to be less pronounced though when resolving small flow features. This situation is due to the fact that the element size must be at least comparable to the size of the simulated flow structures in order to be able to properly represent them.

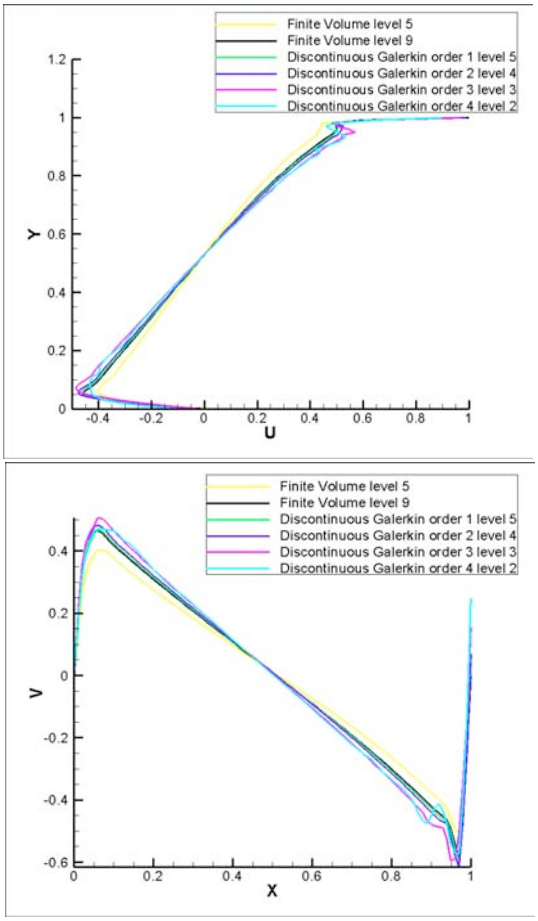

Figure 1. x-velocity at x=0.5(left) and y-velocity at y=0.5(right) for driven cavity flow with Re= 10000

To test the Discontinuous Galerkin solver on a more challenging application we simulated flow (without tracer transport) in the static mixer problem described in section A6.1. Figure 2 compares the averaged axial velocity profiles in a cross section right after the mixer. The difficulties that were seen in the driven cavity plots are even more obvious here: The Discontinuous Galerkin results capture well the positions and the values of extrema, but a coarse grid resolution prevents good representation of fine flow structures, even more so in the quadratic case. Fortunately, in addition to a high order discretisation, the Discontinuous Galerkin method possesses excellent adaptivity capabilities in grid resolution and approximation order that we plan to put to good use in addressing this issue.

The next test (Figure 3) concerns the power spectra of the axial velocity component at the point located on the main axis of the mixer. The experimental measurements (peak at ~0.36 Hz) agree rather well with the Finite Volume results, but both DG frequencies are a bit off: ~ 0.4 for the piecewise linear approximation on level 3 and ~0.43 for the piecewise quadratic approximation on level 2. One possible explanation is the absence of an LES model in our DG implementation resulting in an unrealistically low value of the viscosity term.

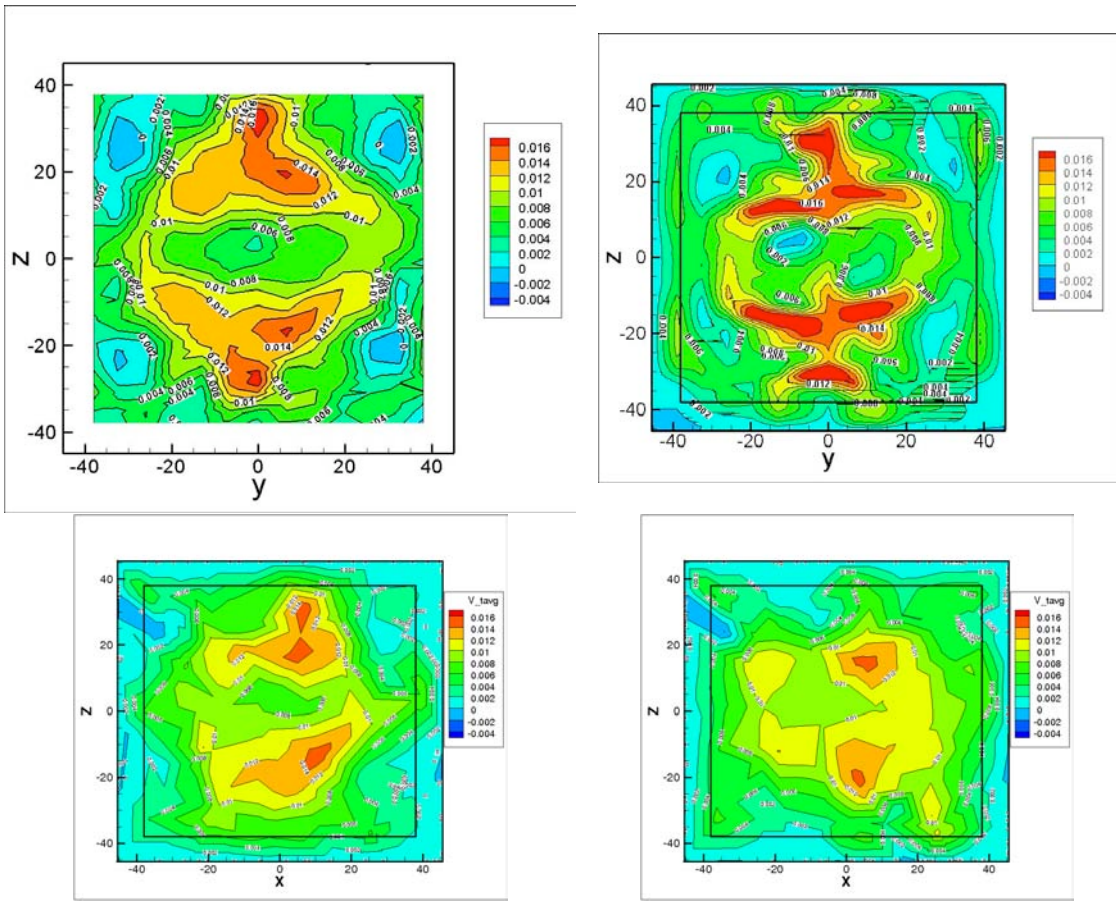

Figure 2. Axial velocity after the mixer
From left to right: top row: experiment, linear finite volumes at level 5; base row: linear DG at level 3, quadratic DG at level 2

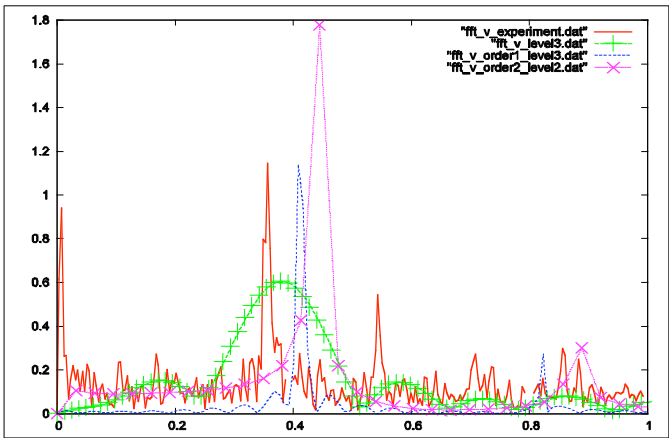

Figure 3. Power spectra of the axial velocity
Experiment, FV on level 3, linear DG on level 3, quadratic DG on level 2

References

Aizinger, V., Hauser, A., & Wittum, G. (2010). Simulation of Flow and Transport in a Static Mixer Using Adaptive and Higher Order Numerical Methods. In H. Bockhorn et al. (Eds.), Heat and Mass Transfer, Micro and Macro Mixing: analysis, simulation and numerical calculation (pp. 245-262). Berlin: Springer.

A6.3: Multiphase Flows

Peter Frolkovič, Dmitry Logashenko, Christian Wehner, Gabriel Wittum

One of the most active research fields in computational fluid dynamics is the numerical simulation of incompressible two-phase flow. This great interest has contributed to the development of many, often substantially different numerical methods for this kind of problems. One of them is based on the level set formulation in which the interface between two phases is represented implicitly by the zero level set of a smooth function (see also Section M4). This approach is easier to handle than other methods, that use a direct representation of the dynamic interface (e.g. Lagrangian-type methods, moving grids).

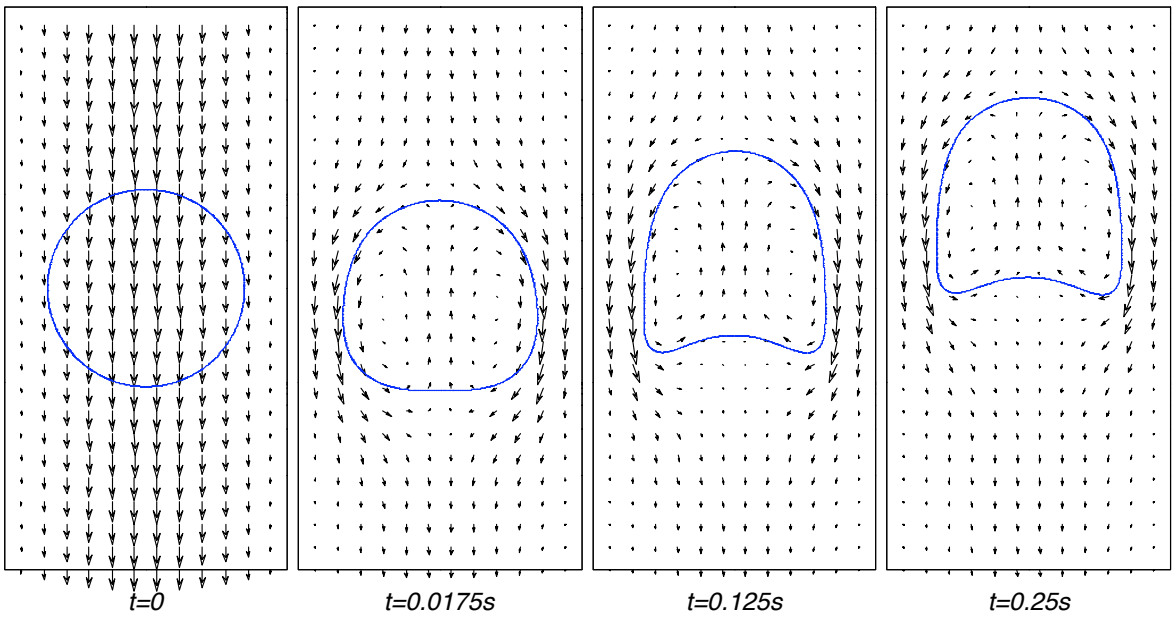

Figure 1. Evolution of a rising bubble in counterflow

The flux-based level set method for two-phase flow we developed (Frolkovič et al. 2008, Frolkovič et al. 2010) uses a sharp treatment of the numerical interface and requires no artificial post-processing steps for stable behavior. In numerical test examples computed with *ug*, it showed good mass conservation properties and negligible parasite currents.

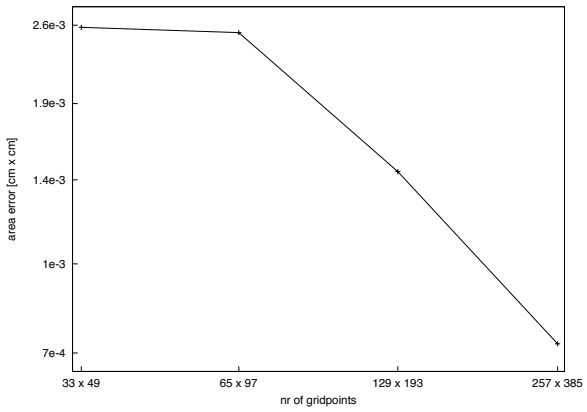

Figure 2. Error in the volume of the bubble at time t=0.25 on different grids for the experiment depicted in Figure 1

The method applies analogous finite volume discretisations to the local balance formulations for the conservation of momentum, mass and level sets on identical vertex-centered control volumes. To enable the sharp treatment of the interface condition in the method, we extend the approximation spaces for the pressure and the velocity by additional degrees of freedom for the elements intersected by the interface. This method can be implemented by a relatively simple extension of an existing finite volume discretisation for the single-phase Navier-Stokes equations. In our case, we used the collocated discretisation from Nägele and Wittum (2007). As discretisation method for the level set equation we use the flux-based level set method (Frolkovič and Mikula 2007).

The approximation of the curvature is computed using quadratic interpolation of the level set function on a refined grid. In each time step, we refine only the elements that are near or at interface and use this locally refined grid only for the numerical solution of the level set equation.

It is common, to use a signed distance function as initial level set function, that means a distance function for the interface with negative sign in the inside region and positive sign outside. In general, the level set function can develop very steep or flat gradients in the region around the interface during computation. This causes essential difficulties in numerical computations, e.g., inaccurate computation of the curvature. To avoid this, it is reasonable to replace the level set function at certain time steps with a signed distance function, that has the same zero level set. This "reinitialisation" process is done by solving a reinitialisation equation using the flux-based level set method.

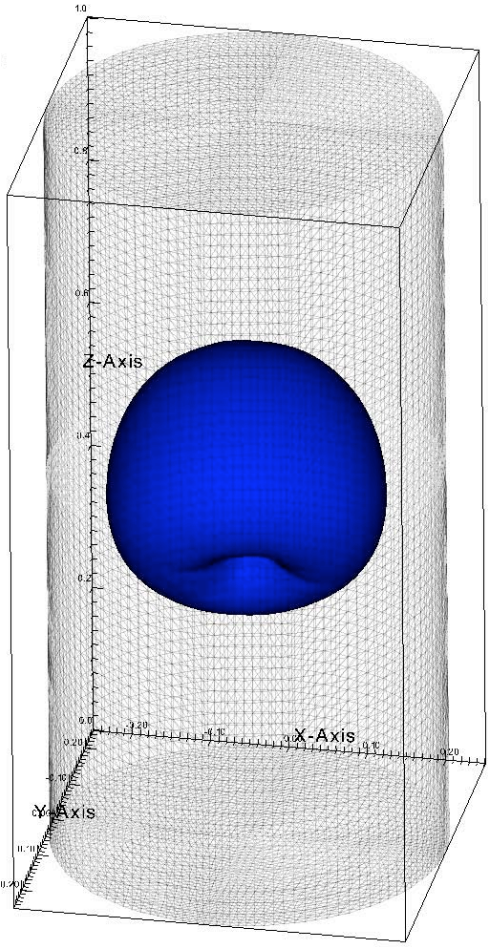

Figure 3. Simulation of a rising bubble in 3D

Numerical tests confirmed convergence and stability of the described method. For sufficiently fine grids, grid-independent numerical solutions for the tested problems were obtained. The test problem illustrated in figure 1 is the simulation of a rising bubble in counterflow. The density is set to 0.995 g/cm³ outside the bubble and 0.001107 g/cm³ inside, the viscosity is set to 0.104 dyn s/cm² outside and 0.048 dyn s/cm² inside, the surface tension factor is set to 2 dyn/cm and the gravitation constant is 980 cm/s². A parabolic profile of the inflow velocity is prescribed as boundary condition on the top (the maximum velocity is 4 cm/s), zero velocities are prescribed on the left and right side and on the lower side a zero stress outflow-boundary condition is used. Initially, the bubble is a circle with radius $R=0.175$ cm. During the computation, the bubble is pressed upwards due to gravitation, but at the same time, the incoming fluid hinders the bubble to move up. Although the interface is deformed, the volume of the bubble should remain constant.

Numerical mass conservation is not guaranteed by the level set formulation, so conservation of mass is an important issue for two-phase flow level set methods. In Figure 2, the mass conservation error observed on different grid levels for the test problem at time $t=0.25$ is plotted, we note convergence to zero with first order of accuracy.

Figure 3 presents an analogous test case of a rising bubble in a cylinder in three dimensions.

References

Frolkovič, P., Logashenko, D., Wehner, C., & Wittum, G. (2010). Finite volume method for two-phase flows using level set formulation. Preprint 2010-10, Department of Mathematics and Descriptive Geometry, Slovak University of Technology, Bratislava 2010.

Frolkovič, P., Logashenko, D., & Wittum, G. (2008). Flux-based level set method for two-phase flows. In R. Eymard, J.-M. Herard (Eds.), Finite Volumes for Complex Applications V (pp. 415-422). London: ISTE and Wiley.

Frolkovič, P., & Mikula, K. (2007). High-resolution flux-based level set method. SIAM Journal on Scientific Computing, 29(2), 579–597.

Nägele, S., & Wittum, G. (2007). On the influence of different stabilisation methods for the incompressible Navier-Stokes equations. Journal of Computational Physics, 224(1), 100–116.

A7: Computational Electromagnetism
A7.1: The Low Frequency Case

Oliver Sterz, Andreas Hauser, Gabriel Wittum

An important class of electromagnetic problems comprises low-frequency applications where the magnetic energy dominates the electric energy. Examples are devices from power engineering like motors, generators, transformers and switch gears as well as medical hyperthermia applications in cancer therapy. Here, the eddy-current approximation of the full Maxwell equations can be used to describe the electromagnetic fields. The governing equations read

$$\mathbf{curl}\,\mathbf{E} = -i\omega\mu\mathbf{H}\,, \quad \mathbf{curl}\,\mathbf{H} = \mathbf{J}_G + \sigma\mathbf{E} \quad \text{in } \mathbb{R}^3\,,$$

where **E** and **H** are the electric and the magnetic field respectively; $\mathbf{J}_G$ is an excitation current density, σ denotes the conductivity and μ the permeability.

The eddy-current model is transformed into a variational formulation with the electric field as an unknown variable. For the computation of real-world problems, the adaptive finite element software EMUG (electromagnetics on unstructured grids) has been developed, based on the simulation toolbox $\mathcal{UG}$. The discretization is carried out by so-called edge elements (Whitney-1-forms) as the most natural choice. In particular, edge elements have the advantage that discrete potentials are computationally available.

To solve the linear systems of equations with up to two million unknowns on a single-processor machine, a fast method is essential. Multigrid methods are applied since they offer optimal complexity. The smoothing in the multigrid cycles needs special treatment and is based on a Helmholtz decomposition, see Hiptmair (1999). To ensure the optimal complexity even for locally adapted grids, the smoothing is restricted to the refined region (local multigrid). In the case of non-conductive sub-domains, the stiffness matrix becomes singular. An approximate projection procedure is applied to prevent cancellation errors caused by increasing kernel components of the solution, see Sterz (2002).

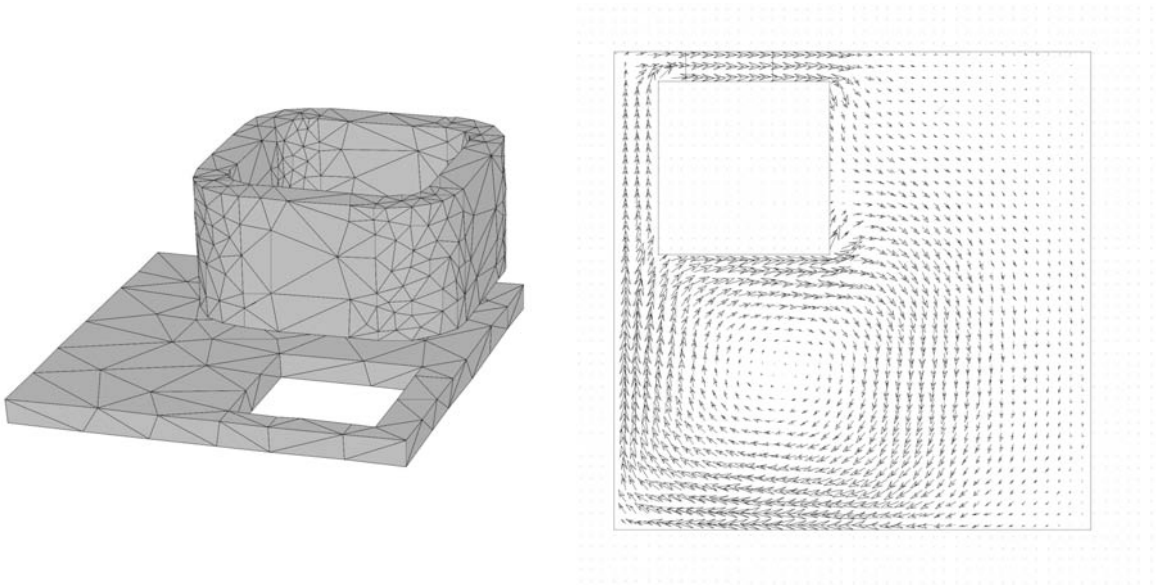

Figure 1. Coarse triangulation of the TEAM benchmark problem 7, the air-region triangulation is not displayed. The problem consists of an excitation coil that induces eddy currents in the aluminium plate below (left). Induced current distribution in the middle of the aluminium plate (right).

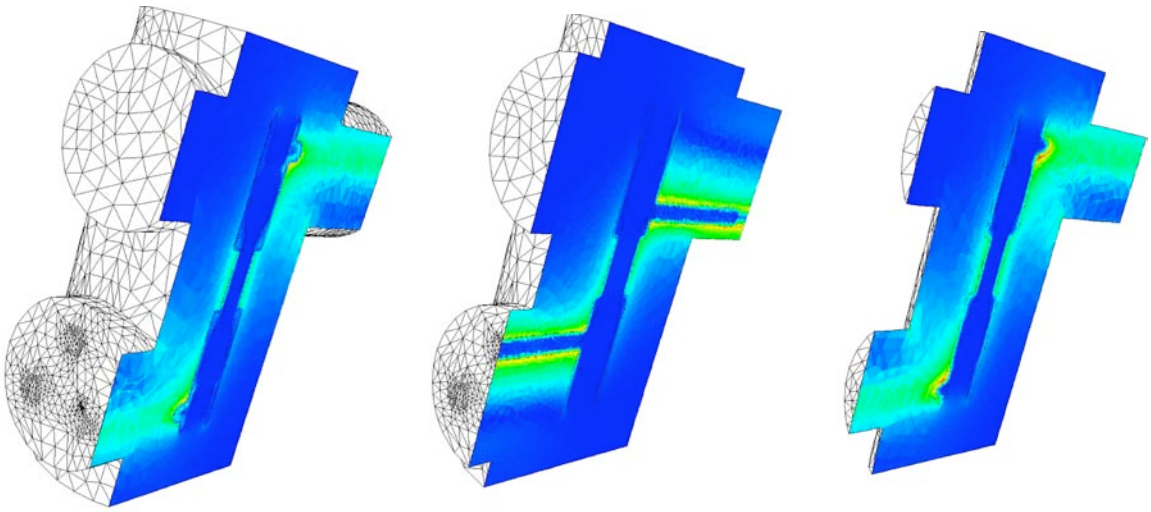

Figure 2. Magnitude of the magnetic field in a gas-insulated switch gear along different cutting planes

The software EMUG has been successfully employed for benchmark problems (see Figure 1) as well as realistic applications (see Figure 2). A parallel prototype of the electromagnetic simulation tool is currently being developed.

From the known fields and currents, force densities and Ohmic losses can easily be computed. The Ohmic losses give rise to heat generation in the conductors. In order to compute the temperatures in general cooling, effects of fluid flow, diffusion and radiation must be considered. This will lead to coupled problems of electromagnetics and heat transfer (multiphysics) since the conductivity depends on the temperature.

References

Hiptmair, R. (1999). Multigrid method for Maxwell's equations. SIAM Journal on Numerical Analalysis, 36(1), 204–225.

Hiptmair, R. & Sterz, O. (2003). Current and voltage excitations for the eddy current model. Eidgenössische Technische Hochschule, Research report / Seminar für Angewandte Mathematik No. 2003-07.

Sterz, O. (2002). Multigrid for time harmonic eddy currrents without gauge. In Scientific Computing in Electrical Engineering. Proceedings of the 4th International Workshop Scientific Computing in Electrical Engineering, Eindhoven, The Netherlands, June 23–28, LNCSE. Berlin: Springer.

Sterz, O. (2003). Modellierung und Numerik zeitharmonischer Wirbelstromprobleme in 3D. Whitney- Elemente, adaptive Mehrgitterverfahren, Randelemente. Dissertation, Universität Heidelberg.

Sterz, O., Hauser, A., & Wittum, G. (2006). Adaptive Local Multigrid Methods for the Solution of Time Harmonic Eddy Current Problems. IEEE Transactions on Magnetics, 42(2), 309-318.

A8: Reduction of Numerical Sensitivities in Crash Simulations

Raphael Prohl, Alfio Grillo, Gabriel Wittum

The simulations of crash tests are very sensitive numerical procedures, which require very accurate and robust algorithms in order to handle numerical instabilities. In addition to these, also physical instabilities, which may be due, for example, to the bifurcation behavior of the material under asymmertic loading, have to be detected and correctly treated by the numerical procedures in order to obtain reliable results. In this context, our task in the project "HPC-10 Reduzierung numerischer Sensitivitäten in der Crashsimulation auf HPC-Rechnern" is to identify and eliminate numerical instabilities and improve the mathematical analysis of the physical ones.

In a first step we started with the examination of the stability of some algorithms taken from the industry, where full-vehicle-models are normally used. We reduced these models in order to investigate their main features and dealed with formulating an appropriate mathematical model of a crash test. To this end we considered a non-linear material behavior for large elastic and plastic strains. This led to a non-linear system of partial differential equations coupled with an evolution law for plastic distortions. The latter law was expressed through a plastic flow rule. We concentrate on geometrical and kinematical non-linearities, non-linear material description, elasto-plastic material description, contact simulations, and their impact on the observed instabilities. To perform contact simulations we closely cooperate with the group of Prof. R. Krause.

Our mathematical model is based on the introduction of a hyperelastic stored energy function W, so that the second Piola-Kirchhoff stress tensor reads

$$S_e = \frac{\partial W}{\partial E}.$$

We adopt the Kröner's multiplicative decomposition of the deformation gradient $F = F_e F_p$, where F_e and F_p denote the elastic part of deformation and the plastic distortions, respectively. The crucial step in formulating the model is the determination of an evolution law for F_p. Initially we used an associative flow rule, which is determined by the principle of maximum plastic dissipation and a flow condition f, cf. J.C. Simo and T.J.R. Hughes (1998). By letting B, ρ_0, τ, $C_p = F_p^T F_p$ and $b_e = F_e F_e^T$ denote body forces, the reference density, the Kirchhoff stress tensor, the plastic Cauchy-Green strain tensor and the elastic finger tensor, respectively, the equations to be solved are (formulated in Lagrangian description):

$$\begin{aligned} -\operatorname{DIV}(FS_e) &= \rho_0 B \\ \frac{\partial \overline{C_p}^{-1}}{\partial t} &= -\frac{2}{3}\gamma \operatorname{tr}[b_e] F^{-1} \frac{\operatorname{dev}[\tau]}{\|\operatorname{dev}[\tau]\|} F^{-T} \\ \gamma \geq 0,\ f(\tau) &\leq 0,\ \gamma f(\tau) = 0 \end{aligned}$$

The model presented above will be extended to a rate-dependent elasto-plastic model, consistent to the work of Micunovic et al. in 2011.

The numerical computations of the quasi-static case are performed by an incremental procedure which contains a non-linear sub-problem in every single incremental step. To treat the governing equations of plasticity, we firstly adopted the well-established return-mapping-algorithm and the consistent-tangent-method for the linearization therein. As remarked in Wieners (2007), this plasticity-algorithm may be turn instable because it computes stresses that do not necessarily satisfy the global equilibirum equations. Therefore we developed a new class of solution methods with better mathematical properties by reviewing the plasticity problem in the context of nonlinear programming. We achieve higher robustness by additionally linearizing the constitutive equations and the governing equations of

plasticity. Hence, our method is an extension of the algorithm proposed in Wieners (2007) to the case of finite deformations.

The implementation of the return-mapping-algorithm for finite deformations in our software framework $\mathcal{UG}$ has been tested by some benchmark problems. As a reference for our numerical tests, we used a shear/compression-test of the unit-cube with perfect plastic behavior and the well-documented necking of a circular bar as an example for exponential hardening behavior.

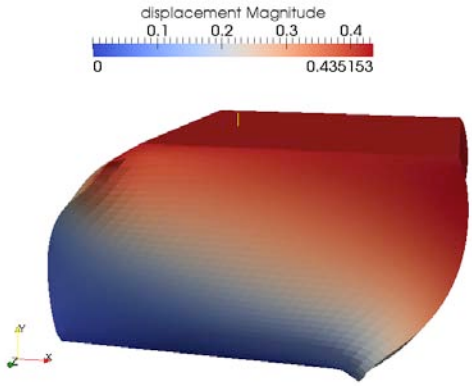

Figure 1. Unit cube in a shear/compression test

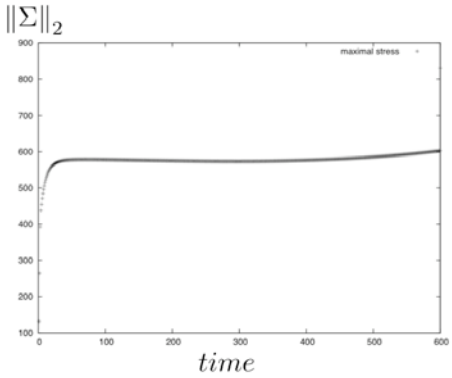

Figure 2. Max. Stress at the midpoint of the cube

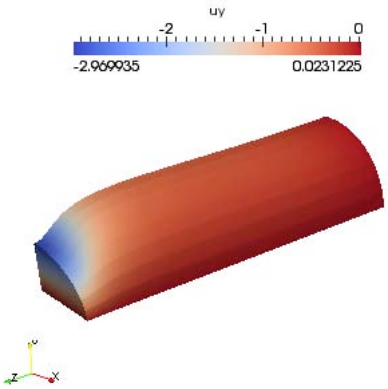

Figure 3. 1/8th of circular bar in a tensile test

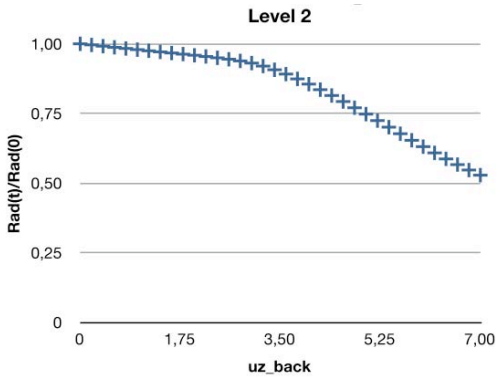

Figure 4. Change of necking area in time

References

Krause, R. (2009). A Non-Smooth Multiscale Method for Solving Frictional Two-Body Contact Problems in 2D and 3D with Multigrid Efficiency. SIAM Journal on Scientific Computing, 31(2), 1399-1423.

Micunovic, M.V., Albertini, C., Grillo, A., Muha, I., Wittum, G., & Kudrjavceva, L. (2011). Two dimensional waves in quasi rate independent viscoplastic materials. Journal of Theoretical and Applied Mechanics, 38(1), 47-74.

Wieners, C. (2007). Nonlinear solution methods for infintesimal perfect plasticity. Journal of Applied Mathematics and Mechanics, 87(8-9), 643-660.

A10, M9, T8: 3D Visualisation of Heidelberg Castle in 1680

Babett Lemke, Matthias Kleiser, Michael Lampe, Arne Nägel, David Wittum, Gabriel Wittum
in co-operation with Matthias Untermann, History of Art Heidelberg University.

The goal of the project is to create a virtual scene movie, in which the camera flies through the Castle of Heidelberg, as it was in the late 17th century. Around the year 1680, the castle‘s architectural value and its upgrading state reached its historical peak, while today most of the buildings are either ruined or even have disappeared completely. So these buildings first have to be completed using all the accessible information such as old engravings, paintings, construction plans and reconstructions already conducted.

The scene itself is then built as a wireframe model using CAD-modelling software, allowing three-dimensional visualisation of any kind of objects as well as generating photorealistic scenes and animations in high quality. The individual buildings and the area surrounding Heidelberg Castle are composed from basic objects and graphic primitives using the modelling functions of the CAD software.

To get a realistic view of the scene, the surfaces are finished with materials and textures, obtained from corresponding digital photos or existing libraries. The textures used in our model are restricted to simple material structures, while all relevant architectural contours, especially the visible structures near the camera's flight path, are modelled in greater detail.

In the course of modelling, we found that plenty of the objects had to many details to be modelled fully. This refers in particular to the facades of Otto-Heinrichs-Bau and Friedrichsbau which contain a lot of elaborate ornaments and statues. It was immediatley clear that complexity made it impossible to model these details as three dimensional objects. Thus we were left with texture mapping. Modern modelling software provides sophisticated methods of texture mapping, however, they are still lacking reality in modeling 3d objects for a moving observer.

To answer the question, what path an observer or a camera is allowed to follow while preserving the illusion of a full three dimensonal object even though modeling uses some sort of texture mapping, characteristics of three dimensional viewing have been derived and described mathematically (Lemke, 2007). This mathematical model describes the difference between percieving a three dimensional object and a two dimensional view using various kinds of texture mapping. The corresponding criteria allow to choose a path for the camera across the virtual scene a priori, and to select a texture mapping still preserving the illusion, but strongly reducing modelling complexity in each point of the path. Finally, light and surface effects contribute substantially which are included in the model.

Figure 1. Ökonomiegebäude and Brunnenhalle today

Figure 2. CAD-model of Ökonomiegebäude and Brunnenhalle

Figure 3. Ottheinrichs-Bau: Portal (from: Koch/ Seitz, Das Heidelberger Schloß)

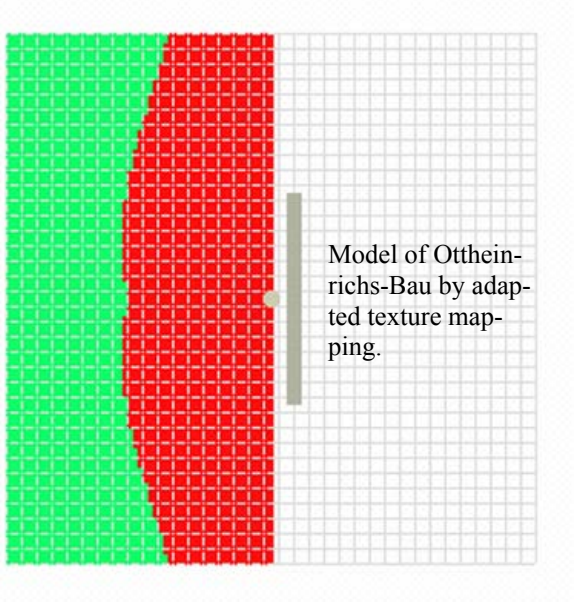

Figure 4. Allowed (green) and forbidden (red) observer locations around the portal of Ottheinrichs-Bau

The flight through the scenery of Heidelberg Castle is then realised in a sequence of single images, defined by position, view direction and zoom factor of the camera, all separately rendered and combined to a movie scene. In order to give an impression of smooth motion, ≥ 25 frames per second are necessary. This, together with realistic light effects, requires great computational power. We chose ray tracing as the rendering technique. This technique will be performed by POVRAY, an open-source software, which we extended for the purpose of internet computing. The software will run also on parallel clusters.

The rendering task is to be organised within the framework of a competition, where packages of single scenes are provided for work via internet. Participants download, render and then send back the images to a collecting and controlling server station. Its software and the web interface has also been developed at SiT in close co-operation with the Institute for Theoretical Astrophysics at the University of Tübingen. The pictures separately rendered are finally put together as a movie sequence, a virtual flight through Heidelberg Castle in the year 1680. This project has no financial support, it is run by students on a voluntary basis.

Ths visualisation methods developed here will be applied also to other objects like the visualisation of neural cells processed by NeuRA (see A2).

References

Lemke, B. (2007). Merkmale dreidimensionaler Objektwahrnehmung - Eine mathematische Beschreibung. Diplomarbeit, Mathematik, Universität Heidelberg.

Koch, J., & Seitz, F. (1887). Das Heidelberger Schloss. 2 Bände, Darmstadt.

A11: Computational Acoustics: Eigenmodes of Musical Instruments

Martin Rupp, Gabriel Wittum

What determines the sound of a guitar? A string can vibrate with all natural multiples of its fundamental frequency. The fundamental frequency is also called the first harmonic overtone, the second harmonic overtone is twice the fundamental frequency and so on. It is the amplitude of the first ten harmonic overtones which characterise the tone. A vibrating string alone hardly produces any audible sound at all, so all string instruments (like the guitar or the piano) need resonance bodies. When a string is excited, the vibration is carried over to the resonance body, which, due to its larger area, makes the vibration audible.

However, these resonance bodies have resonance frequencies, so the amplification is not independent of the frequency: Frequencies close to a resonance frequency will be amplified more than others, but do also fade away faster, because the resonance body drains more energy from the vibrating string resulting in a higher damping of this frequency. In other words: The amplitudes of the overtones of a vibrating string are filtered by the resonance body. This also supports Schumann's theory of the so-called "formants", i.e. amplitudes of overtones (Schumann 1929): An overtone is amplified stronger than others if its frequency lies in a frequency range which is characteristic for an instrument, independent from the fundamental frequency of the tone or the order of the overtone (when played with the same intensity).

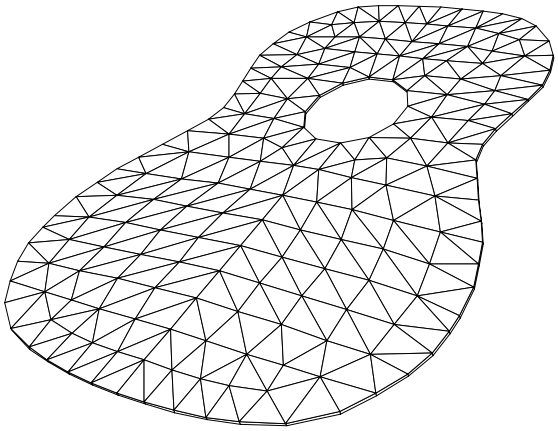

Figure 1. Simple geometry for the guitar top plate

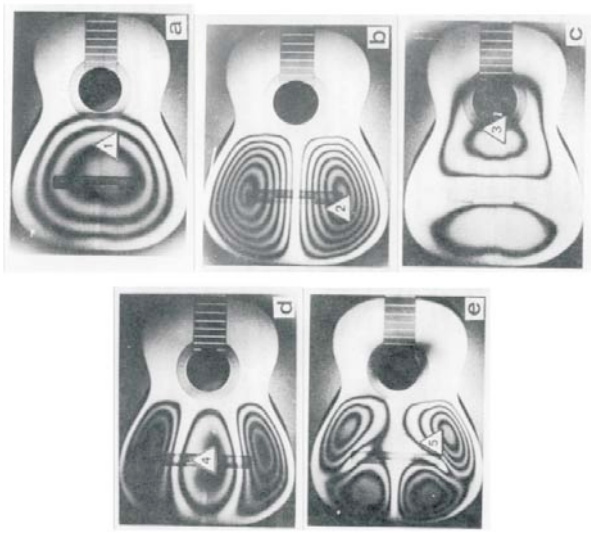

Figure 2. Experimental results from Molin/Stetson (Jansson 1983)

We started studying the top plate of a guitar. This is the first step towards characterizing the formants of this instrument by computation. The elasticity of the top plate is modeled by linear elasticity, so we get a system of partial differential equations. Because wood has different strength (elasticity coefficients) in the direction from the roots to the top, from the inner to the outer annual rings, and tangential to the annual rings, we get an anisotropic elasticity tensor.

In our approach, we directly used a full three-dimensional model, because we want to study the three-dimensional effect of the bracings of the top plate. Bracings are wooden sticks glued to the top and the back plate to support the large free thin surface area of the plates. Since they allow the resonance body to be larger and thinner, and therefore the guitar to be louder, they can be found in every guitar since the introduction of the traditional fan-bracing by Antio de Torres Juan in the 19th century. The top plate is over 30 cm long and wide, but only around 2 mm thick (Figure 1), resulting in a very challenging geometry.

The discretisation is done by finite elements. The computation of resonance frequencies of the resulting system leads to a generalised eigenvalue problem $Ax = \lambda Bx$. The eigenvectors with the smallest eigenvalues correspond to

the eigenmodes with the lowest frequency. We are interested in the five to six eigenmodes with lowest frequency. We solve these eigenvalue problems with a special kind of projection method, the Local Optimal Block Preconditioned Gradient (LOBPCG) Method, introduced in 2001 by Knyazev. With this method, we can calculate several eigenvalues at once. Another advantage of LOBPCG is that it does not need much space in computer memory.

As the name LOBPCG suggests, we need to precondition it, that means, we have to find a approximate solution x of the linear equation system $Ax = b$. For this purpose we use an Algebraic Multigrid (AMG) Method, since geometric multigrid is not able to cope with the highly anisotropic nature of the discretisation matrix A, which results from the anisotropic geometry and the anisotropic elasticity tensor of wood. Another problem is the large number of free boundaries: Since the top plate is only clamped at the outer edges, the top and the bottom are free boundaries. This causes problems with standard AMG methods, so we chose to use the Filtering Algebraic Multigrid (FAMG) method introduced by Christian Wagner in 2000. This AMG method is especially advantageous for linear elasticity problems with large number of free boundaries.

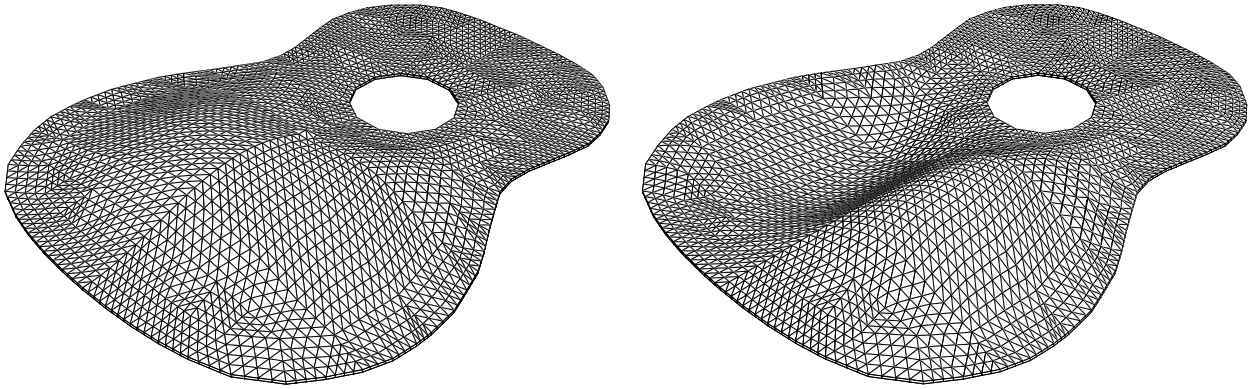

Figure 3. Results of our simulation, first (177 Hz) and second (200 Hz) eigenmode of the guitar top plate

In our work (Rupp 2009), we calculated the eigenmodes of the guitar top plate without bracings (Figure 3), and found reasonable agreement with the results from Jansson (1983; Figure 2), although the results show that the influence of the bracings cannot be neglected. In the next step, we will incorporate bracings in our model, and, in a later one, the coupling with the air inside the guitar. We also studied the behaviour of LOBPCG and similar algorithms depending on the strength of the preconditioner and how far "backwards" the algorithm may look, showing that for hard problems (in terms of solving the system $Ax = b$), the calculation is faster when the algorithm may look farther behind, whereas for easy problems, it can be beneficial to do this only for the last eigenvalues.

References

Jansson, E. V. (1983). Function: construction and quality of the guitar. Papers given at a seminar organised by the Commitee for the Acoustics of Music, Royal Swedish Academy of Music, Stockholm.

Knyazev, A. V. (2001). Toward the Optimal Preconditioned Eigensolver: Locally Optimal Block Preconditioned Conjugate Gradient Method. SIAM Journal of Scientific Computing, 23(2), 517-541.

Nägel A., Falgout R. D., & Wittum G. (2008). Filtering algebraic multigrid and adaptive strategies. Computing and Visualization in Science, 11(3), 159-167.

Schumann, E. (1929). Physik der Klangfarben. Habilitationsschrift, Universität Berlin.

Rupp, M. (2009). Berechnung der Resonanzschwingungen einer Gitarrendecke. Diplomarbeit, Fakultät Mathematik, Universität Heidelberg.

Wagner C. (2000). On the algebraic construction of multilevel transfer operators. Computing, 65(1), 73-95.

M1: Fast Solvers for Large Systems of Equations: Filtering Algebraic Multi-Grid (AMG) and Transforming Iterations

Ingo Heppner, Babett Lemke, Arne Nägel, Christian Wagner, Christian Wrobel, Gabriel Wittum

Introduction

The aim of this project is to develop efficient methods to compute approximate inverses or preconditioners for large systems of linear algebraic equations

$$A\,u = f, \tag{1}$$

with a sparse system matrix A and vectors of variables (unknowns) u and right-hand side f ($A \in \mathbb{R}^{n*n}$, $u, f \in \mathbb{R}^n$), not necessarily arising from the discretisation of second-order elliptic partial differential equations (PDEs) on a grid $\mathfrak{G}$ resolving the domain Ω ($\Omega \in \mathbb{R}^d$, $d \in \{1, 2, 3\}$).

The basic idea behind all multi-grid methods is the use of corrections computed on a coarser grid (coarse-grid corrections) with a corresponding smaller system of linear equations whenever an explicit iteration method (smoother) is unable to relax the error efficiently in order to accelerate convergence for a given fine-grid problem. This principle can be applied recursively on a sequence (hierarchy) of coarser and coarser grids, where each grid level is responsible for eliminating a particular frequency bandwidth of errors. To apply the method, one needs, in addition to the hierarchy of grids, smoothers (maybe level dependent), coarse-grid analogues of (1) (i.e. coarse-grid operators) and intergrid transfer (interpolation) operators to transfer residuals and corrections between the grid levels.

For the efficiency of standard (geometric) multi-grid, a “smoothed error” (i.e. an error that can no longer be efficiently reduced by the smoother) has to be smooth in a *geometrical* sense. Otherwise, linear interpolation, and therefore the coarse-grid correction, does not work well enough. But in general “smoothed error” may not be smooth in a geometrical sense: A closer look (e.g. at anisotropic problems) shows that if the coarse-grid correction fails, a “smoothed error” can, in general, only be regarded as “*algebraically* smooth” (in the sense that it is the result of an algebraic smoothing operation) and is no longer eliminated. In addition, it would be preferable for a solver for an algebraic set of equations that it doesn't need such an auxiliary construction as a geometric hierarchy of grids.

In order to apply the multi-grid idea to more general problem classes, algebraic multi-grid (AMG) is an attempt to abstract or generalise the multi-grid ingredients “grid”, “linear interpolation” and “smoothness” (better denoted as “slowness-to-converge”), which are by nature spatial or geometrical, to algebraic concepts: The term “grid” is replaced by “the graph of the system matrix”, and the concepts of “linear interpolation” and “smoothness” are generalised in an algebraic sense (“algebraised”). From this point of view, it may be better to refer to an “algebraic multi-graph method”.

The emphasis in AMG is on automatic coarsening and adaptation to the problem to be solved (optimally, to get a black-box solver). Algebraic multi-grid methods consist of a set-up phase in which the coarse graphs, the intergrid transfer operators and the coarse-grid operators are constructed in a (more or less) purely algebraic manner. Especially the coarse-level operators A_H are constructed by the Galerkin approach

$$A_H = r\,A_h\,p, \tag{2}$$

where A_h denotes the system matrix on the respective next finer level, and r and p denote the restriction and prolongation operator respectively.

After the set-up phase, standard multi-grid algorithms with the operators constructed above can be applied in the usual way to get the approximate inverse of (1). All algorithms introduced in the following are based on the software toolbox UG ("Unstructured Grids", Bastian and Wittum 1994; Lang and Wittum 2005).

Automatic Coarsening (AC)

In many scientific and engineering applications, the spatial objects under consideration have very complicated shapes containing a huge number of geometrical details on different scales. AC (Feuchter et al. 2003) is a multi-grid solver for the discretisation of partial differential equations on such complicated domains. As input the algorithm only requires a given grid, fine enough to resolve such complicated shapes, and the discretisation on this grid, instead of a hierarchy of discretisations on coarser grids. In a set-up phase, these coarse auxiliary grids are generated in a black-box fashion trying to resemble the structure of the given grid, i.e. its "element density", and are used to define purely algebraic intergrid transfer and coarse-grid operators. This adaptation process results in a stack of geometrically nested auxiliary grids $\mathfrak{G}_i \supset \Omega$, $i = 0, \ldots, l_{max}$.

Thus, to a certain extent this approach is similar to AMG: for a given fine grid, a hierarchy of coarser grids is created. However, this is not in the spirit of algebraic multi-level approaches since there is no matrix dependence, neither of coarse grid selection nor of building the intergrid transfer and coarse grid operators. Also, as opposed to AMG, the coarsening process does not proceed from the given fine grid towards increasingly coarser grids but an adaptation process moves from a very coarse grid towards the given fine grid(s). This approach can therefore be called "semi-algebraic".

Since a naive implementation of this accommodation process would require a lot of search operations with complexity $O(N^2)$ (N being the number of elements in the given grid), we utilise a quadtree data structure for a far better complexity of $O(j)$ (j being the number of levels), accelerating the set-up phase significantly.

Schur-complement multi-grid (SchurMG)

The Schur-complement multi-grid method was constructed as a robust multi-grid method for the interface problem arising from the discretisation of the convection-diffusion equation with strongly discontinuous coefficients in groundwater flow (Wagner et al. 1997). It is based on an idea by Reusken (Reusken 1994). These and the coarse grid operators are matrix dependent, but the coarse-grid selection is not (as in AC), so that this method can also be called "semi-algebraic". The coarse-grid selection of the fine grid and the reordering of the vector of unknowns u (and also of right-hand side vector f) so that all variables belonging to fine-grid points and all variables belonging to coarse-grid points are blocked and consecutive, induces a 2 x 2 block structure of the system matrix A. Block factorisation then leads to inverses of the fine-fine block and the Schur complement which would provide the solution in one step if computed exactly. Since the matrix is neither sparse nor easy to invert, one has to approximate the system matrix (lumping) to get a recursively applicable method. One can show that the Schur complement of the modified system matrix corresponds to the Galerkin approach with appropriate intergrid transfer operators.

Standard AMG

The set-up phase of the classical AMG method, in the following called RSAMG, as introduced in the fundamental paper (Ruge and Stüben 1987), is based on the concept of "strong coupling" and the notion of "slow-to-converge" error which guide the automatic coarsening process and the construction of appropriate intergrid transfer operators to ensure that each fine variable is well interpolated from a (small) subset of coarse variables. Coarse-grid equations are constructed by the Galerkin approach.

Here, a variable v_i is said to be "strongly connected to" another variable v_j from its neighbourhood if for a fixed parameter ϑ ($0 < \vartheta \leq 1$):

$$|a_{ij}| \geq \vartheta \max_{l \neq i} (|a_{il}|). \tag{3}$$

The aim of the coarsening process is that each fine variable has at least one strong coupling to a coarse variable to achieve good interpolation and that there is, as far as possible, no pair of coarse variables that are strongly connected to each other (i.e. coarse variables should form a maximal independent set) to limit the size of the coarse grid and thus the work which has to be done on it. The interpolation weights are then determined via the solution of the residual equation for an error variable.

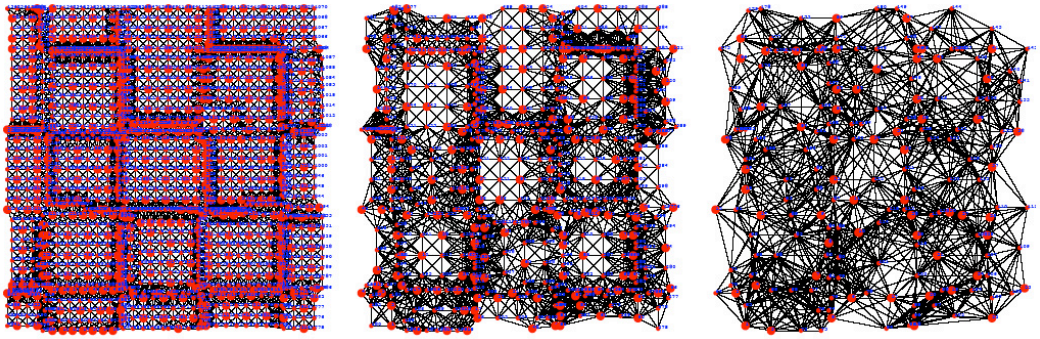

Figure 1. RSAMG coarsening of an originally uniform grid for a diffusion problem with checkerboard heterogeneity. The interfaces are clearly visible on the coarse grid (left)

Filtering and Filtering Algebraic Multigrid

Filtering is another technique for solving linear systems $Ax = b$. It is based on the filtering property: Find an approximate inverse M, such that:

$$Mt = At, t \in T \text{ with a "testing space" } T,$$

yielding a linear iteration of the type

$$x_{new} = x_{old} - M^{-1}(Ax_{old} - b).$$

Depending on T, the resulting method can be tailored to be a smoother or a corrector as described in (Wittum 1992). It is possible to derive the filtering space T adaptively during the iteration by Adaptive Filtering (Wagner and Wittum 1997). The efficiency of the filtering approach was demonstrated in these papers. However, only so-called filtering decompositions were available to construct filters. These are based on block incomplete decompositions and thus are limited to structured grids only. We continued this development with the two-frequency decompositions (Logaschenko 2003; Buzdin and Wittum 2004; Buzdin et al. 2008).

In order ro generalise this method to unstructured grids Filtering Algebraic Multigrid, FAMG, (Wagner 2000a, b; Nägel 2005) has been developed. This multigrid method is one of the most advanced AMG solvers available and features a filtering property for the construction of the grid transfers operators. In particular the smoother is considered for the construction of the grid transfer-operators, which grants an optimised coarse-grid correction operator. The method has been parallelized by Wrobel, yielding a robust and at the same time efficient overall solver (Wrobel 2001). Additionally, it has been combined with the Adaptive Filtering technique (Nägel 2008). Generalizations for systems of PDEs is an ongoing focus of research.

The method has been successfully employed to compute a strategy for bioremediation of an aquifer or to elucidate the interactions between structure and function for biological barrier membranes. Moreover, it is used as a preconditioner for the computation of eigenmodes of musical instuments and in various other applications.

AMG for systems of equations

The methods so far were developed to solve the equations originating from the discretisation of one (scalar) PDE. In order to handle algebraic equations arising from the discretisation of systems of PDEs as well, the multi-grid methods SchurMG and RSAMG are extended.

There are two possible ways of doing this:

1. Take the system matrix A in its "natural order", which means "equation-wise blocking", and define coarse-grid sets and interpolation separately for each of the unknown functions. This is the so-called "unknown" approach. In general, this may lead to more than one grid hierarchy (with accompanying algorithmic and computer resource problems).

2. Collect all variables defined on the same set of grid points (which assumes a non-staggered original fine grid) and apply the algorithm in a “blockwise” fashion, where the block of all variables corresponding to the same grid point is relaxed, coarsened and interpolated together. This is the “point-block” approach, which we implemented in UG since this is more natural to UG's data structure and avoids much of the problems associated with the “unknown" approach.

References

Bastian, P., & Wittum, G. (1994). Robustness and adaptivity: The UG concept. In P. Hemker, P. Wesseling (Eds.), Multigrid Methods IV. Proceedings of the Fourth European Multigrid Conference, Amsterdam 1993. Basel: Birkhäuser.

Buzdin, A., & Wittum, G. (2004). Two-frequency decomposition. Numerische Mathematik, 97, 269–295.

Buzdin, A., Logashenko, D., & Wittum, G. (2008). IBLU decompositions based on Pade approximants. Numerical Linear Algebra with Applications, 15(8), 717–746.

Feuchter D., Heppner I., Sauter S.A., & Wittum G. (2003). Bridging the gap between geometric and algebraic multigrid methods. Computing and Visualization in Science, 6, 1-13.

Lang, S., & Wittum, G. (2005). Large scale density driven flow simulations using parallel unstructured grid adaptation and local multigrid methods. Concurrency Computation, 17(11), 1415 - 1440.

Logaschenko, D. (2003). Verallgemeinerte filternde IBLU-Zerlegungen der Ordnung l. Dissertation, Mathematik, Universität Heidelberg.

Nägel, A (2005). Filternde algebraische Mehrgitterverfahren und Anwendungen. Diplomarbeit, Universität Heidelberg.

Nägel, A., Falgout, R., & Wittum, G. (2008). Filtering algebraic multigrid and adaptive strategies. Computing and Visualization in Science, 11, 159–167.

Nägel, A. (2009). Löser für große Gleichungssystem in der Biophysik und den Lebenswissenschaften. Dissertation, Universität Heidelberg.

Reusken, A. (1994). Multigrid with matrix-dependent transfer operators for convection-diffusion problems. Multigrid Methods. Proceedings of the fourth European Multigrid Conference, Hemker, P.W., and Wesseling, P. (Eds.), Basel: ISNM Birkhäuser.

Ruge, J. W., & Stüben, K. (1987). Algebraic Multigrid. Multigrid Methods. In McCormick, S.F. (Ed.), Frontiers in Applied Mathematics, Vol. 5, SIAM Philadelphia, Pennsylvania.

Wagner, C., Kinzelbach, W., & Wittum, G. (1997). Schur-complement multi-grid - a robust method for groundwater flow and transport problems. Numerische Mathematik, 75, 523-545.

Wagner, C., & Wittum, G. (1997). Adaptive Filtering. Numerische Mathematik, 78, 305-328.

Wagner, C. (2000a). On the algebraic construction of multilevel transfer operators. Computing, 65, 73-95.

Wagner, C. (2000b). Ein algebraisches Multilevelverfahren - Entwicklung und Anwendung auf einen Sanierungsfall. Habilitationsschrift, Mathematik, Universität Heidelberg.

Wittum, G. (1992). Filternde Zerlegungen: Schnelle Löser für große Gleichungssysteme. Skripten zur Numerik Bd. 1. Stuttgart: Teubner.

Wrobel, C. (2001). Die Parallelisierung des filternden algebraischen Mehrgitterverfahrens zum Lösen partieller Differentialgleichungen. Dissertation, Universität Heidelberg.

M2.1: Multiscale Modelling of Biological Tissues

Alfio Grillo, Gabriel Wittum

Multiscale modelling aims to provide a detailed description of complex systems throught the simultaneous study of a selected number of processes that, although characterised by different scales of observation, interact reciprocally.

Biological materials constitute a field of research in which multiscale modelling finds a natural application, and the up-to-date concept of multi-physics is a direct consequence of the interplay of many intermingled phenomena that, making a living system “alive”, embrace several disciplines, such as mechanics, thermodynamics, electromagnetism, chemistry, and of course biology. This fascinating interdisciplinary subject requires advanced mathematical models, accurate numerical methods, and precise experiments.

Our main topic of research in this area is the study of the thermo-mechanics of growth and remodelling of biological tissues. Tissues are complex systems which, within their simplest approximation, may be thought of as mixtures of deformable solids and a fluid comprising several chemical agents. An example of solid constituent is given by the skeleton of the tissue. The fluid serves as carrier of substances that are destined to, or are by-products of, metabolic reactions. This picture may be re-formulated by regarding the solid constituents as deformable porous media in the interstitial space of which some fluid, and the chemical substances dissolved in it, experience transport processes. These processes are influnced by stimuli of various nature (for example, change of shape of the tissue, generation of internal distortions and stresses, exposure to thermal gradients, etc.), which may be triggered by the interaction of the tissue with its surrounding environment. We speak of growth when all these phenomena lead to the variation of mass of the tissue. We refer to remodelling when the internal structure of the tissue changes in time.

Three scales can be singled out for our purposes. The smallest one could be identified with the molecular scale; the intermediate scale could be given by the level of observation attained by using a "hypothetical" microscope to look at cellular and intercelluarl processes as well as the internal structure of the tissue. Finally, the largest scale (which could be said to be "macroscopic") is associated with the scale of the laboratory, i.e. the scale at which the collective properties of the tissues are determined.

Part of our research is based on the characterisation of a hypothetical tissue at the mesoscale, and the subsequent retrievement of the fundamental field equations and constitutive relations that describe the behaviour of the tissue at the macroscopic scale. This procedure, carried out through the use of Hybrid Mixture Theory (e.g., Bennethum et al. 2000, and references threin), is meant to relate the physical quantities featuring in the macroscopic balance laws with their mesoscale counterparts, and to account for the internal structure of biological materials. This is crucial for developing self-consistent theories whose goal is to describe the overall behaviour of a tissue in response to both microstructural and environmental factors.

In our contributions, particular emphasis has been thrown onto kinematic and thermodynamic aspects of growth and remodelling. Within the framework of Extended Thermodynamics (Liu and Müller 1983), and employing the Coleman-Noll method (Coleman and Noll 1963), we proposed an evolution law for growth and mass transfer, in which the driving mechanism for mass transfer and growth was a generalised Eshelby-like tensor that included the chemical potential of the fluid (Grillo et al. 2009a). Our results were similar to those determined by other authors, e.g. Loret and Simoes (2005), and Fusi et al. (2006). Subsequently, we revised and extended our findings to the case of a fibre-reinforced growing tissue (Grillo et al. 2009b). Here, we included the concept of "non-standard dynamics" put forward by DiCarlo and Quiligotti (2002) and used by Olsson and Klarbring (2008) in the context of remodelling. By viewing growth and remodelling as anelastic processes, we showed that the fundamental kinematic quantity describing growth, i.e. the rate of anelastic distortion, also called inhomogeneity velocity "gradient" by Epstein and Maugin (2000), is related to the Mandel stress tensor of the solid and to the chemical potential of the constituents of the fluid. We also showed that, in response to growth, the evolution of the anelastic part of deformation may yield fibre reorientation. Our results were meant to put together growth and remodelling according to the picture given by Imatani and Maugin (2002). Some remarks about the issue of incompressibility have been given by Federico et al. (2009).

Further investigations, revisions and improvements of our previsouly published results about the determination of evolution laws for the tensor of growth-induced distortions were provided by Grillo and Wittum (2010a,b). Here, the issue of Eshelbian coupling, discussed by DiCarlo and Quiligotti (2002), was framed in the context of Mixture Theory (analogous results have recently been proposed also by Ambrosi et al. (2010)). The distinction between growth and transfer processes was made visible through the fact that, in the evolution law of the distortion tensor induced by mass transfer, the Eshelbian coupling is augmented by the imbalance of the chemical potential of the substance which is transferred from one phase to the other. Finally, evolution laws involving fractional derivatives have been proposed by Atanackovic et al. (2010). This subject is currently under investigation.

References

Ambrosi, D., Preziosi, L., & Vitale, G. (2010). The insight of mixture theory for growth and remodeling. ZAMP, 61, 177-191.

Atanackovic, T., Grillo, A., Wittum, G., & Zorica, D. (2010). An application of fractional calculus to growth mechanics. 4th Workshop "Fractional Differentiation and its Applications" (FDA10), 18-20. X, 2010, Badajoz, Spain.

Bennethum, L. S., Murad, M. A., & Cushman, J. H. (2000). Macroscale Thermodynamics and the Chemical Potential for Swelling Porous Media. Transport in Porous Media, 39, 187-225.

Coleman, B. D., & Noll, W. (1963). The thermodynamics of elastic materials with heat conduction and viscosity. Archive for Rational Mechanics and Analysis. 13, 167-178.

DiCarlo, A., & Quiligotti, S. (2002). Growth and balance. Mechanics Research Communications, 29, 449-456.

Epstein, M., & Maugin, G. A. (2000). Thermomechanics of Volumetric Growth in Uniform Bodies. International Journal of Plasticity, 16, 951-978.

Federico, S., Grillo, A., & Wittum, G. (2009). Consideration on Incompressibility in Linear Elasticity. Nuovo Cimento C, 32(1), 81-87.

Fusi, L., Farina, A., & Ambrosi, D. (2006). Mathematical Modelling of a Solid-Liquid mixture with mass exchange between constituents. Mathematics and Mechanics of Solids, 11, 575-595.

Grillo, A., Wittum, G., Giaquinta, G., & Micunovic, M. V. (2009). A Multiscale Analysis of Growth and Diffusion Dynamics in Biological Materials. International Journal of Engineering Science, 47, 261-283.

Grillo, A., Federico, S., Wittum, G., Imataini, S., Giaquinta, G., & Micunovic, M. V. (2009). Evolution of a Fibre-Reinforced Growing Mixture. Nuovo Cimento C, 32(1), 97-119.

Grillo, A. & Wittum, G. (2010). Considerations on growth and transfer processes in multi-constituent materials. Manuscript submitted for publication.

Grillo, A. & Wittum, G. (2010). Growth and mass transfer in multi-constituent biological materials. American Institute of Physics, CP1281. ICNAAM, Numerical Analysis and Applied Mathematics. International Conference, Vol. 1, Ed. by T. Simos, G. Psihoyios, and Ch. Tsitouras, 355-359.

Imatani, S., & Maugin, G. A. (2002). A Constitutive Model for Material Growth and its Application to Three-Dimensional Finite Element Analysis. Mechanics Research Communications, 29, 477-483.

Liu, I. S., & Müller, I. (1983). Extended Thermodynamics of classical and degenerate gases. Archive for Rational Mechanics and Analysis, 83, 285-332.

Loret, B., & Simoes, F. M. F. (2005). A Framework for Deformation, Generalized Diffusion, Mass Transfer and Growth in Multi-Species Multi-Phase Biological Tissues. European Journal of Mechanics, 24, 757-781.

Olsson, T., & Klarbring, A. (2008). Residual stresses in soft tissues as a consequences of growth and remodelling: an application to an arterial geometriy. European Journal of Mechanics, 27, 959-974.

M2.2: Multiscale Numerics, Homogenisation and Coarse Graining

Ivo Muha, Sabine Stichel, Alfio Grillo, Gabriel Wittum

Most laws in the natural sciences are correct only up to error terms which depend on certain parameters and which are small only for a certain parameter range. Furthermore, many of these laws describe dependencies between macroscopic quantities which arise by averaging microscopic quantities. In this case, it is often possible to compute the parameters of the macroscopic laws from the physics of the micro problems and to quantify the error of the macroscopic law with respect to the microscopic law. This process is called "homogenisation".

In the case of media with periodic heterogeneities (this case occurs rather frequently for industrially produced composites), there are explicit rules for computing the parameters of the macroscopic law. Essentially, the technique is to solve a representative problem on a small reference cell. For stochastic problems it is necessary to compute many realizations.

A recent application of homogenisation is used for modelling diffusion through human stratum corneum (cf. A1). The geometry of the stratum corneum consists of tetrakaidekahedra. Due to the complexity of the geometry and the difference in length scales involved in its microstructure, solving the equation directly on detailed microstructure is of high computational cost. We obtain a macroscopic effective diffusion tensor by homogenisation (cf. Muha et al. 2010b) and thereby significantly reduce the computational cost of modelling transdermal diffusion. A detailed description of application of homogenisation theory on tetrakaidekahedra has been given in Muha et al. Some results for the cell problem are shown in Fig. 1.

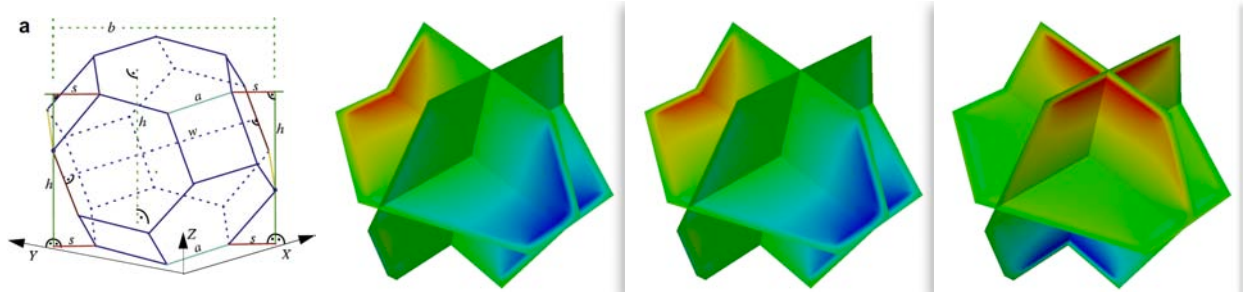

(a) (b) (c) (d)

Figure 1. **(a) Geometry of a tetrakaidekahedron.**
(b)-(d) Solution of the cell problem, in x- (b), y- (c) and z-direction (d)

For the case of media with non−periodic heterogeneities, a new method, called Coarse Graining, was introduced. The idea of Coarse Graining is developed in Attinger et al. (2002) based on filtering procedures. It can be understood as a combination of volume averaging and using local fine-scale solutions for upscaling. The concept of Coarse Graining is smoothing a function for local volumes in order to get a function on a higher resolution scale. This smoothing corresponds to cutting off high frequencies of the solution. While accurate approximations for effective permeability values are known for the case of global upscaling, we give an explicit scale-dependent effective permeability.

The theoretical upscaling was extended to a numerical scheme (cf. Eberhard et al. 2004) for a local upscaling of the permeability field, similar to the method of homogenisation. It is shown that, for a periodic setting with periodic media, the effective permeability is equivalent to the homogenised coefficient. The numerical treatment offers the opportunity of computing and testing all theoretical results of the Coarse Graining method. The latter are in good agreement with numerical results. Numerical Coarse Graining also allows us to compute the theoretically derived results to a higher order of the variance, for which the results of the perturbation theory are no longer valid.

Numerical Coarse Graining can be used on any level of an arbitrary given grid hierarchy. For the use on unstructured non-aligned elements appropriate boundary conditions for the cell problem have to be used (cf. Muha et al., 2010a). For aligned square grids a special kind of mixed boundary conditions proved to yield much better results than other boundary conditions. Hence we generalised these boundary conditions to arbitrary elements by approximating the elements with aligned squares and then defining the boundary conditions on the new sequence of boundary pieces.

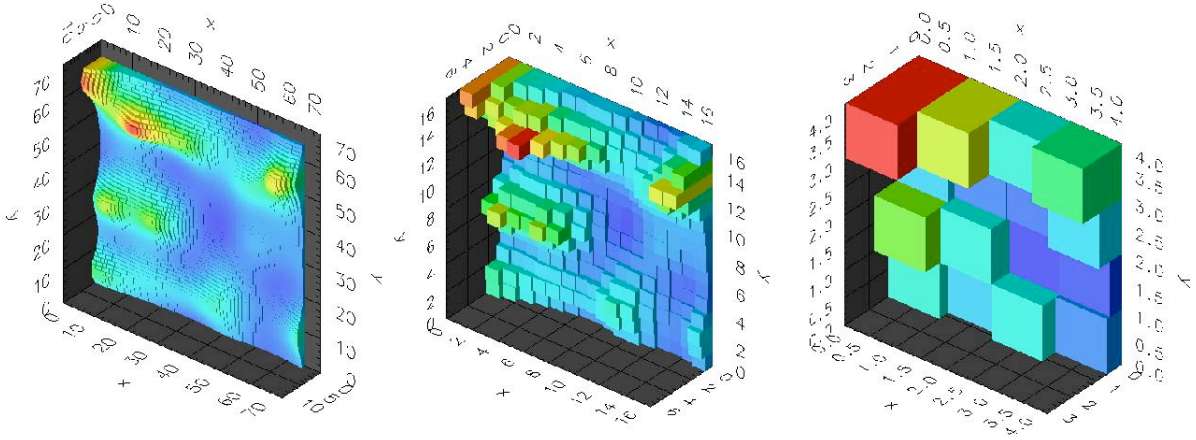

Figure 1. To illustrate the iterative coarse graining of the permeability we plot the longitudinal effective coefficients in the isotropic case: 64, 16, 4 elements, variance 0.5. The original field is given on the 64x64-grid shown on the left.

References

Attinger, S., Eberhard, J., & Neuss, N. (2002). Filtering procedures for flow in heterogeneous porous media: Numerical results. Computing and Visualization in Science, 5(2), 67-72.

Eberhard, J., Attinger, S., & Wittum, G. (2004). Coarse graining for upscaling of flow in heterogeneous porous media. SIAM Multiscale Modeling and Simulation, 2(2), 269-301.

Eberhard, J., Popovic, D., & Wittum, G. (2008). Numerical upscaling for the eddy-current model with stochastic magnetic materials, Journal of Computational Physics, 227(8), 4244-4259.

Muha, I., Stichel, S., Attinger, S., & Wittum, G. (2010a). Coarse graining on arbitrary grids. SIAM Multiscale Modeling and Simulation 8(4), 1368-1382.

Muha, I., Naegel, A., Stichel, S., Grillo, A., Heisig, M., & Wittum, G. (2010b). Effective diffusivity in membranes with tetrakaidekahedral cells and implications for the permeability of human stratum corneum. Journal of Membrane Science 368(1-2), 18-25.

M3: Finite Volume Element Methods of Arbitrary Order

Andreas Vogel, Gabriel Wittum

Finite Volume Methods are an effective discretisation technique to solve partial differential equations that arise from physical conservation laws. They are used in a variety of applications such as computational fluid dynamics, convection-diffusion problems or flow problems in porous media. The most attractive property of a finite volume method is that the approximative solution satiesfies a discrete convervation law. More precisely, on discrete control volumes B_h - also called "box"-volumes - the discrete solution u_h staisfies the equation (e.g. for a scalar conservation law)

$$\frac{\partial}{\partial t}\int_{B_h} u_h \, dx = -\int_{\partial B_h} f(u_h)\cdot n \, dS,$$

which states that the temporal change of the conserved quantity u_h in the control volume is in balance with the flux $f(u_h)$ over the boundary of the control volume.

The Finite Volume Element Method (FVEM) is a variant of the Finite Volume Methods that use a Finite Element mesh and Finite Element ansatz functions to decompose the physical domain and to represent the discrete solution, respectively. Therefore, it inherits such attractive features like unstructured grid approaches, local grid refinements, unstructured multigridding and parallelisation from the Finite Element Method, but still remains a conservative scheme.

The FVEM using linear ansatz functions has been described and analysed in e.g. Bank and Rose (1987), Heinrich (1987) and Hackbusch (1989). This method is successfully used in realistic problems and is a standard feature of the software toolbox UG.

From the Finite Element context higher order methods are well known. These are characterised by higher order polynomial ansatz spaces, which lead to asymtotically higher convergence order, i.e. roughly speaking a desired approximation error can be achieved with less effort when a certain smoothness of the exact solution is given. Therefore, it is desirable to use higher order finite volume methods, combining fast convergence rates with discrete conservativity and applicability on unstructured grids.

The key points to develop FVEM of arbitrary order are the choice of trial functions and the construction of the control volumes B_h. A quadratic FVEM has been proposed and analysed in Liebau (1996). Recent results for quadratic schemes can also be found in Xu and Zou (2005).

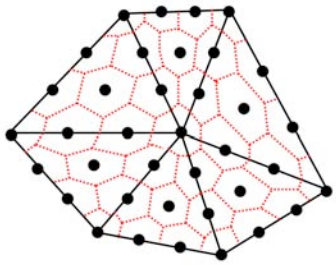

Figure 1. Control Volumes for a cubic trial space

We proposed an arbitrary order FVEM using nodal shape functions with piecewise polynomials of degree $p > 1$ (see Vogel and Wittum, 2009). The box volumes are constructed by a barycentric technique. For example in 2D the elements are divided into subelements first (see Figure 2). Then, barycenters and edge midpoints are connected by straight lines for every subtriangle. Applying this procedure on every element of the grid leads to a non-overlapping decomposition of the domain into control volumes. Figure 1 gives an example for cubic shape functions on triangles.

This generalisation of the standard FVEM to higher order has been implemented in the software toolbox UG. It is available for arbitrary order on hybrid grids in 2D (Triangles, Quadrilaterals) and 3D (Tetrahedra, Hexahedra).

Several numerical experiments using the new discretisation schemes have been performed and can be found in Vogel (2008). A typical result of a convergence rate study for a 2D convection-diffusion problem is displayed in Figure 3. The error between exact solution u and approximated solution u_h for the H^1- and L^2-Norm is shown versus the number of unkowns. Since the effort for the computation of the approximative solution is proportional to the num-

ber of unkowns, these results are a convincing example how the higher order FVEM can be used to achive better solutions with less effort.

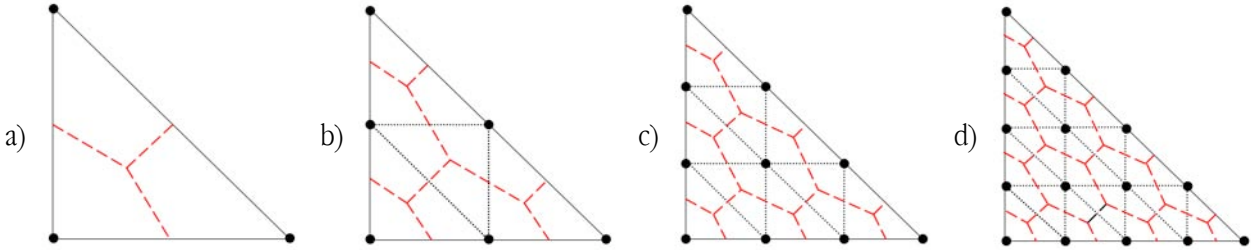

Figure 2. Triangles, Subtriangles and Control Volumes for different FVE schemes: a) linear (p=1), b) quadratic (p=2), c) cubic (p=3) and d) quartic (p=4)

A more detailed measurement of the convergence rates gives the following results: For the H^1-Norm an optimal order convergence rate is found, i.e.,

$$||u - u_h||_{H^1} \leq Ch^p,$$

where p denotes the polynomial degree of the choosen trial functions. The optimal convergence rate in L^2-Norm is found for odd degree trial functions. For even degree trial functions, the order is one order below optimal, i.e.

$$||u - u_h||_{L^2} \leq Ch^m,$$

where $m = p$ when p is even and $m = p+1$ when p is odd.

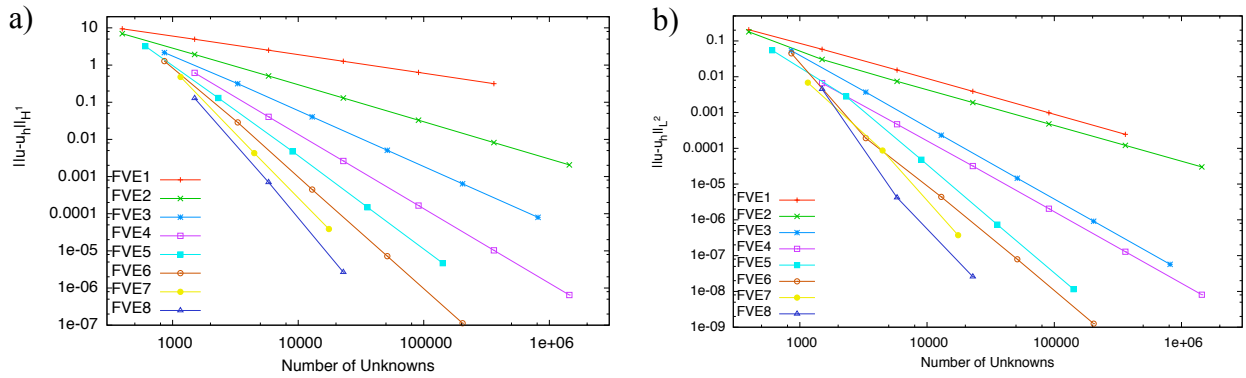

Figure 3. Convergence Rates for a 2D model problem for different Finite Volume Element schemes of order *p* (FVEp)

References

Bank, R. E., & Rose, D. (1987). Some error estimates for the box method. SIAM Journal on Numerical Analysis, 24(4), 777–787.

Hackbusch, W. (1989). On first and second order box schemes. Computing, 41, 277-296.

Heinrich, B. (1987). Finite Difference Methods on Irregular Networks - A generalized approach to second order elliptic problems. Basel: Birkhäuser.

Liebau, F. (1996). The finite volume element method with quadratic basis functions. Computing, 57(4), 281-299.

Vogel, A. (2008). Ein Finite-Volumen-Verfahren höherer Ordnung mit Anwendung in der Biophysik. Diploma thesis, University of Heidelberg.

Vogel, A., Xu, J. & Wittum, G. (2010). A generalization of the vertex-centered Finite Volume scheme to arbitrary high order. Computing and Visualization in Science, 13(5), 221-228.

Xu, J., & Zou, Q. (2005). Analysis of linear and quadratic finite volume methods for elliptic equations. Preprint AM298, Math. Dept., Pennsylvania State University.

M4: Level Set Method

Peter Frolkovič, Christian Wehner, Gabriel Wittum

Free boundaries occur in a wide range of applications, e.g. in two-phase flow, image processing or modelling of combustion. The level-set method, introduced by Osher and Sethian in 1988, is a method for tracking moving interfaces. The main idea is to model the moving boundary as zero level set of a function. The movement of the free boundary can then be modeled as initial boundary value problem. The resulting partial differential equations are usually linear or non-linear hyperbolic equations.

The focus of our work is to develop methods to solve the arising hyperbolic equations on unstructured grids in ug and to apply these methods to practical problems.

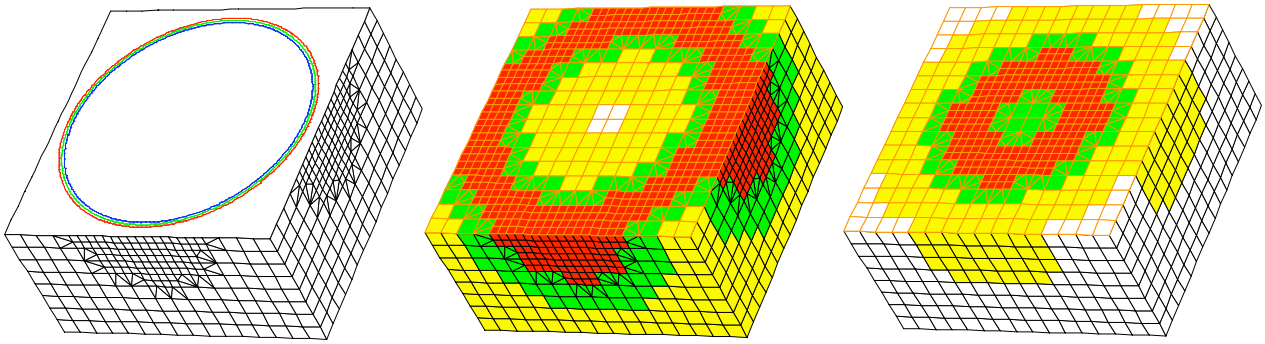

Level set function | Grid for the intial condition | Grid at the last time step

Figure 1. Shrinking of a sphere in 3 dimensions computed with flux-based level set method in ug

The flux-based level set method (Frolkovič and Mikula 2007) is a finite-volume method for a general hyperbolic equation of the form

$$\partial_t u + \vec{v} \cdot \nabla u = f.$$

In the level set context this equation describes the movement of the interface under the velocity $\vec{v}$. If the velocity is given as external velocity field the above equation is a linear advection equation, the case $\vec{v} = F\,\nabla u\,/\,||\nabla u||$ leads to the level set equation for movement in normal direction $\partial_t u + F||\nabla u|| = f.$

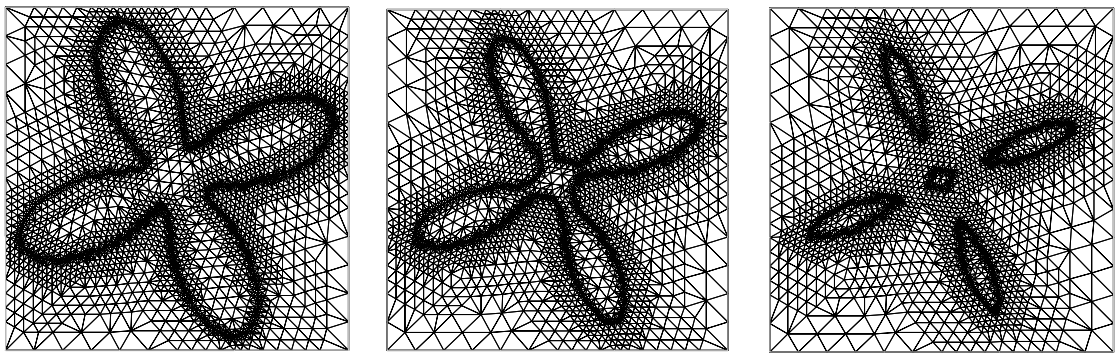

Figure 2. Shrinking quatrefoil on adaptive grid

The flux-based level set method is explicit in time and is stable under a given time step restriction (CFL constraint). Tests in ug with several popular benchmarks confirmed second order convergence for sufficiently smooth solutions and showed good mass conservation properties of the method, when it was applied to problems with divergence-free velocity. This is important because mass conservation is not guaranteed by the level-set formulation.

The flux-based level set method was investigated further for rectangular grids and was used for the computation of general arrival time functions, which can e.g. be used for the modelling of fire spread (Frolkovič and Wehner 2009).

Further applications of the method were the simulation of an atherosclerotic lesion (Eberhard and Frolkovič 2006), the surface evolution in image segmentation of 3D biological data (Frolkovič et al. 2007) and the simulation of groundwater flow using the r^{3}t-software tool (see section A5.2).

Yet another application was the computation of two-phase flow with *ug* (Frolkovič et al. 2010). For this problem type, it is well-known, that the level set function has to be reparametrised from time to time to guarantee stable computations, so a method for this "reinitialisation" of the level set function on unstructured grids was developed. Both the interface tracking and the reinitialization equation were solved using the flux-based level set method.

Several test examples showed that the overall two-phase flow level set method is convergent and gives good results concerning mass conservation.

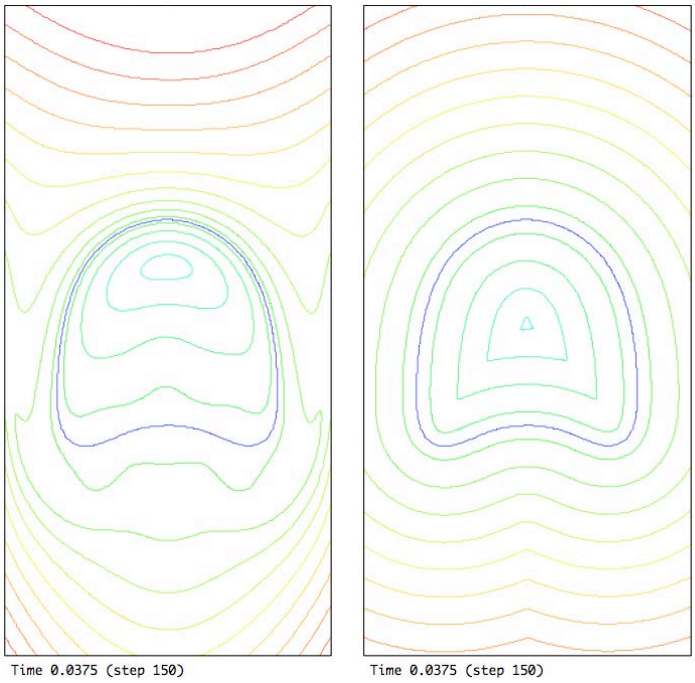

Figure 3. Reinitialisation of the level set function in a simulation of a rising bubble

The pictures show the level set function before and after solving the reinitialisation equation. The zero level set (the blue line) remains the same, but after reinitialising the level set function is a signed distance function, that does not suffer from steep and flat gradients.

References

Eberhard, J., & Frolkovič, P. (2006). Numerical simulation of growth of an atherosclerotic lesion with a moving boundary. IWR-Preprint. Retrieved from http://archiv.ub.uni-heidelberg.de/volltextserver/volltexte/2006/6477/pdf/IWRpreprintEberhardFrolkovic2006.pdf

Frolkovič, P., Logashenko, D., Wehner, C., & Wittum, G. (2010). Finite volume method for two-phase flows using level set formulation. Preprint 2010-10, Department of Mathematics and Descriptive Geometry, Slovak University of Technology, Bratislava 2010.

Frolkovič, P., Logashenko, D. & Wittum, G. (2008). Flux-based level set method for two-phase flows, In R. Eymard, J.-M. Herard (Eds.), Finite Volumes for Complex Applications V (pp. 415-422). London: ISTE and Wiley.

Frolkovič, P., & Mikula, K. (2007a). Flux-based level set method: a finite volume method for evolving interfaces. Applied Numerical Mathematics, 57(4), 436-454.

Frolkovič, P., & Mikula, K. (2007b). High-resolution flux-based level set method. SIAM Journal on Scientific Computing, 29(2), 579-597.

Frolkovič, P., Mikula, K., Peyrieras, N., & Sarti, A. (2007). A counting number of cells and cell segmentation using advection-diffusion equations. Kybernetika, 43(6), 817–829.

Frolkovič, P., & Wehner, C. (2009). Flux-based level set method on rectangular grids and computations of first arrival time functions. Computing and Visualization in Science, 12(5), 297-306.

M5.1: Parameter Estimation for Bingham Fluids and Optimal Geometrical Design of Measurement Devices

Dmitry Logashenko, Bernd Maar, Volker Schulz, Gabriel Wittum

As early as 1996, we issued the first multigrid method for solving a full pde optimisation problem. We applied this methods to several problems such as the parameter estimation and inverse modelling of groundwater flow, topology optimisation (Dreyer et al. 2000) and optimal geometry and experiment design. In the following, we present an example of the latter topic.

In a joint effort with Braun GmbH (Friedrichshafen, Germany), we have developed a model-based measurement technique which allows the simultaneous determination of all model parameters of certain Bingham flow models, for example for ceramic pastes. Pastes are used, for example in the production of bricks or bodies of catalytic converters. Usually, they are extruded, where the quality of the extrusion product depends on the velocity distribution of the flow within the extrusion device. Recently, substantial progress has been achieved in the development of numerical simulation techniques for paste extrusion based on Bingham models. However, in practice, these numerical techniques can only be used if certain parameters of the underlying flow model are known. These parameter values cannot be accessed by direct measurements, but are usually determined in a process involving a rather high empirical effort and using analytical approximation approaches. The efforts show that numerical methods can be set up for the estimation of the model parameters from measurements of normal stresses, which need only twice as much computing time as a pure flow simulation. Furthermore, all interesting parameters are estimated simultaneously and automatically.

At every measurement, the fluid is pressed through the measurement device shown in Figure 1. The normal stress is measured at several points on the upper wall. Then, the flow model of this fluid, i.e. the Bingham equations, is discretised and the normal stresses at the measurement points are expressed in terms of the discrete solution and the fluid parameters. The comparison of these analytic stresses and the measured ones gives rise to a least square problem with non-linear constraints. For the estimation of the parameters, this problem is solved using a reduced SQP method.

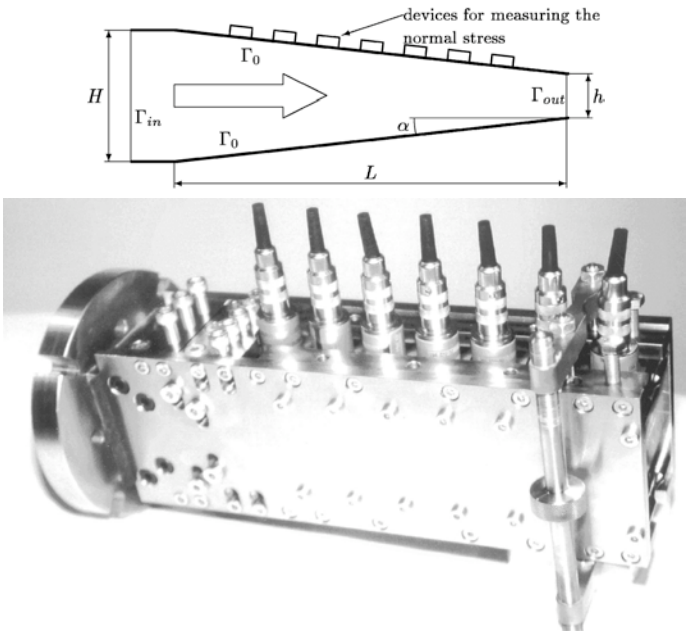

Figure 1. Schematic draft and photo of measurement device

However, the statistical reliability of this approach is rather low for this measurement device. We carried out the shape optimisation of the device, resulting in the geometry shown in Figure 2. The confidence intervals of measurements are then substantially focused, as presented in Table 1.

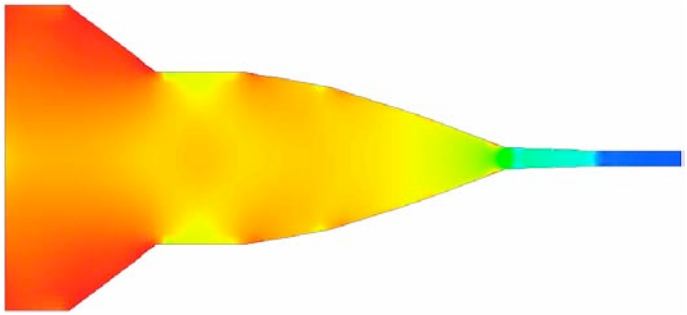

Figure 2. The optimised measurement device

Parameter	Value	The simple device	The optimised device
Bingham viscosity [bar s]	0.302	±26.3	±0.00421
yield stress [bar]	3.03	±38.5	±0.0520
sliding factor [bar s / m]	0.497	±46.2	±0.0640
sliding limit [bar]	0.180	±1.5	±0.0819

Table 1. Confidence intervals of the parameters

References

Dreyer, Th., Maar, B., & Schulz, V. (2000). Multigrid Optimization in Applications. Journal of Computational and Applied Mathematics, 120(1-2), 67-84.

Hazra, S. B., & Schulz, V. (2002). Numerical Parameter Identification in Multiphase Flow through Porous Media. Computing and Visualization in Science, 5(2), 107-113.

Johannsen, K., Oswald, S., Held, R., & Kinzelbach, W. (2006). Numerical simulation of three-dimensional saltwater-freshwater fingering instabilities observed in a porous medium. Advances in Water Resources, 29(11), 1690-1704.

Logashenko, D., Maar, B., Schulz, V., & Wittum, G. (2001a). Optimal geometrical design of Bingham parameter measurement devices. In: Hoffmann, Karl-Heinz (Ed.) et al., Fast solution of discretized optimization problems. Int. Ser. Numer. Math. 138, (pp. 167-183). Basel: Birkhäuser.

Logashenko, D., Maar, B., Schulz, V., & Wittum, G. (2001b). Optimal geometrical design of Bingham parameter measurement devices. International Series of Numerical Mathematics (ISNM), 138, 167-183.

Maar, B., & Schulz, V. (2000). Interior Point Multigrid Methods for Topology Optimization. Structural Optimization, 19(3), 214-224.

Schulz, V., & Wittum, G. (1998). Multigrid optimization methods for stationary parameter identification problems in groundwater flow. In Hackbusch, W., Wittum, G. (eds.), Multi-Grid Methods V. Lecture Notes in Computational Science and Engineering, Vol. 3 (pp. 276-288), Heidelberg: Springer.

Schulz, V., & Wittum, G. (1999). Transforming smoothers for Optimization Saddlepoint Problems. Computing and Visualization in Science, 4, 207-219.

Wittum, G., Schulz, V., Maar, B., & Logashenko, D. (2003). Numerical methods for parameter estimation in Bingham-fluids. In W. Jäger, H.-J. Krebs (eds.), Mathematics - Key Technology for the Future (pp. 204-215), Berlin: Springer.

M5.2: Parameter Estimation for Calcium Signalling

Gillian Queisser, Gabriel Wittum

A recurring challenge in neurobiology is finding experimental methods to access biological parameters within cell tissue or single cells. Measuring diffusion properties of molecules in vivo or in vitro, opposed to an artificial experimental setting, poses difficulties since these parameters are only indirectly accessible. Literature on diffusion properties of cellular and nuclear calcium is sparse. Until now only one publication touching on that topic is known to us (Allbritton et al. 1992). Furthermore, in Allbritton et al. (1992) experiments are not carried out in vitro, but in an artificial setting using cytosolic-like media.

In other neuroscience projects of the G-CSC, calcium diffusion properties are part of underlying mathematical models. We therefore saw the need to quantify calcium diffusion by developing inverse modelling tools, based on experimental data. A prerequisite for developing an adequate parameter estimation method, is to know what kind of data is recordable experimentally. A method for investigating the diffusion barrier properties of the nuclear membrane was published by the Bading lab at the IZN in Heidelberg (Eder and Bading 2007). Laser-assisted calcium uncaging methods allow controlled release of calcium in the cell, and the spatio-temporal development of this calcium signal can be recorded. For the schematics of this method see Figure 1.

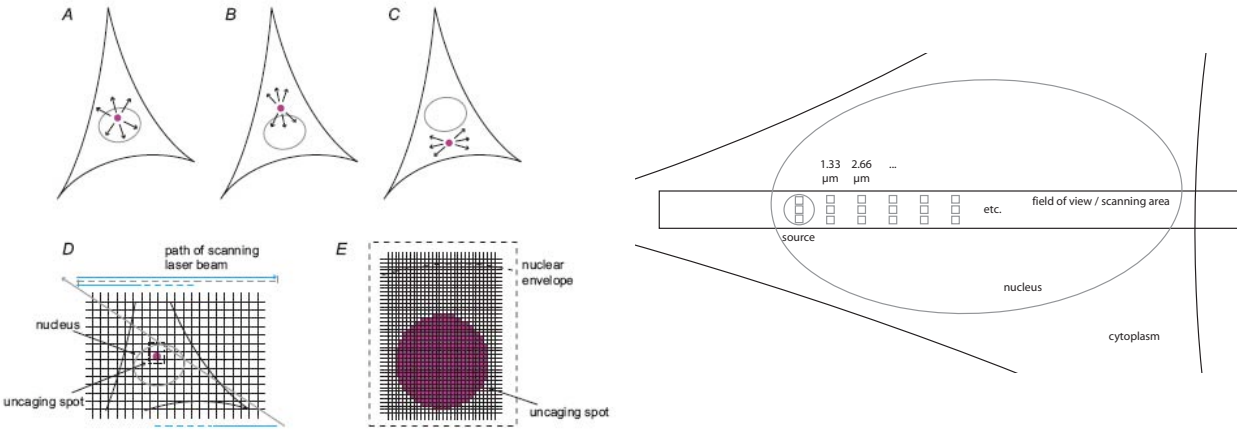

Figure 1. Left: Set up of the laser-assisted calcium uncaging experiments. Calcium can be locally released by a UV-laser, either in the nucleus or in the cytosol of single cells. Right: Measuring spatio-temporal calcium patterns; a linear recording band is defined, averaging data vertically (accounting for experimental variability) and measuring at discrete point in horizontal direction.

This data can be used to estimate the diffusion coefficient of cellular calcium (nuclear or cytosolic). As an objective function for the optimisation problem we define

$$F(D) := \sum_{i=1}^{N} \sum_{j=1}^{M} (u_{ij}(D) - c_{ij})^2$$

where D denotes the diffusion coefficient of nuclear calcium, which is to be estimated, c the experimental data in space and time (i and j resp.) and u the model data resp. to D. Finding an optimal model fit for the experimental data means minimising the objective function F. Local approximation and minimisation of the objective function yields a linearised quadratic function of the form

$$\min \sum_{i,j} \left(u_{ij}(D^{(q)}) - c_{ij} + \frac{\partial u_{ij}}{\partial D^{(q)}} \cdot \Delta D^{(q)} \right)^2$$

with

$$\Delta D^{(q)} := D^{(q+1)} - D^{(q)}$$

The minimisation problem then reduces to calculating the zero derivative of u resp. to D and the model data u, which we retrieve from simulating a calcium diffusion process. The details of deriving the following equations for our optimisation problem can be found in Queisser (2008):

For model data u solve

$$\frac{\partial u}{\partial t} = div(D\nabla u(x,t))$$

and for the derivative of F resp. to D (denoted by g), solve

$$\frac{\partial g(x,t)}{\partial t} = div(D\nabla g(x,t)) + div(\nabla u(x,t))$$

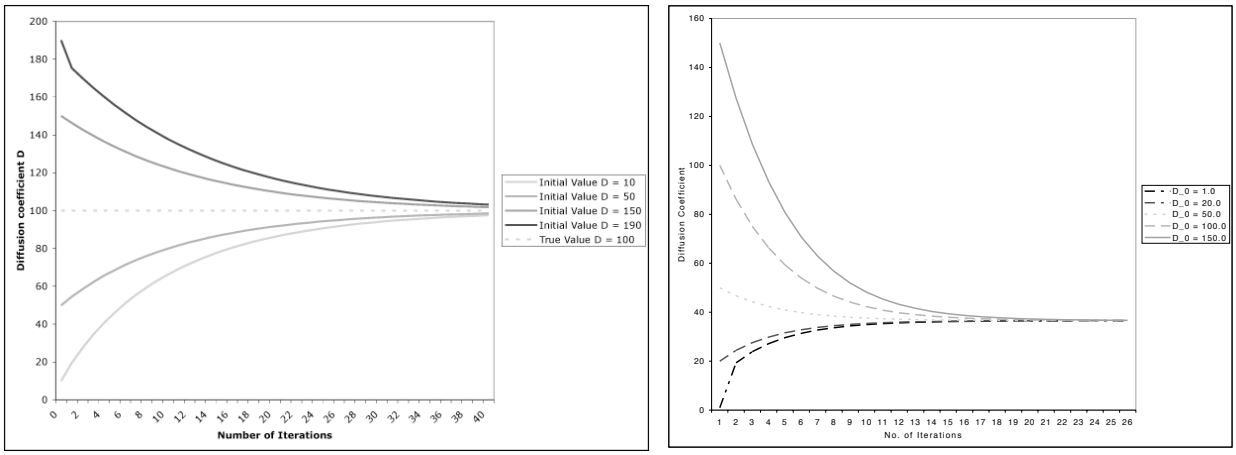

Figure 2. Left: Convergence of parameter estimation runs independent of the starting values for D. The test coefficient was set to $D=100$, convergence to this value is quadratic. Right: Using data from laser-assisted calcium uncaging the parameter estimation model shows stable convergence independent of the starting value for D to approx. 40 um ^ 2/s. This is in agreement to previously published data (Allbritton et al. 1992).

Using $\mathcal{uG}$ we then can solve the above equations, which are only coupled in one direction, meaning one can solve, in each time step, the first equation and with that data solve the second equation. The updating of the diffusion coefficient after each simulation cycle is done by stepping in the steepest decent direction, retrieved from calculating the zero derivative of F with an appropriate step length, which can be calculated using standard optimisation techniques like a line-search method. This parameter estimation method for nuclear calcium has been investigated in a test environment and subsequently applied to the experimental data from laser-assisted calcium uncaging. Results are shown in Figure 2 (Queisser & Wittum, submitted). The inverse model shows two major things. First, data published by Albritton et al. (1992) can be verified by this parameter estimation model, showing that the diffusion coefficient for calcium in the uncaging experiments lies at approx. 40 um ^ 2/s and secondly assuming a diffusion process as the underlying biophysical process for nuclear calcium is a legitimate estimation (the inverse model converges).

References

Allbritton, N.L., Meyer, T., & Stryer, L. (1992). Range of Messenger Action of Calcium Ion and Inositol 1,4,5-Triphosphate. Science, 258, 1812-1815.

Eder, A., & Bading, H. (2007). Calcium signals can freely cross the nuclear envelope in hippocampal neurons: somatic calcium increases generate nuclear calcium transients. BMC Neuroscience, 8, 57.

Queisser, G., (2008). The Influence of the Morphology of Nuclei from Hippocampal Neurons on Signal Processing in Nuclei. Dissertation, University of Heidelberg.

Queisser, G. & Wittum, G. (2011). Investigating the Diffusion Properties of Nuclear Calcium. Biological Cybernetics, 105(3-4), 211-216.

M8, M9, T7: Geometry Modelling and Grid Generation

Dirk Feuchter, Alexander Fuchs, Andreas Hauser, Sebastian Reiter, Martin Stepniewski, Gabriel Wittum

Many physical processes occur in rather complex domains. For simulating phenomena with practical relevance, mapping these domains onto a computational domain and triangulating them can only be carried out with powerful and specialised tools. In order to cope with the specific properties of the problems that are treated in numerical simulations, different approaches are required to preserve the special characteristics of the associated geometries during discretisation.

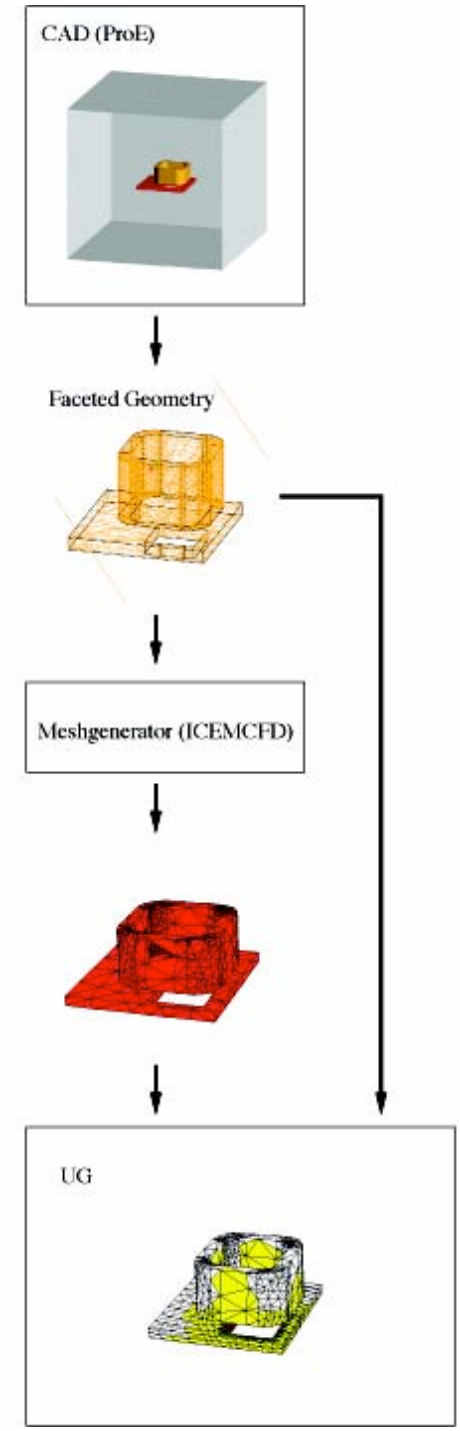

Figure 1. Path from CAD-tool (ProE) to UG

First, a rather general way of utilising arbitrary CAD geometries is presented, while the second approach is adopted for highly anisotropic domains occurring in simulating groundwater flow or transdermal diffusion of xenobiotics into the epidermis. A third approach allows the fully automated generation of tetrahedral grids from arbitrary piecewise linear surface geometries. All approaches produce grids ready for simulation with UG.

Finally a new approach to successive multigrid refinement is described. The required preprocessing for this technique is currently being integrated into our toolchain.

CAD Geometries

In many industrial applications, the starting point for a numerical simulation is the modelling and discretisation of CAD geometries. To model complex geometries, the 3D-modeller ProE is applied. This also enables the import of neutral files via IGES and STEP interfaces which in turn allows geometries generated by other software on different platforms to be considered. Then, a very fine surface mesh is generated in ProE that now acts as the new approximated domain, which is either imported into UG or into the powerful mesh generator ICEMCFD. This grid generator tool is able to triangulate complex geometries, resulting in a volume mesh with far more than 10 million elements that is finally imported into UG via a linear domain interface. The data transfer between the several tools is realised by Perl converters and depicted in the figure on the left-hand side.

Three examples of real-world geometries are presented in Figure 1, 2 and 3. Electromagnetics and heat transfer are simulated using these geometries. The first figure gives insight into a module of a static mixer. Figure 2 represents a part of an electrical device with lamellae for cooling, while the last figure shows a gas-isolated switch gear. The number of volume elements varies from 5,000 to 100,000 elements on the coarse grid and from 200,000 up to and more than 64 million on the finest grid that approximates the very fine surface mesh sufficiently and thus the original geometry.

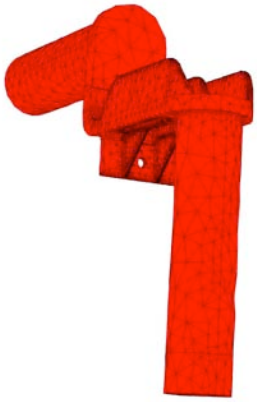

Figure 2. Medium voltage switch (ABB)

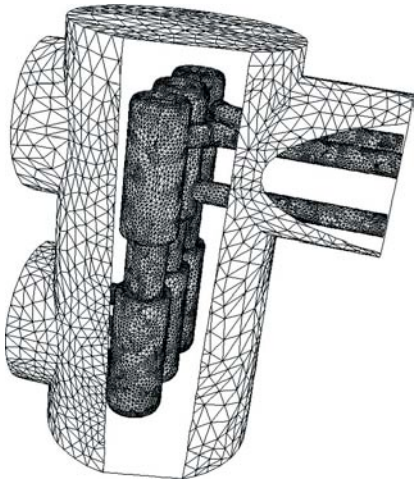

Figure 3. Gas-insulated switching gear: full configuration

Geometry and grid generation for anisotropically layered domains

Solving partial differential equations in geoscientific applications (e.g. density-driven flow) or in pharmaceutical applications (e.g. transdermal diffusion of xenobiotics into the epidermis (stratum corneum)) implies a complex preprocessing for geometry modelling and grid generation. Geoscientific domains are often assemblies of layers with a dimension of many kilometres in the horizontal direction, but a dimension of only some metres in the vertical direction. This yields the typical strong anisotropy. Further geological characteristics possibly occur: layers crop out, sometimes contain lenses or fractures, display overhangs (e.g. salt domes) or faults. Layered domains of cells such as the stratum corneum consist of many corneocytes which are approx. 30 μm wide and 1 μm in height and are surrounded by a homogeneous lipid layer of 0.1 μm. Simulations of such anisotropically layered domains require grids with suitable sizes and shapes of the elements. We develop methods for geometry and grid generation using the file formats "lgm" and "ng" used in our numerical simulation system UG to describe complex geometries and grids. First, with vertical lines and a protrusion technique, LD_Modeller2.5D creates geometries and grids consisting of triangles, quadrilaterals in 2D and prisms and hexahedra in 3D, suitable for a certain kind of geoscientific "L"ayered "D"omain.

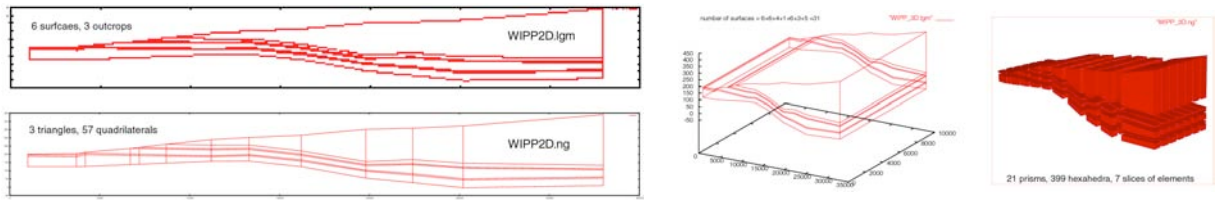

Figure 4. The WIPP domain, a typical highly anisotropic domain from hydrogeology

In a second approach, we model more complicated layered domains, using the gridding methods of surfer or any data interpolation software which is able to describe a separating surface between two layers based on geological input data (e.g. borehole data). With a thickness approach, LD_Modeller3D can include domains with geological characteristics (as above), leading to a consistent assembly of all layers available to the 3D simulation process with UG. In a second step, the grid generator of LD_Modeller3D creates hybrid meshes consisting of pyramids, tetrahedra, prisms and mainly hexahedra. Using vertical lines during the grid generation leads to good element angles.

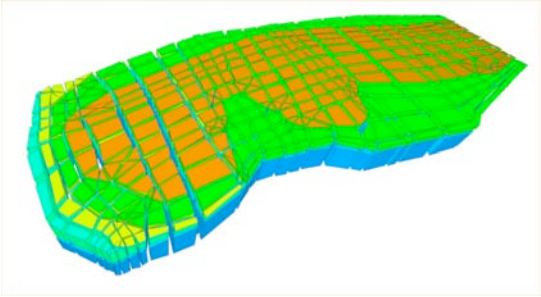

Figure 5.
A 3d grid of Norderney, an East-Frisian island in the North Sea. The grid consisting of hexahedra, prisms, pyramids and tetrahedra is generated by Ld_Modeller3d and follows the geometry.

In case of anisotropically layered domains such as the epidermis, Cuboid_Modeller describes each corneocyte as a cuboid. The corneocytes and the lipid layers are both meshed uniquely with hexahedra. In a second approach, we use nested tetrakaidekahedra, describing a corneocyte in the lipid layer. Tetrakaidekahedra are suitable because they overlap, and it is possible to create a dense packing of 100%. Tkd_Modeller creates a geometry file in the lgm-format and a hybrid grid consisting of hexahedra, prisms, pyramids and tetrahedra in the ng-format.

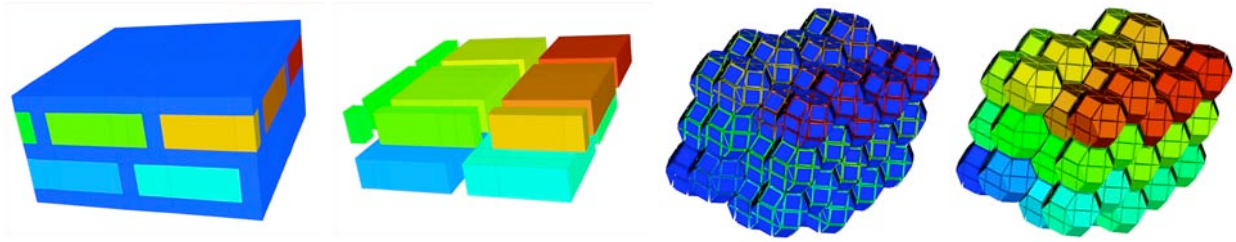

Figure 6. Geometry and grid of two different 3D models for human stratum corneum. On the left the corneocytes are modelled by cuboids, on the right by tetrakaidekhedra.

Additionally, we developed the grid generator ARTE, based on ART (Almost Regular Tetrahedra). ARTE keeps to interior faces and is able to expand prescribed internal faces to thin layers and to generate prisms for anisotropic layers. Special algorithms are developed for treating intersecting faces.

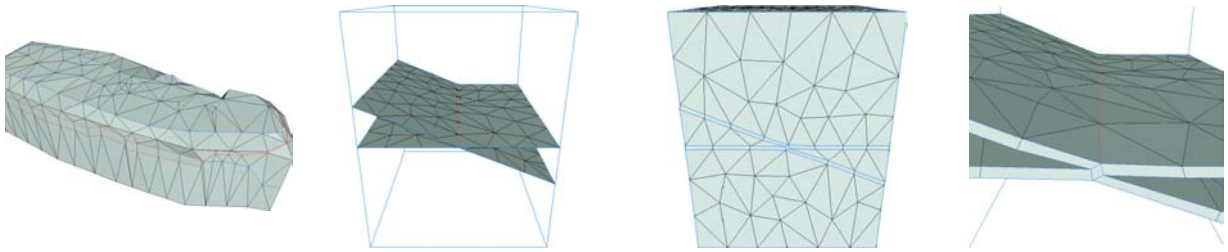

Figure 7. Thin layer grids generated by ARTE
From left to right: Grid of the Norderney domain. The next three images show the expansion of intersecting interior faces to thin layers with special treatment of layer intersections.

Fully automated tetrahedral grid generation

Implemented as a module of the grid management library *libGrid*, the tool *volUtil* builds the bridge between plain surface geometries and the final numerical simulation on the complete volume geometries with the simulation tool UG. Accessing the library TetGen (Si 2006), *volUtil* is able to generate high quality tetrahedralisations of arbitrary complex piecewise linear 3D surface geometries with holes, inner boundaries, interlacings etc. using the Constrained Delauney method. Surface geometry import, volume grid generation and data export to UG can be easily executed seperately or all by one command. *volUtil* provides the opportunity to specify various important parameters such as maximum radius-edge ratio of the tetrahedrons, maximum tetrahedron volume constraints, geometry region information etc.

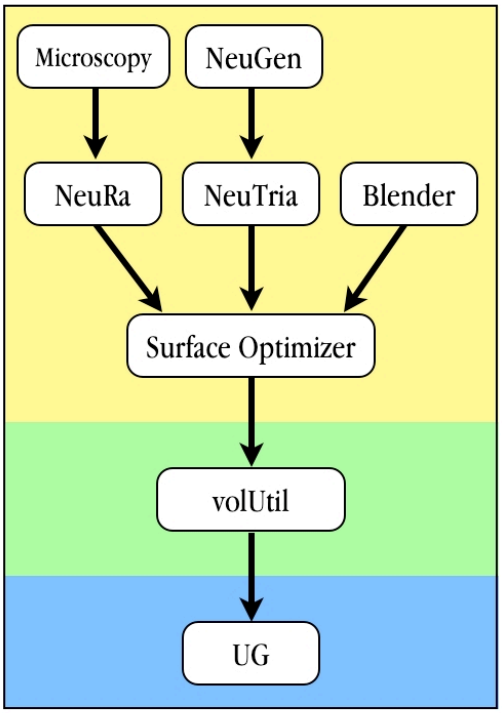

Figure 8. Toolchain for grid generation

The required surface geometries can be easily created, imported and edited with the 3D-graphics software BLENDER. Yet, a major part of the surface geometries dealt with comes from neurobiological data. In this context we are interested in both the reconstruction of geometries from microscopy data and the generation of synthetic cells, which adhere to biologically measured anatomical fingerprints. The first point is handled by the surface reconstruction program NeuRa [A2.1], the second by the neuron generation programs NeuGen and NeuTria [A2.6]. Due to its modular design, the toolchain can be easily extended by other surface grid construction packages.

Before actually generating the volume grid, the surface optimiser can be used to considerably reduce the amount of triangles required for an adequate representation of the original data. At the same time it smoothes the surface and thus removes artefacts that were unintentionally introduced during surface reconstruction.

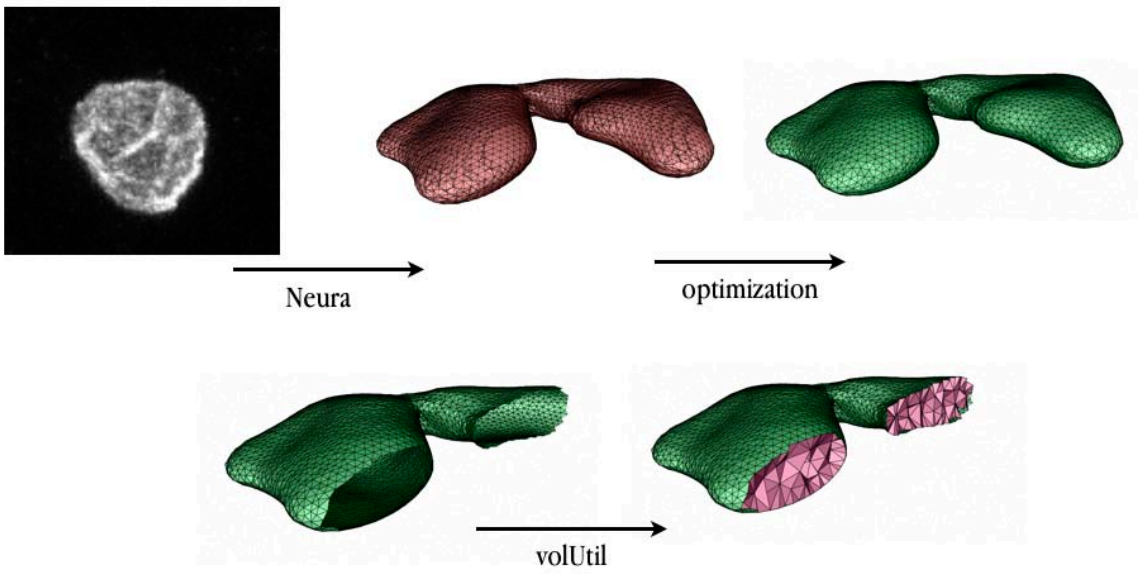

Figure 9. Workflow from microscopy to volume grid

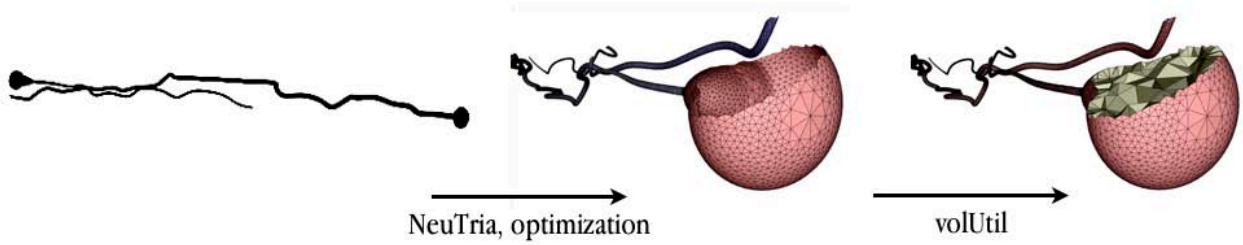

Figure 10. Workflow from NeuGen to volume grid

Subdivision Surface Refinement

Subdivision Surface Refinement is a technique to describe either interpolating or approximating 2D smooth surfaces, which result as the limit of the successive refinement of a piecewise linear control mesh and (re-)positioning of its vertices. Vertices of the refined mesh are positioned using weighted averages of the vertices of the unrefined mesh. With Loop's scheme (Loop 1987), which is based on B-Spline approximation, the limit surface is ensured to be two times continuously differentiable everywhere except for irregular vertices, where the surface is only one time continuously differentiable. Furthermore, this method can be applied to regular 2D geometries of arbitrary topology.

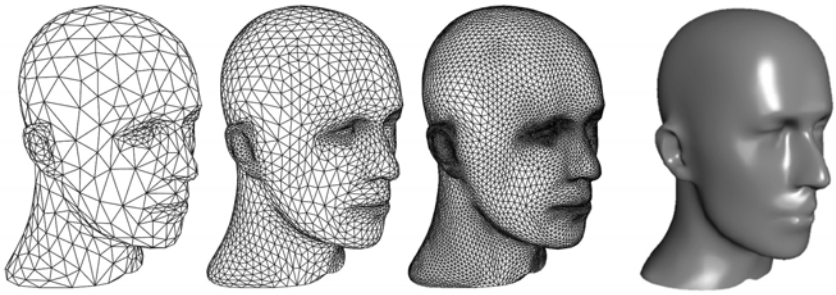

Figure 11. Successive subdivision refinement steps and limit surface (from Zorin et al. 2000)

Multigrid methods require successive refinement. The classical approach is based on a geometrical projection, where the refined mesh is projected onto a separate boundary description. This method is prone to error and likely to cause problems on geometries with inversions, which occur quite often in neurobiological data. In this case subdivision refinement represents a promising alternative. After an initial surface-fitting step, which can be done during surface-optimisation, successive Subdivision Refinement automatically leads to a grid whose boundary approximates the surface geometry of the original data. While this technique is not intended to replace the classical refinement methods, it is a stable, robust and fast alternative, perfectly suited for geometries based on neurobiological data.

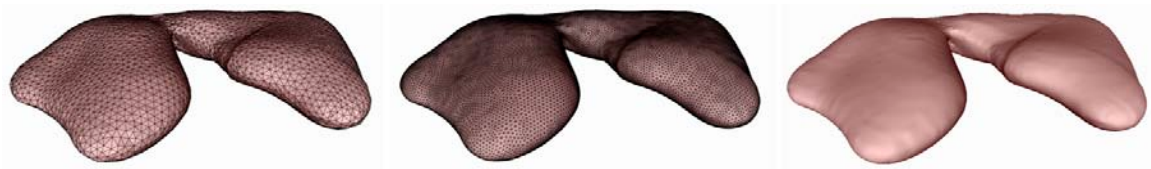

Figure 12. Subdivision Refinement applied on a nucleus during simulation with $\mathcal{UG}$

References

Feuchter, D., Stemmermann, U., & Wittum, G. (2001). Description and Generation of Geometries and Grids for Layered Domains. 17th GAMM Seminar on Construction of Grid Generation Algorithms, ISBN 3-00-007753-7. Retrieved from http://www.mis.mpg.de/conferences/gamm/2001/GAMM_2001_Abstracts_7.html

Feuchter, D., Heisig, M., & Wittum, G. (2006). A geometry model for the simulation of drug diffusion through stratum corneum. Computing and Visualization in Science, 9(2), 117-130.

Fuchs, A., & Wittum, G. (2003). Grid Generation for Domains with Thin Layers. WiR-Preprint, 02/03, Heidelberg.

Loop, C. (1987). Smooth Subdivision Surfaces Based on Triangles. M.S. Mathematics thesis, University of Utah, USA.

Si, H. (2006). TetGen - A Quality Tetrahedral Mesh Generator and Three-Dimensional Delauney Triangulator, User's Manual. Retrieved from http://tetgen.berlios.de/

Zorin, D., DeRose, T., Levin, A., Schröder, P., Kobbelt, L., & Sweldens, W. (2000). Subdivision for Modeling and Animation. SIGGRAPH 2000 Coursenotes. Retrieved from: http://www.cs.rutgers.edu/~decarlo/readings/subdiv-sg00c.pdf

T4: Visualisation: VRL/UG Interface

Michael Hoffer, Christian Poliwoda, Gabriel Wittum

VRL is a flexible library for automatic and interactive object visualisation on the Java platform. It provides a visual programming interface including meta programming support and tools for real—time 3D graphic visualisation.

Mapping programme functionality to graphical interfaces is traditionally a manual and work—intensive process. VRL tries to simplify the creation of user interfaces by using a declarative approach. Instead of giving specific instructions on how to generate the user interface it is only necessary to define the functionality of the user interface. VRL analyses the functionality provided by the Java objects that shall be visualised and uses three types of visual components to create a graphical user interface that reflects the functionality provided by the object: object visualisations, method visualisations and parameter visualisations (see Figure 1). Parameter visualisations are the most individual part of the VRL GUI generation. Therefore VRL provides a plugin interface that allows to add custom visualisations. This includes interactive 2D and 3D visualisations. In addition to the automatic visualisation, it is possible to specify data dependencies. This is necessary to define complex workflows. All connections are type safe. It is possible to define custom contracts for data validation. The messaging system notifies the user about incorrect input. VRL can also execute external tools, i.e., perform tasks that are usually performed on the command line. Thus, it is able to integrate external tools for defining a problem specific workflow which consists of several independent tools. Although not limited to a specific domain, VRL components are optimised for technical simulation. Figure 2 shows an example visualisation:

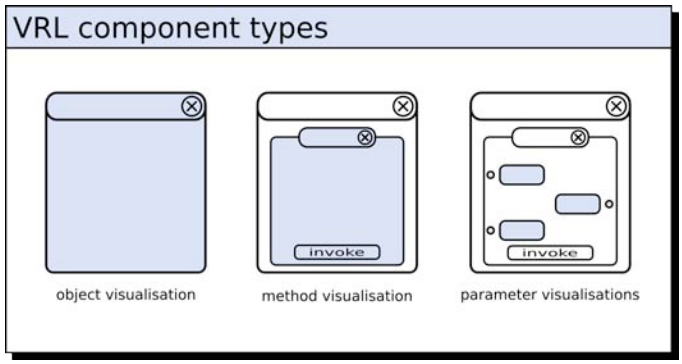

Figure 1. VRL component types

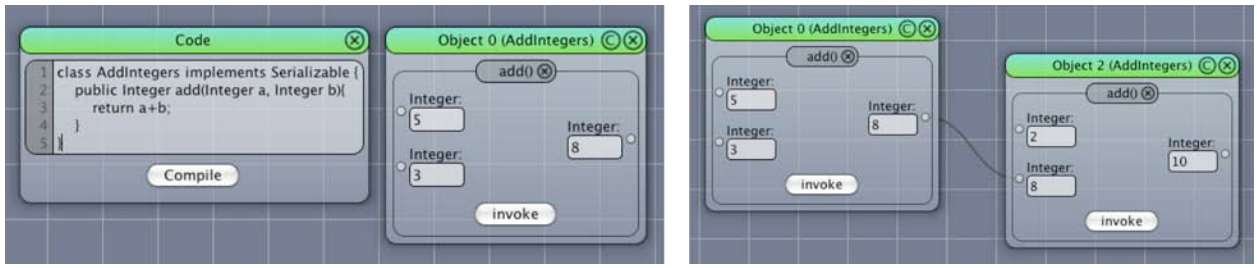

Figure 2. Visualisation of a simple Java object

To define method calls independently from data dependencies, VRL enables the definition of a linear control flow (see Figure 3). With this additional information it is possible to compile a VRL workflow as Java class with one method. Instances of this class can be visualised like any other Java object. Another important aspect is the usage of the visually formulated functionality by any other Java based software. This includes non—graphical applications.

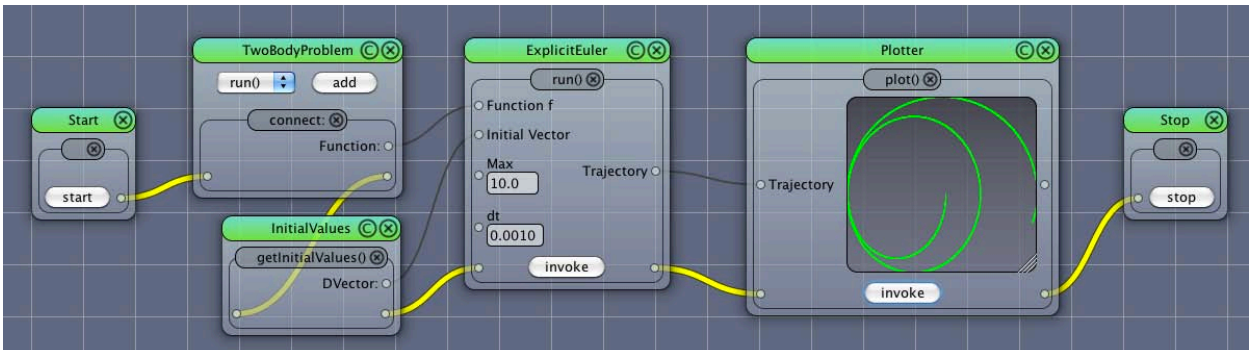

Figure 3. Visualisation of the control flow

Usually UG-based workflows are console dependant tasks which involve also other tools. Because simulation workflows can be complex it is necessary to provide a graphical user interface which is able to reflect the flexibility and complexity of UG. By using an intuitive graphical user interface, UG can be handled by a wider range of users. For UG 3 VRL is used to convert a visually defined workflow to UG script files. Figure 4 shows a graphical UG application for the detailed computation of permeation through human skin.

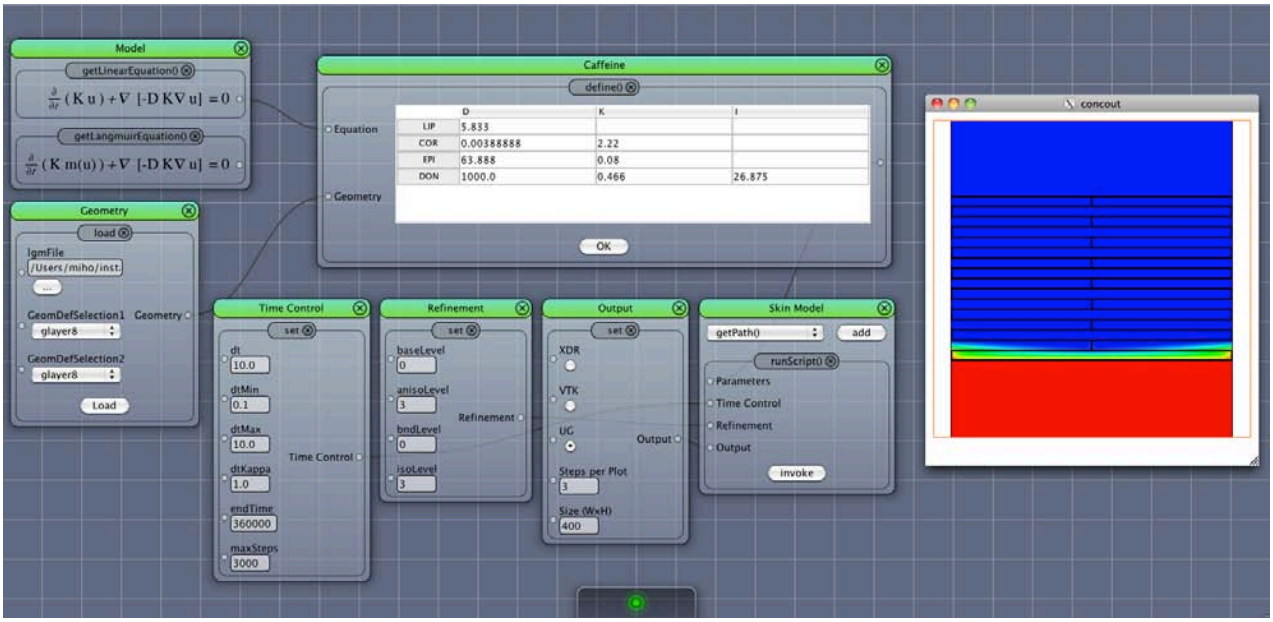

Figure 4. UG 3 application for the detailed computation of permeation through human skin

Converting visual workflows to script files has several limitations we want to overcome. For example, it is not possible to automatically create the visual components to interact with UG. Combining VRL, UG and other libraries and frameworks in one application is complicated as many different technologies are involved.

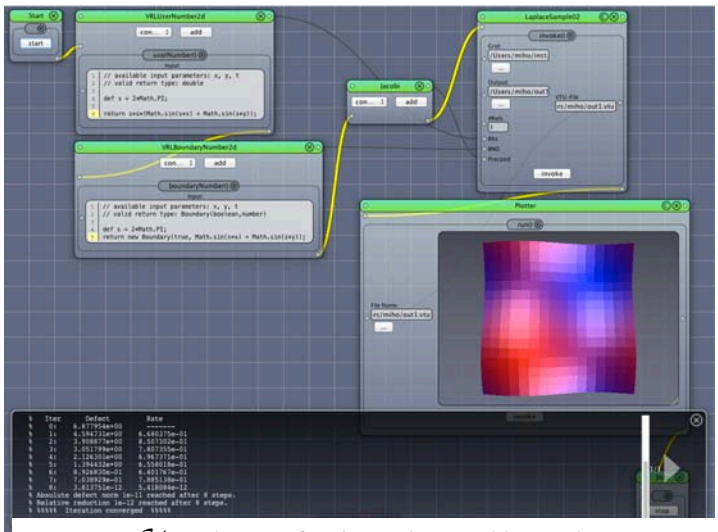

Figure 5. UG 4 application for the Laplace problem (2d)

To address these issues we created a direct VRL/Java binding for UG 4 in addition to the LUA binding. UG 4 provides a flexible registration service that we use to create Java classes that can be visualized by VRL. The class hierarchy of the original UG classes is preserved. Thus, it is possible to directly use the visualisation capabilities of VRL to create UG-based workflows. Furthermore, the VRL editor can be used for text–based UG programming on the Java platform.

Figure 5 shows a graphical UG 4 application for the Laplace problem. This is an application that combines a visual workflow that defines the basic application logic and text–based programming for the detailed definition of the numerical problem.

Combining text–based programming and visual workflow management enables the creating flexible and powerful applications. Our tests show that this approach is promising and allows for completely new and dynamic applications.

T5: Simulation Software Library SG

Dmitry Logashenko, Gabriel Wittum

As a counterpart of *ug*, we developed the library SG (structured grids). This is an efficient tool for computations on topologically rectangular grids of arbitrary dimension. It profits from the special data structures for the representation of these grids. Furthermore, for efficient simulations of high-dimensional problems, it supports the combination technique for sparse grids (Zenger, 1990). The current version of the library (SG2) is capable of handling a wide range of discretisations of systems of PDEs on structured grids, including e.g. time-dependent non-linear problems on staggered grids, and contains efficient numerical solvers, e.g. multigrid methods. It provides a flexible object-oriented programming interface for numerical methods with the possibility of reading method-specific parameters from initialisation files. The combination technique is parallelised on the base of the MPI library. SG is implemented in C++ programming language and is platform independent.

The main field of the applications of SG are high-dimensional problems. In the combination technique for the sparse grids, the system of the PDEs is discretised and solved independently on several grids obtained from the same coarse grid by anisotropic refinement. Figure 1 demonstrates this method in 2 dimensions. The numerical solution on the sparse grid is a linear combination of the numerical solutions on the red and the blue regular grids, which are computed independently of each other. The accuracy of this solution is approximately equivalent to that of the solution on the full regular grid with stepsize h, provided the solution is sufficently smooth. But in high-dimensional cases, the number of degrees of freedom on all the grids involved in the combination technique is essentially smaller then for the full regular grid with the same grid step. Furthermore, the computations of the solutions on the regular grids in the combination technique can be performed on different processors without communication. This allows very efficient parallelisation of the computations. This approach was used for high dimensional problems in the computational finance (see Section A3).

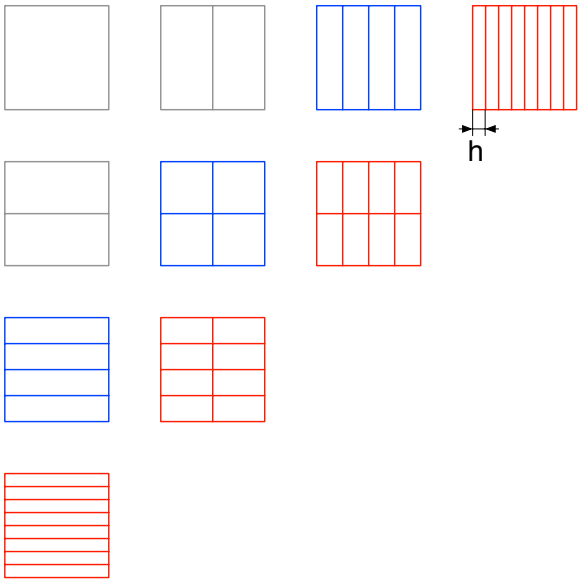

Figure 1. Combination technique for the sparse grids

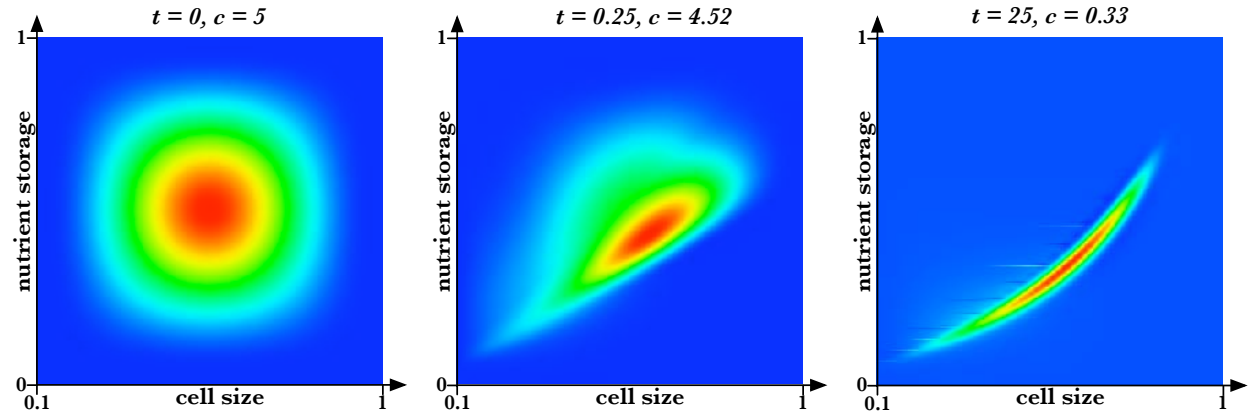

Figure 2. Simulation of biological cell growth with SG2

We also applied this approach for simulations of population dynamics. Figure 2 presents results of a simulation of the biological cell growth in a stirred tank. The medium containing the cells (e.g. bacteria) and the nutrient is considered to be well mixed so that it is homogenious. The nutrient is described by its concentration c in the medium. The cells consume the nutrient and store it in their internal nutrient storage. Furthermore, they convert this nutrient to biomass characterised by cell size. The whole cell population is therefore described by the number density function characterising the distribution of the cells in coordinate system "cell size $\times$ stored nutrient" (these values are scaled). The model describing these processes is a system of an integro- partial differential equation for the number density function and an ordinary differential equation with an integral term for the concentration c (see Fischer et al. 2006) in the coordinates space, time, cell size and stored nutrient. This system is solved using the combination technique for the sparce grids which allows also efficient treatment of the integral terms. More complicated biological models involving more parameters for the description of the population can be handled in the same way.

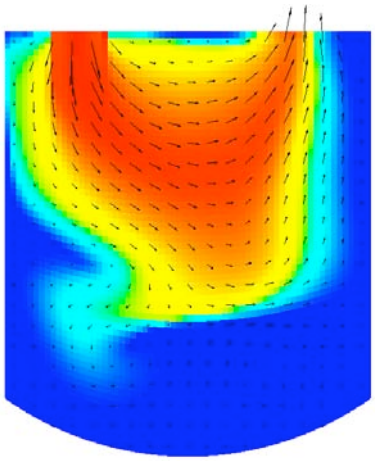

Figure 3: Simulation of flow and transport in a stirred tank with SG

SG2 can be also used for efficient computations on regular structured (non-sparse) grids. Figure 3 presents a simulation of the Navier-Stokes flow coupled with the transport in a stirred tank. In this example, the discretisation of the Navier-Stokes equations is based on staggered grids.

Further applications include image processing. The possibility to link SG2 as an external library to other software was used in Mang et al. 2009 for a method tracking fibers in the brain. In this application, the SG2 solvers were used to simulate the self-diffusion in small areas of the brain to determine the direction of the fibers and showed very good performance.

References

Fischer, T., Logashenko, D., Kirkilionis, M., & Wittum, G. (2006). Fast Numerical Integration for Simulation of Structured Population Equations. Mathematical Models and Methods in Applied Sciences, 16(12), 1987-2012.

Mang, S. C., Logashenko, D., Gembris, D., Wittum, G., Grodd, W., & Klose, U. (2010). Diffusion Simulation Based Fiber Tracking using Time-of-Arrival Maps. Magnetic Resonance Materials in Physics, Biology and Medicine, 23(5-6), 391-398.

Zenger, C. (1990): Sparse Grids. SFB-Bericht 342/18/90, Lehrstuhl für Informatik V, TU München.

T8: NeuGen: A Tool for the Generation of Realistic Morphology of Cortical Neurons and Neural Networks in 3D

Jens Eberhard, Alexander Wanner, Sergei Wolf, Gillian Queisser, Gabriel Wittum

NeuGen (Eberhard et al. 2006) is a tool for the efficient generation and description of dendritic and axonal morphology of realistic neurons and neural networks in 3D. It is based on experimental data. The 'in silico' neurons are based on cells of cortical columns in the neocortex. The software is available at http://www.neugen.org

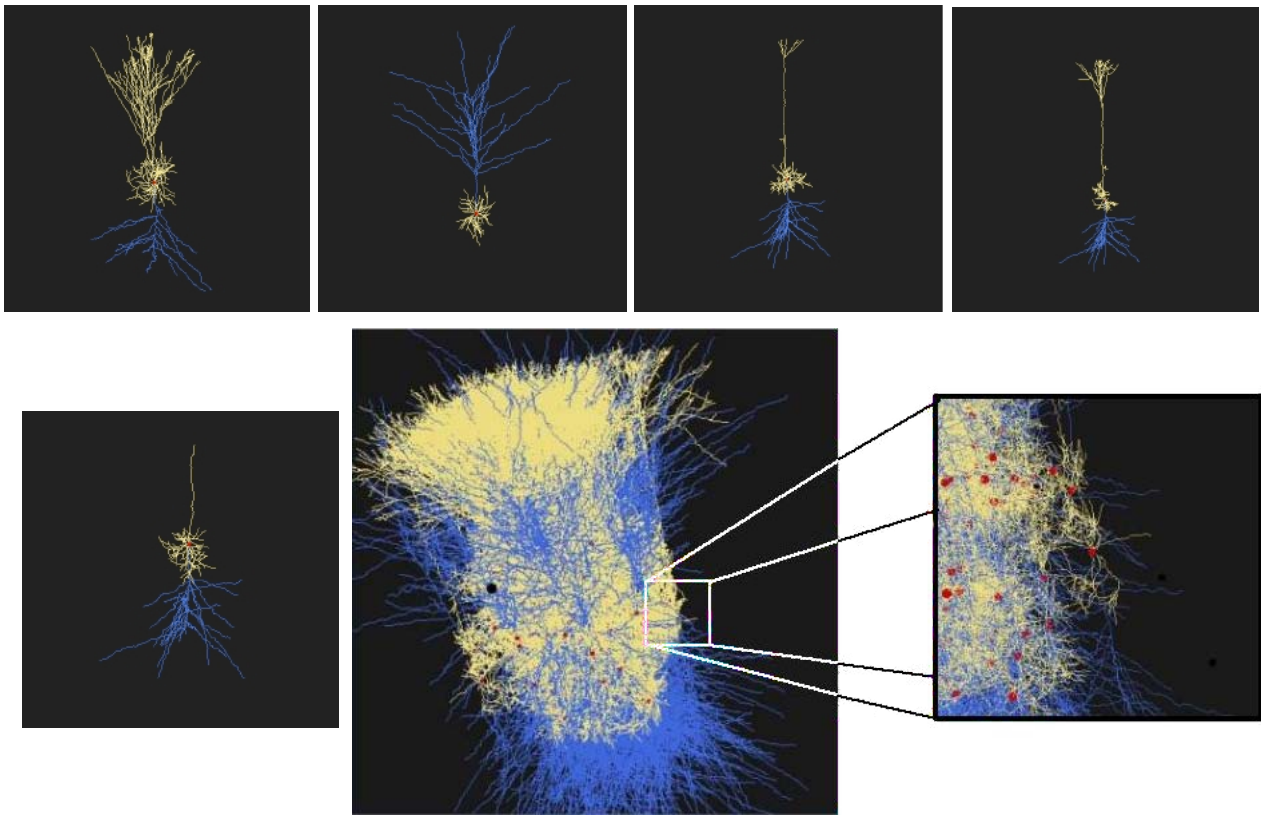

Figure 1. From left: L2/3 pyramidal cell, L4 spiny stellate cell, L5A pyramidal neuron, L5B pyramidal neuron , L4 starpyramidal cell, network with 100 cells

The idea for the development of NeuGen has been to be able to simulate networks of synaptically connected neurons in a cortical column. The NeuGen project is mainly a result of the fact that experimental data is available nowadays to extract the anatomical fingerprints of the cells and to generate synthetic neuron geometries.

NeuGen is an on-going software project which will be extended by additional features. A graphical user interface is included in the newest NeuGen version which makes program control and assignment of values to the configuration parameters very easy. In recent developments, we began developing a neuroanatomical model of the hippocampus. New classes of neurons, e.g. granule cells, CA1 pyramidal cells and CA3 pyramidal cells and different types of interneurons have been implemented.

References

Wolf, S., Grein, S., & Queisser, G. (2011). Employing NeuGen 2.0 to automatically generate realistic morphologies of hippocampal neurons and neural networks in 3D. Manuscript submitted for publication.

Eberhard, J. P., Wanner, A., & Wittum, G. (2006). NeuGen: A tool for the generation of realistic morphology of cortical neurons and neural networks in 3D. Journal of Neurocomputing, 70(1-3), 327-342.

NeuGen: http://www.neugen.org

T9: NeuTria: A Tool for the Triangulation of Realistic Morphologies of Cortical Neurons and Neural Networks in 3D

Niklas Antes, Sebastian Reiter, Gillian Queisser, Gabriel Wittum

NeuTria is a software tool for generating closed 3-d surface grids from abstract spatial information. One example is the generation of neurons and networks from abstract data provided by NeuGen.

In NeuGen (Eberhard et al. 2006) the geometry is composed of frustums, see Figure 1 (right). For detailed 3-d models of cellular and sub-cellular signal processing we need a closed surface of the neurons, whereas the list of frustums does not define closed surfaces.

NeuTria is a software tool to generate an approximation of the given "raw data" and calculates closed surfaces – composed of triangles – from NeuGen-generated files. It also creates a geometry of synapses, which in NeuGen only is provided as electrophysical data. Because the lists of frustums describing a dendrite or an axon are too angular, the program also generates a smoothed graph along a dendrite. Very difficult is the generation of correct geometries at intersections and soma.

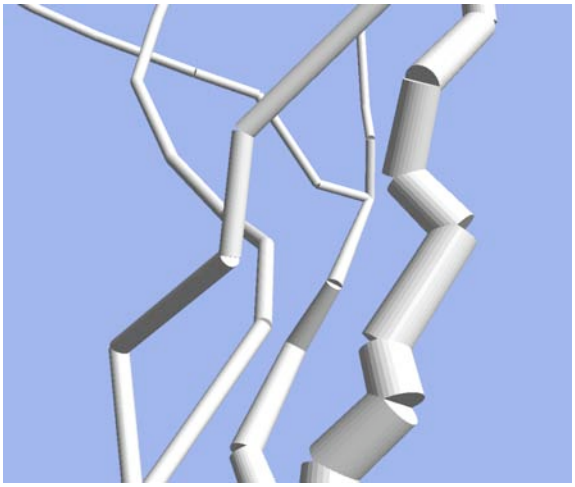

Figure 1. The geometry of dendritic branches is represented as a sequence of frustums. The sections are devided into compartments.

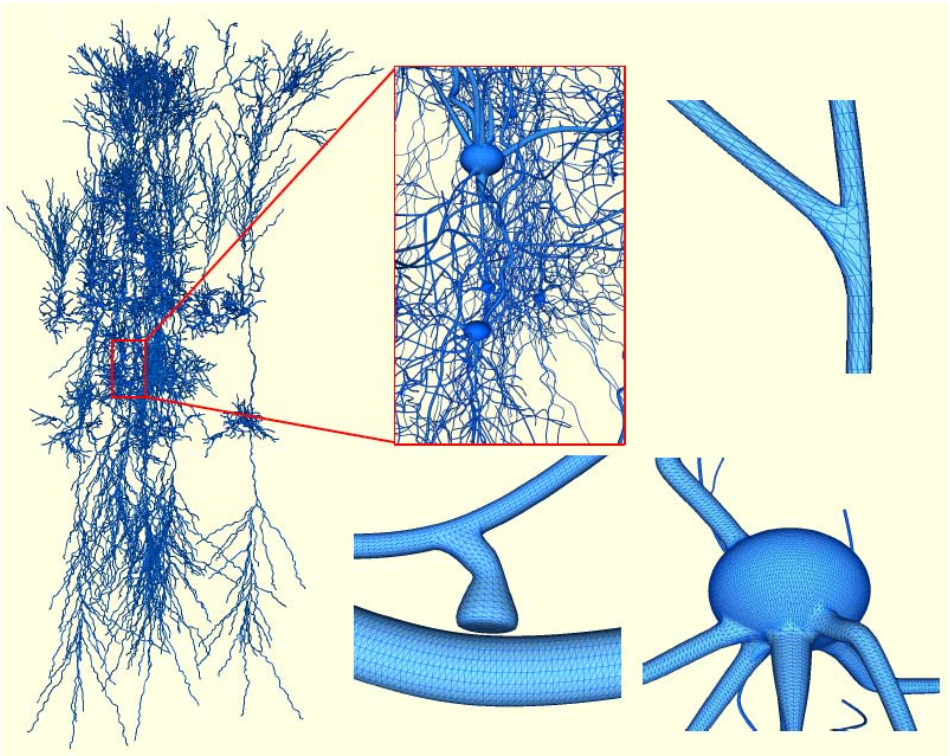

Figure 2.
Left: A generated network for a cortical column with 20 cells.
Right top: A dendritic branching point. A synapse (middle) and soma (right).

References

Antes, N. (2009): Ein Werkzeug zur Erzeugung von Oberflächengeometrien von Neuronen. Staatsexamensarbeit, Fakultät Mathematik, Universität Heidelberg.

Eberhard, J. P., Wanner, A., & Wittum, G. (2006). NeuGen: A tool for the generation of realistic morphology of cortical neurons and neural networks in 3D. Neurocomputing, 70(1-3), 327-342.

CF1: Asset/Liability Management in Insurance

Thomas Gerstner

Much effort has been spent on the development of stochastic asset-liability management (ALM) models for life insurance companies in the last years. Such models are becoming more and more important due to new accountancy standards, greater globalisation, stronger competition, more volatile capital markets and long periods of low interest rates. They are employed to simulate the medium and long-term development of all assets and liabilities. This way, the exposure of the insurance company to financial, mortality and surrender risks can be analysed. The results are used to support management decisions regarding, e.g., the asset allocation, the bonus declaration or the development of more profitable and competitive insurance products. The models are also applied to obtain market-based, fair value accountancy standards as required by Solvency II and the International Financial Reporting Standard.

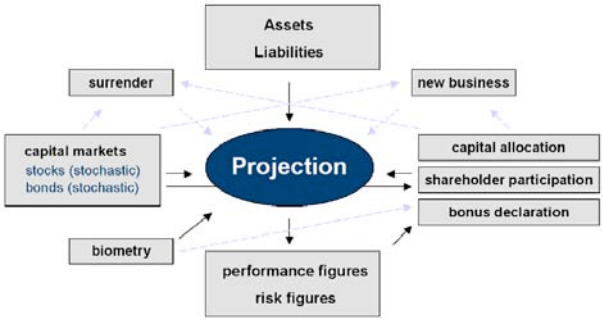

Due to the wide range of path-dependencies, guarantees and option-like features of insurance products, closed-form representations of statistical target figures, like expected values or variances, which in turn yield embedded values or risk-return profiles of the company, are in general not available. Therefore, insurance companies have to resort to numerical methods for the simulation of ALM models. In practice, usually Monte Carlo methods are used which are based on the averaging of a large number of simulated scenarios. These methods are robust and easy to implement but suffer from an erratic convergence and relatively low convergence rates. In order to improve an initial approximation by one more digit precision, Monte Carlo methods require, on average, the simulation of a hundred times as many scenarios as have been used for the initial approximation. Since the simulation of each scenario requires to run over all relevant points in time and all policies in the portfolio of the company, often very long computing times are needed to obtain approximations of satisfactory accuracy. As a consequence, a frequent and comprehensive risk management, extensive sensitivity investigations or the optimisation of product parameters and management rules are often not possible.

In this project, we focus on approaches to speed up the simulation of ALM models. To this end, we rewrite the ALM simulation problem as a multivariate integration problem and apply quasi-Monte Carlo and sparse grid methods in combination with adaptivity and dimension reduction techniques for its numerical computation. Quasi-Monte Carlo and sparse grid methods are alternatives to Monte Carlo simulation, which are also based on a (weighted) average of different scenarios, but which use deterministic sample points instead of random ones. They can attain faster rates of convergence than Monte Carlo, can exploit the smoothness of the integrand and have deterministic upper bounds on their error. In this way, they have the potential to significantly reduce the number of required scenarios and computing times.

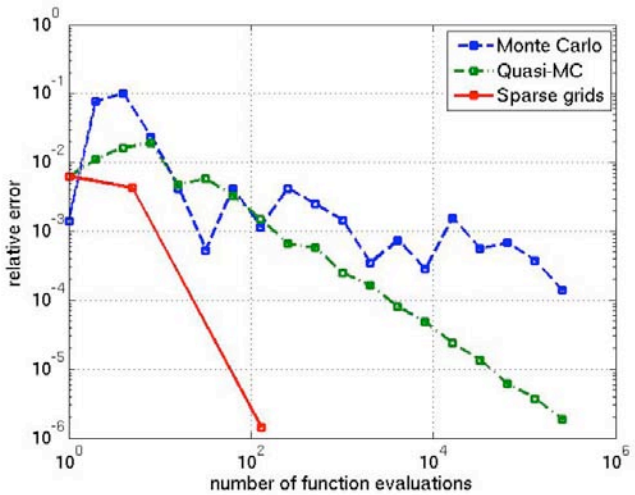

CF2: Valuation of Performance-Dependent Options

Thomas Gerstner

Companies make big efforts to bind their staff to them for long periods of time in order to prevent a permanent change of executives in important positions. Besides high wages, such efforts use long-term incentives and bonus schemes. One widespread form of such schemes consists in giving the participants a conditional award of shares. If the participant stays with the company for at least a prescribed time period he will receive a certain number of company shares at the end of the period.

Typically, the exact amount of shares is determined by a performance criterion such as the company's gain over the period or its ranking among comparable firms (the peer group). This way, such bonus schemes induce uncertain future costs for the company. For the corporate management and especially for the shareholders, the actual value of such bonus programmes is quite interesting. One way to determine an upper bound on this value is to take the price of vanilla call options on the maximum number of possibly needed shares. This upper bound, however, often significantly overestimates the true value of the bonus programme since its specific structure is not respected.

Contingent claim theory states that the accurate value of such bonus programmes is given by the fair price of options which include the used performance criteria in their payoff. Such options are called performance-dependent options. Their payoff yields exactly the required shares at the end of the bonus scheme. This way, performance-dependent options minimise the amount of money the company would need to hedge future payments arising from the bonus scheme.

Similar performance comparison criteria are currently used in various financial products, for example many hedge funds are employing so-called portable alpha strategies. Recently, pure performance-based derivatives have entered the market in the form of so-called alpha certificates. Here, typically the relative performance of a basket of stocks is compared to the relative performance of a stock index. Such products are either used for risk diversification or for pure performance speculation purposes.

In this project, we develop a framework for the efficient valuation of fairly general performance-dependent options. Thereby, we assume that the performance of an asset is determined by the relative increase of the asset price over the considered period of time. This performance is then compared to the performances of a set of benchmark assets. For each possible outcome of this comparison, a different payoff can be realised.

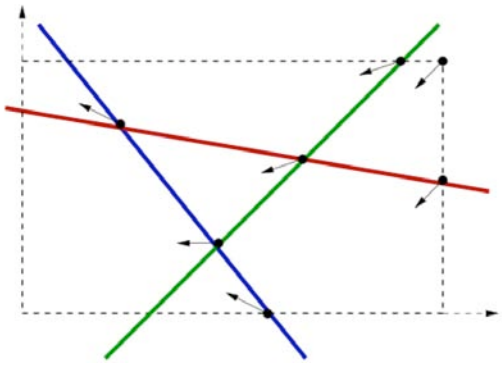

We use multidimensional stochastic models for the temporal development of all asset prices required for the performance ranking. The martingale approach then yields a fair price of the performance-dependent option as a multidimensional integral whose dimension is the number of stochastic processes used in the model. In so-called full models the number of stochastic processes equals the number of assets. In reduced models, the number of processes is smaller. Unfortunately, in neither case direct closed-form solution for these integrals are available. Moreover, the integrand is typically discontinuous which

makes accurate numerical solutions difficult to achieve. In this project we develop numerical methods to solve these integration problems. For reduced models, tools from computational geometry are developed, such as the fast enumeration of the cells of a hyperplane arrangement and the determination of its orthant decomposition.

References

Gerstner, T., & Griebel, M. (2009). Sparse grids. In Encyclopedia of Quantitative Finance, J. Wiley & Sons.

Gerstner, T., Griebel, M., & Holtz, M. (2007). The effective dimension of asset-liability management problems in life insurance. In Proc. Third Brazilian Conference on Statistical Modelling in Insurance and Finance (pp. 148-153).

Gerstner, T., Griebel, M. & Holtz, M. (2009). Efficient deterministic numerical simulation of stochastic asset-liability management models in life insurance. Insurance: Mathematics and Economics, 44(3), 434-446.

Gerstner, T., Griebel, M., Holtz, M., Goschnick, R., & Haep, M. (2008). A General Asset-Liability Management Model for the Efficient Simulation of Portfolios of Life Insurance Policies. Insurance: Mathematics and Economics, 42(2), 704-716.

Gerstner, T., Griebel, M., Holtz, M., Goschnick, R., & Haep, M. (2008). Numerical Simulation for Asset-Liability Management in Life Insurance.In H.-J. Krebs and W. Jäger, Mathematics - Key Technology for the Future (pp. 319-341). Berlin: Springer.

Gerstner, T., & Holtz, M. (2008). Valuation of performance-dependent options. Applied Mathematical Finance, 15(1), 1-20.

Gerstner, T., & Holtz, M. (2006). Geometric tools for the valuation of performance-dependent options. In M. Costantino and C. Brebbia (Eds.), Computational Finance and its Application II (pp. 161-170). London: WIT Press.

Gerstner, T., Holtz, M., & Korn, R. (2007). Valuation of performance-dependent options in a Black-Scholes framework. In J.H. Miller et al. (Eds.), Numerical Methods for Finance (pp. 203-214). Boca Raton: Chapman & Hall/CRC.

List of Publications 2006-2012

Peer-reviewed

Buzdin, A., Logaschenko, D., & Wittum, G. (2008). IBLU Decompositions Based on Padé Approximants. Numerical Linear Algebra with Applications, 15(8), 717-746.

Eberhard, J. P., Wanner, A., & Wittum, G. (2006). NeuGen: A tool for the generation of realistic morphology of cortical neurons and neural networks in 3D. Journal of Neurocomputing, 70(1-3), 327-342.

Eberhard, J., Popovic, D., & Wittum, G. (2008). Numerical upscaling for the eddy-current model with stochastic magnetic materials. Journal of Computational Physics, 227(8), 4244-4259.

Federico, S., Grillo, A., & Wittum, G. (2009). Considerations on Incompressibility in Linear Elasticity. Il Nuovo Cimento C, 32(1), 81-87.

Feuchter, D., Heisig, M., & Wittum, G. (2006). A geometry model for the simulation of drug diffusion through stratum corneum. Computing and Visualization in Science, 9(2), 117-130.

Fischer, T., Kirkilionis, M., Logashenko, D., & Wittum, G. (2006). Fast Numerical Integration for Simulation of Disperse Systems. Mathematical Models and Methods in Applied Sciences, 16(12), 1987-2012.

Frolkovic, P., & Kacur, J. (2006). Semi-analytical solutions of contaminant transport equation with nonlinear sorption in 1D, Computational Geosciences, 3(10), 279-290.

Frolkovic, P., & Mikula, K. (2007). High-resolution flux-based level set method. SIAM Journal on Scientific Computing, 29(2), 579-597.

Frolkovic, P., & Mikula, K. (2007). Flux-based level set method: a finite volume method for evolving interfaces. Applied Numerical Mathematics, 57(4), 436-454.

Frolkovič, P., Mikula, K., Peyrieras, N., & Sarti, A. (2007). A counting number of cells and cell segmentation using advection-diffusion equations. Kybernetika, 43(6), 817–829.

Frolkovic, P., Wehner, C. (2009). Flux-based level set method on rectangular grids and computations of first arrival time functions. Computing and Visualization in Science, 12(5), 297-306.

Frolkovic, P., Logashenko, D., & Wittum, G. (2008). Flux-based level set method for two-phase flows. In R. Eymard, J.-M. Herard (Eds.), Finite Volumes for Complex Applications V (pp. 415-422). London: ISTE and Wiley.

Gordner, A., & Wittum, G. (2007). Low Machnumber Aeroacoustics --- A direct one-grid approach. Journal of Numerical Mathematics, 15(1), 7–29.

Grillo, A., Federico, S., Wittum, G., Imatani, S., Giaquinta, G., & Micunovic, M. V. (2009). Evolution of a Fibre-Reinforced Growing Mixture. Il Nuovo Cimento C, 32(1), 97-119.

Grillo, A., Lampe, M., Logashenko, D., Stichel, S. & Wittum, G. (2012). Simulation of salinity- and thermohaline-driven flow in fractured porous media. Journal of Porous Media, 15(5), 439-458.

Grillo, A., Lampe, M., & Wittum, G., (2010). Three-dimensional simulation of the thermohaline-driven buoyancy of a brine parcel. Computing and Visualization in Science, 13, 287-297.

Grillo, A., Lampe, M., & Wittum, G. (2011). Modelling and Simulation of Temperature-Density-Driven Flow and Thermodiffusion in Porous Media. Journal of Porous Media, 14(8), 671-690.

Grillo, A., Logashenko, D., Stichel, S., & Wittum, G. (2010). Simulation of Density-Driven Flow in Fractured Porous Media. Advances in Water Resources, 33(12), 1494-1507.

Grillo, A. & Wittum, G. (2010). Growth and mass transfer in multi-constituent biological materials. In T. Simos et al. (Eds.), ICNAAM 2010: International Conference of Numerical Analysis and Applied Mathematics 2010. American Institute of Physics, Conference Proceedings. Volume 1281, pp. 355-359.

Grillo, A., Wittum, G., Giaquinta, G., & Micunovic, M. V. (2009). A Multiscale Analysis of Growth and Diffusion Dynamics in Biological Materials. International Journal of Engineering Science, 47(2), 261-283.

Hansen, S., Henning, A., Nägel, A., Heisig, M., Wittum, G., Neumann, D., Kostka, K. H., Zbytovska, J., Lehr, C. M., & Schäfer, U. F. (2008). In-silico model of skin penetration based on experimentally determined input parameters. Part I: Experimental determination of partition and diffusion coefficients. European Journal of Pharmaceutics and Biopharmaceutics, 68(2), 352-367.

Hansen, S., Naegel, A., Heisig, M., Wittum, G., Neumann, D., Kostka, K., Meiers, P., Lehr, C. M., & Schaefer, U. F. (2009). The Role of Corneocytes in Skin Transport Revised - A Combined Computational and Experimental Approach. Pharmaceutical Research, 26, 1379-1397.

Hauser, A., Wittum, G. (2008). Analysis of Uniform and Adaptive LES in Natural Convection Flow. In J. Meyers et al. (Eds.), Quality and Reliability of Large-Eddy Simulations (pp. 105-116), Dordrecht: Springer.

Heumann, H., & Wittum, G (2009). The tree edit distance, a measure for quantifying neuronal morphology. Neuroinformatics, 7(3), 179-190.

Johannsen, K., Oswald, S., Held, R., & Kinzelbach, W. (2006). Numerical simulation of three-dimensional saltwater-freshwater fingering instabilities observed in a porous medium. Advances in Water Resources, 29(11), 1690-1704.

Johannsen, K. (2006). Multigrid Methods for Nonsymmetric Interior Penalty Discontinuous Galerkin Methods. Computing and Visualization in Science, to appear.

Jungblut, D., Queisser, G., & Wittum, G. (2012). Inertia Based Filtering of High Resolution Images Using a GPU Cluster. Computing and Visualization in Science, 14(4), 181-186.

Logashenko, D., Fischer, T., Motz, S., Gilles, E.-D., & Wittum, G. (2006). Simulation of Crystal Growth and Attrition in a Stirred Tank. Computing and Visualization in Science. 9(3), 175-183.

Mang, S. C., Logashenko, D., Gembris, D., Wittum, G., Grodd, W., & Klose, U. (2010). Diffusion Simulation Based Fiber Tracking using Time-of-Arrival Maps. Magnetic Resonance Materials in Physics, Biology and Medicine, 23(5-6), 391-398.

Metzner, M., & Wittum, G. (2006). Computing low Mach-number flow by parallel adaptive multigrid. Computing and Visualization in Science, 9(4), 259-269.

Micunovic, M.V., Albertini, C., Grillo, A., Muha, I., Wittum, G., & Kudrjavceva, L. (2011). Two dimensional waves in quasi rate independent viscoplastic materials. Journal of Theoretical and Applied Mechanics, 38(1), 47-74.

Mo, Z., Zhang, A., & Wittum, G. (2009). Scalable Heuristic Algorithms fo the Parallel Execution of Data Flow Acyclic Digraphs. SIAM Journal on Scientific Computing, 31(5), 3626-3642.

Muha, I., Grillo, A., Heisig, M., Schönberg, M., Linke, B., & Wittum, G. (2012). Mathematical modeling of process liquid flow and acetoclastic methanogenesis under mesophilic conditions in a two−phase biogas reactor. Bioresource Technology, 106, 1-9.

Muha, I., Lenz, H., Feuchter, D., Handel, S., & Wittum, G. (2009). VVS eine Software zur Optimierung des Einlagerungsprozesses in Horizontalsilos. Bornimer Agrartechnische Berichte, 68, 35-43.

Muha, I., Naegel, A., Stichel, S., Grillo, A., Heisig, M. & Wittum, G. (2011). Effective diffusivity in membranes with tetrakaidekahedral cells and implications for the permeability of human stratum corneum. Journal of Membrane Science 368(1-2), 18-25.

Muha, I., Stichel, S., Attinger, S., & Wittum, G. (2010). Coarse graining on arbitrary grids. SIAM Multiscale Modeling and Simulation 8(4), 1368-1382.

Nägel, A., Falgout, R. D., & Wittum, G. (2008). Filtering algebraic multigrid and adaptive strategies. Computing and Visualization in Science, 11(3), 159-167.

Naegel, A., Hansen, S., Neumann, D., Lehr, C., Schaefer, U. F., Wittum, G., & Heisig, M. (2008). In-silico model of skin penetration based on experimentally determined input parameters. Part II: Mathematical modelling of in-vitro diffusion experiments. Identification of critical input parameters. European Journal of Pharmaceutics and Biopharmaceutics, 68, 368-379.

Nägel, A., Heisig, M., & Wittum, G. (2009). A comparison of two- and three-dimensional models for the simulation of the permeability of human statum corneum. European Journal of Pharmaceutics and Biopharmaceutics, 72(2), 332-338.

Naegel, A., Heisig, M., & Wittum, G. (2011). Computational modeling of the skin barrier. Methods Molecular Biology 763, 1-32.

Naegel, A., Heisig, M., & Wittum, G. (in press). Detailed modeling of skin penetration - an overview. Advanced Drug Delivery Reviews.

Nägele, S., & Wittum, G. (2007). On the Influence of Different Stabilisation Methods for the Incompressible Navier-Stokes Equations. Journal of Computational Physics, 224(1), 100-116.

Queisser, G., Wiegert S. & Bading H. (2011). Structural dynamics of the nucleus: Basis for Morphology Modulation of Nuclear Calcium Signaling and Gene Transcription. Nucleus, 2(2), 98-104.

Queisser, G., Wittmann, M., Bading, H., & Wittum, G. (2008). Filtering, reconstruction and measurement of the geometry of nuclei from hippocampal neurons based on confocal microscopy data. Journal of Biomedical Optics, 13(1), 014009.

Queisser, G. & Wittum, G. (2011). Investigating the Diffusion Properties of Nuclear Calcium. Biological Cybernetics, 105(3-4), 211-216.

Reisinger, C., & Wittum, G. (2007). Efficient Hierarchical Approximation of High-Dimensional Option Pricing Problems. SIAM Journal for Scientific Computing, 29(1), 440-458.

Sterz, O., Hauser, A., & Wittum, G. (2006). Adaptive Local Multigrid Methods for the Solution of Time Harmonic Eddy Current Problems. IEEE Transactions on Magnetics, 42(2), 309-318.

Stichel, S., Logashenko, D., Grillo, A., Reiter, S., Lampe, M. & Wittum, G. (2012). Numerical methods for flow in fractured porous media. In J.M.P.Q. Delgado (Ed.), Heat and Mass Transfer in Porous Media (volume 13 of Advanced Structured Materials, pp. 83-113). Berlin: Springer.

Vogel, A., Xu, J. & Wittum, G. (2010). A generalization of the vertex-centered Finite Volume scheme to arbitrary high order. Computing and Visualization in Science, 13(5), 221-228.

Voßen, C., Eberhard, J., & Wittum, G. (2007). Modeling and simulation for three-dimensional signal propagation in passive dendrites. Computing and Visualization in Science, 10(2), 107-121.

Wittmann, M., Queisser, G., Eder, A., Bengtson, C. P., Hellwig, A., Wiegert, J. S., Wittum, G., & Bading, H. (2009). Synaptic activity induces dramatic changes in the geometry of the cell nucleus: interplay between nuclear structure, histone H3 phosphorylation and nuclear calcium signaling. The Journal of Neuroscience, 29(47), 14687-14700.

Xylouris, K., Queisser G., Wittum G. (2010). A Three-Dimensional Mathematical Model of Active Signal Processing in Axons. Computing and Visualization in Science, 13(8), 409-418.

Non peer reviewed

Atanackovic, T., Grillo, A., Wittum, G., & Zorica, D. (2010). An application of fractional calculus to growth mechanics. 4th Workshop "Fractional Differentiation and its Applications" (FDA10), 18-20. X, 2010, Badajoz, Spain.

Eberhard, J., & Frolkovič, P. (2006). Numerical simulation of growth of an atherosclerotic lesion with a moving boundary. IWR-Preprint. Retrieved from http://archiv.ub.uni-heidelberg.de/volltextserver/volltexte/2006/6477/pdf/IWRpreprintEberhardFrolkovic2006.pdf

Frolkovič, P., Logashenko, D., Wehner, C., & Wittum, G. (2010). Finite volume method for two-phase flows using level set formulation. Preprint 2010-10, Department of Mathematics and Descriptive Geometry, Slovak University of Technology, Bratislava 2010.

Gordner, A., Nägele, S., & Wittum, G. (2006). Multigrid methods for large-eddy simulation. In W. Jäger et al. (Eds.), Reactive Flows, Diffusion and Transport. Berlin: Springer.

Grillo, A., Logashenko, D., & Wittum, G. (2009). Mathematical Modelling of a Fractured Porous Medium. Oberwolfach Report No. 12/2009. Within the Mini-Workshop "Numerical Upscaling for Flow Problems: Theory and Applications." Mathematisches Forschungsinstitut Oberwolfach, 1.3.-7.3.2009.

Grillo, A., Logashenko, D., & Wittum, G. (2009). Study of Transport Problem in a Two-Dimensional Porous Medium. In the Proceedings of the COSSERAT+100 International Conference on the Legacy of "Théorie des Corps Déformables" by Eugéne and Francois Cosserat in the centenary of iths publication. École des Ponts ParisTech, 15th-17th of July 2009.

Jungblut, D., Karl, S., Mara, H., Krömker, S., & Wittum, G. (2009). Automated GPU-based Surface Morphology Reconstruction of Volume Data for Archeology. SCCH 2009.

Micunovic, M. V., Grillo, A., Muha, I., & Wittum, G. (2009). Two Dimensional Plastic Waves in Quasi Rate Independent Viscoplastic Materials. In the Proceedings of the ESMC2009, 7th EUROMECH, Lisbon, Portugal, 7th-11th September 2009.

v. Rohden, C., Hauser, A., Wunderle, K., Ilmberger, J., Wittum, G., & Roth, K. (2006). Lake dynamics: observation and high-resolution numerical simulation. In W. Jäger et al. (Eds.), Reactive Flows, Diffusion and Transport. Berlin: Springer.

Submitted papers and papers in preparation

Buzdin, A., Logashenko, D., & Wittum, G. (2009). Frequency Filtering in the Iterative Solution of Eigenvalue Problems. Manuscript submitted for publication.

Frolkovic, P., & Lampe, M., & Wittum, G. (2011). Numerical simulation of contaminant transport in groundwater using software tools r^3t. Manuscript submitted for publication.

Frolkovic, P., Logashenko, D., Wehner, C., Wittum, G. (2009). Finite volume method for two-phase flows using level set formulation. Manuscript submitted for publication.

Frolkovič, P., Logashenko, D., Wehner, C., & Wittum, G. (2011). Flux-based level set method and applications on unstructured grids. Manuscript submitted for publication.

Grillo, A., & Wittum, G. (2010). Considerations on growth and transfer processes in multi-constituent materials. Manuscript submitted for publication.

Hoffer, M., Poliwoda, C., & Wittum, G. (2011). Visual Reflection Library. A Framework for Declarative GUI Programming on the Java Platform. Manuscript in preparation.

Johannsen, K., & Wittum, G. (2006). A SOR-type smoother for strongly non-symmetric positive definite matrices. Unpublished.

Karl, S., Jungblut, D., Mara, H., Wittum, G., & Krömker, S. (2010). Insights in Manufacturing Techniques of Ancient Pottery: Industrial X-Ray Computed Tomography as a Tool in the Examination of Cultural Material in Museums. Manuscript submitted for publication.

Knodel, M., Queisser, G., Geiger, R., Ge, L. H., Bucher, D., Grillo, A., Schuster C.M. & Wittum, G. (2010). Bouton Sizes are Tuned to Best Fit their Physiological Performances. Manuscript submitted for publication.

Micunovic, M.V., Albertini, C., Grillo, A., Muha, I., & Wittum, G. (2009). Two dimensional waves in quasi rate independent viscoplastic materials. Manuscript submitted for publication.

Muha, I., Heisig, M., Schönberg, M., Linke, B., Wittum, G. (2011). Methanogenesis from acetate under mesophilic condition in a biogas reactor. In preparation.

Muha, I., Stichel, S., Naegel, A., Heisig, M., & Wittum, G. (2009). Using homogenization theory to calculate an effective diffusion tensor for human stratum corneum with tetrakaidekahedral geometry. In preparation.

Muha, I., Zielonka, S., Lemmer, A., Schönberg, M., Linke, B., & Wittum, G. (2012). Do two stage biogas reactors seperate the processes? Bioresource Technology. In preparation.

Naegel A., Hahn T., Lehr C.-M., Schaefer U.F., Heisig M., & Wittum G. (2012). Finite dose skin penetration: Concentration depth profiles - Comparison between experiment and simulation. Manuscript submitted for publication.

Naegel A., Heisig, M., Wittum, G., K.H. Schaller, H. Drexler, & Korinth, G. Prospective evaluation of a sophisticated predictive mathematical model to simulate the percutaneous penetration of caffeine. Manuscript submitted for publication.

Queisser, G. & Wittum, G. (2010). Investigating the Diffusion Properties of Nuclear Calcium. Manuscript submitted for publication.

Reiter, S., Logashenko, D., Stichel, S., Wittum, G., & Grillo, A. (2012). Models and simulations of variable-density flow in fractured porous media. Manuscript submitted for publication.

Schröder, P., Gerstner, T., & Wittum, G. (2012). Taylor-like ANOVA Expansion for high dimensional Problems in Finance. Manuscript submitted for publication.

Selzer D., T. Hahn T., Naegel A., Heisig M., Neumann D., Kostka K.H., Lehr C.M., Schaefer U.F., & Wittum G. (2012). Finite dose skin mass balance including the lateral part - Comparison between experiment, pharmacokinetic modeling, and diffusion models. Manuscript submitted for publication.

Wolf, S., Grein, S., & Queisser, G. (2011). Employing NeuGen 2.0 to automatically generate realistic morphologies of hippocampal neurons and neural networks in 3D. Manuscript submitted for publication.

Wolf, S., Wittum, G. & Queisser, G. (2010). NeuGen3D: The CA1 Region. In preparation.